Mathematical and Experimental Studies on the Temperature Rise of Electric Rotating Machines.

By

Motokiti Mori.

CHAPTER I.

INTRODUCTION.

The present essay reports mathematical and exprimental investigations on the heat problem of electric rotating machines.

The flow of heat in the armature of electric machines is classified into two sorts, the radial heat flow and the axial heat flow, according to the path of the heat which is developed in the armature and dissipated from the cooling surfaces. The inner temperature of each part of the armature is calculated from the thermal relations existing among the slot, teeth and iron core. Considering the effect of the radial ventilating ducts, the radial heat flow of the section perpendicular to the axis of the armature at the middle point of the axial length is discussed, since the temperature in this plane is surely higher than in any other cross section. In this plane the temperature of the periphery of the armature is distributed regularly with the pulsation which corresponds to the slot pitch. Therefore the peripheral temperature can be expressed by Fourier's series. The temperature of the teeth can be decided from the temperature of their circumference and the cooling conditions at the boundary. Temperature distribution in the teeth depends upon their form. The sufficient conditions favourable to cool the teeth are obtained generally.

The calculation of the temperature in the radial direction in the armature may be applied to the generators coupled to the water turbine and some small motors, because in such machines the diameter of the armature is comparatively large compared with its axial length. For the numerical example a large synchronous alternator 31,000 KVA, 11,000 V, recently designed and constructed by the Hitachi Electric Works and used at a hydro-electric power station for Railway service, was taken. The results of calculation were compared with the experi-

mental results obtained by using the alternator, and it was found that the calculation coincides approximately with the experiment.

The heat developments due to hysteresis and eddy current have not yet been treated by the function of the magnetic induction in the core. In this article, however, the heat sources are treated as the function of magnetic induction which varies with the position in the core.

For an ordinary electric machine, it may be necessary to calculate the axial distribution of the temperature. The axial temperatures are solved mathematically in connection with the slot, teeth, iron core and the end connector. The temperature distributions both at no-load and at short-circuit are obtained. Moreover it is found that it is possible to estimate the temperature in the case of any loading, if the temperatures at no-load and short-circuit are obtained from practical tests.

The calculation of the axial temperature distribution may be applied to the machine having a long axial length compared with its diameter; for example:—generators or motors having a high revolution as the turbo-generator. The cooling of the turbo-generator might be the essential problem for the machinery maker. Since the temperature of such a high speed machine is likely to rise considerably because the size is generally small compared with the one having a low speed, some special considerations should be required in the design of the machine in order to cool its surface effectively. Therefore it may be sure that this calculation about the axial direction is useful for the design of the high speed machine.

The most part of the heat is dissipated from the cooling surface, but some part is dissipated through the rotating axle or the frame. The heat amount is calculated and estimated by using the equivalent emissibility.

Four differential equations are established among the winding embedded in the slot, iron core, teeth and the end connectors and these differential equations are transformed into integral equations and solved by successive approximation. Therefore the essential terms are not missed.

The temperature of each part of the machine in the loading is separated into the no-load and the short-circuit. As the numerical example, a large turbo-generator is taken, of a capacity of 50,000 KVA, 11,000 V recently designed and constructed in the Hitachi Electric Works and used at a stream power plant. This calculation was applied to this design.

To solve the problem of the temperature about the slot conductor Green's potential function is used and the temperature distribution about some kind of arrangement of slot conductor is calculated. From the calculated results, it is discussed (1) how the temperature distribution varies according to the boundary conditions and (2) where the spot of the highest temperature occurs in the slot and (3) how the spot of the highest temperature transfers according to the thermal conditions. These discussions are divided into two sections; one is no-loading and the other is loading, and the case of loading is again classified into D.C. loading in the D.C. machine and A.C. loading in the A.C. machine. For A.C. loading, the current distribution in the slot conductor is discussed and the temperature distribution is obtained by using the "Alternating current resistance."

Damage to an electric machine occurs generally in the slot winding at over load and it is sure that this damage occurs at the spot of the highest temperature. However, it is difficult to detect the spot of the highest temperature experimentally. If this temperature can be estimated from the results of the calculation, this calculation is indispensable for the design of the slot:—especially for the form of slot, the arrangement of the slot conductor and its insulation. As the numerical example, the synchronous generator 31,000 KVA above mentioned is taken, inner temperature is calculated and results found to coincide approximately with the data experimentally tested.

Next, the heat dissipation from the surface is investigated when the thermal conditions reach a steady state. For this purpose, it is necessary to determine the coefficient of heat dissipation from the cooling surface, i.e. Newton's constant of Newton's cooling law. By this law it is meant that the heat dissipation from the surface is proportional to the temperature difference between the surface and the cooling medium. From this experiment, if the cooling condition varies with the temperature rise of the heated surface, this coefficient can not be taken as constant. From the experimental measurements of the coefficient of the heat diffusion of several kinds of heating surface, it is found that the coefficient of heat diffusion varies with the surface temperature within a wide range and the relation between the coefficient of heat diffusion and the surface temperature is represented approximately by the exponential curve having the saturated character.

The variation of this coefficient depends on the heat conduction and convection in the cooling medium at the near part of the heating surface. Therefore at first the characteristics of the heat conduction

and convection at the surface are investigated by means of the Schlieren method. In order to study the heat diffusion due mostly to the conduction, experiments are made under the condition of forced ventilation in the wind tunnel and in the evacuated vessel. From this result, it is found that both characters are represented by the saturating curves, referred to the surface temperature. The method which is used for detecting the spot of the highest temperature on the heated rotor-periphery is that of Schlieren. Next the coefficient of the heat dissipation from the surface in the case of forced ventilation is determined.

For the comparison of the coefficients of heat diffusion about two surfaces; painted and non-painted, it is found that the painted surfaces is more efficient than the others to dissipate the heat from the surfaces. Referring to the machine having a short hour rating, such as railway motors, the curve of the temperature rise is especially necessary to decide its rating. If the temperature of the machine carrying the constant load is assumed to be followed by the pure exponential curve, the temperature may deviate considerably from the real one, especially in the neighborhood of the saturated state, its deviation is more prominent. Hence this deviation of the temperature rise from the exponential curve is explained by Osborne and Jehle by considering two kinds of time constants according to two groups of materials used in constructing the electric machine. Though it explains the deviation approximately, this theory may not be perfect since the fundamental assumption is based on the pure exponential curves. Their explanation is suitable for the real temperature rise of the electric machine to be represented by the two groups of temperature rising curve having each a particular time constant. However, the time constants of each group of the materials must not be deduced from the exponential curves, but they must be deduced from the temperature rising curve obtained by the variation of Newton's constant in reference to the surface temperature.

Using the coefficient of the heat dissipation obtained from the experiment, the new temperature rise curve is determined and the method to obtain this curve graphically is described. If the curve thus obtained is taken as the fundamental curve of the temperature rise and used to estimate the temperature rise of the practical machine instead of the calculation of the two groups of time constants, a more exact result may be expected.

CHAPTER II.

TEMPERATURE DISTRIBUTION IN THE RADIAL DIRECTION.

The heat developed in the armature of a generator or motor is carried away by the heat flow in the slot, teeth and armature core; one part of the heat developed in the slot winding and in the teeth will flow into the outer cooling medium passing through the surface which is facing the air gap, and another part will be carried away passing through the armature core into the cooling medium.

Thereupon to investigate the heat flow in the armature core only, the temperature of the slot and the teeth must be assumed to be constant and the temperature is calculated from the heat equilibrium between the armature core and the cooling medium by means of the fundamental equations containing the power losses in the armature core.

Next to investigate the heat flow in the teeth only, the heat equilibrium which holds between the teeth and the outer cooling medium, must be studied by assuming the temperature of the slot and the iron core and power losses in the core.

(1) TEMPERATURE OF IRON CORE.

For the sake of simplicity, the problem is discussed only in the plane perpendicular to the axis of the armature, passing at the middle point of the axial length.

Temperature T_p of the periphery of the armature core is considered to be periodically distributed on account of the existence of the slot and the teeth, its periods being based on the slot pitch. Therefore the fundamental period is the same as the slot pitch and the higher harmonics may also appear. Therefore the temperature distribution at the bottom of the slot and the teeth, with respect to the armature periphery can be described naturally as follows.

$$(1) \qquad T_p = T_{p,m} + T_{p,d} \frac{4}{\pi} \sum_{n=0}^{m} \frac{\sin(2n+1)\frac{2\pi}{\lambda_s} y}{(2n+1)}$$

$$n = 0, 1, 2, 3, \ldots\ldots\ldots$$

The coordinates (x, y) are taken as in Fig. 1, where

$T_{p,m}$ = the mean temperature of slot and teeth in °C.

$2T_{p,d}$ = the temperature difference between slot and teeth in °C.

λ_s = the slot pitch in cm.

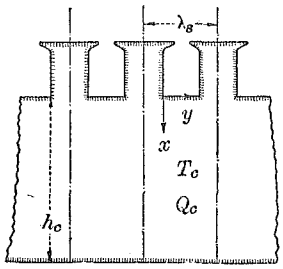

Fig. 1.

The fundamental equation of the heat conduction

$$(2) \qquad \frac{\partial^2 T_c}{\partial x^2}+\frac{\partial^2 T_c}{\partial y^2}=\frac{Q_c}{\sigma_c}$$

is established in the iron core, where

T_c = the temperature of iron core in °C.

Q_c = the heat quantity developed in the iron core in watt/cm³.

σ_c = the thermal conductivity in the radial direction in the iron core in watt/cm, °C.

However, this equation must be solved so as to be satisfied by the next three boundary conditions.

(i) at $x=0$, and between $y=n\lambda_s$ and $\left(n+\frac{1}{2}\right)\lambda_s$, $(n=0, 1, 2, \ldots.)$

$$\left[\frac{\partial T_c}{\partial x}\right]_{x=0}=\frac{\lambda_{s,c}}{\sigma_c}[T_c-T'_p]_{x=0}\,.$$

In the bottom of the slot, the heat flow $\sigma_c\left[\frac{\partial T_c}{\partial x}\right]_{x=0}$ is proportional to the difference between the temperature T'_p of the slot and T_c of the iron core, the proportional constant or Newton's constant being $\lambda_{s,c}$.

$$T'_p=T_{p,m}+T_{p,d}\,.$$

(ii) at $x=0$, and between $y=\left(n+\frac{1}{2}\right)\lambda_s$ and $(n+1)\lambda_s$

$$[T_c]_{x=0}=T''_p\,,$$

where T''_p is the temperature of the bottom of the teeth.

$$T''_p=T_{p,m}-T_{p,d}\,.$$

(iii) at $x = h_c$, and $y = y$.

$$\left[\frac{\partial T_c}{\partial x}\right]_{x=h_c} = \frac{\lambda_{c,0}}{\sigma_c}[T_0 - T_c]_{x=h_c}.$$

This is Newton's cooling law at the surface bounded by the cooling medium, $\lambda_{c,0}$ being Newton's constant at this part of the surface and T_0 being the temperature in the cooling medium.

The solution of equation (2) may be given in the form,

$$T_c = f_1(x) + \sum f_{2,m}(x) f_{3,m}(y). \tag{3}$$

Substituting equation (3) into fundamental equation (2), one obtains

$$\frac{d^2 f_1(x)}{dx^2} - \sum \frac{d^2 f_{2,m}(x)}{dx^2} \cdot f_{3,m}(y) + \sum f_{2,m}(x) \frac{d^2 f_{3,m}(y)}{dy^2} = \frac{Q_c}{\sigma_c}.$$

But as

$$\frac{d^2 f_1(x)}{dx^2} = \frac{Q_c}{\sigma_c}, \tag{4}$$

the above equation will be satisfied

$$\frac{d^2 f_{2,m}(x)}{dx^2} \cdot \frac{1}{f_{2,m}(x)} - \frac{d^2 f_{3,m}(y)}{dy^2} \cdot \frac{1}{f_{3,m}(y)} = 0. \tag{5}$$

The first term of equation (5) is the function of x only, and the second is that of y only, and the sum of these two terms must be always zero. Therefore each term must be constant. If

$$\frac{d^2 f_{3,m}(y)}{dy^2} \cdot \frac{1}{f_{3,m}(y)} = -K, \quad \text{then} \quad \frac{d^2 f_{2,m}(x)}{dx^2} \cdot \frac{1}{f_{2,m}(x)} = K.$$

Put

$$K = \left[\frac{2\pi}{\lambda_s} m\right]^2,$$

then it follows

$$\frac{d^2 f_{2,m}(x)}{dx^2} \cdot \frac{1}{f_{2,m}(x)} = \left[\frac{2\pi}{\lambda_s}\right]^2 m^2,$$

$$\frac{d^2 f_{3,m}(y)}{dy^2} \cdot \frac{1}{f_{3,m}(y)} = -\left[\frac{2\pi}{\lambda_s}\right]^2 m^2.$$

Therefore

$$(6)\qquad \begin{cases} f_{2,m}(x) = A_m e^{-\frac{2\pi}{\lambda_s}mx} + B_m e^{\frac{2\pi}{\lambda_s}mx}, \\ f_{3,m}(y) = C_m \sin\frac{2\pi}{\lambda_s}my + D_m \cos\frac{2\pi}{\lambda_s}my, \end{cases}$$

where A_m, B_m, C_m and D_m are the arbitrary constants of integration.

Thus the solution of (3) is written as follows;

$$T_c = f_1(x) + \sum\Big[A_m e^{-\frac{2\pi}{\lambda_s}mx} + B_m e^{+\frac{2\pi}{\lambda_s}mx}\Big] \times\Big[C_m \sin\frac{2\pi}{\lambda_s}my + D_m \cos\frac{2\pi}{\lambda_s}my\Big].$$

Since the fluctuated temperature distribution at $x = 0$ is represented by the rectangular form in the direction of y-axis as shown in (1), the function f_3 must be given as follows,

$$(7)\qquad f_{3,m}(y) = \frac{4}{\pi}\frac{T_{c,d}}{A_m}\cdot\frac{\sin(2n+1)\frac{2\pi}{\lambda_s}y}{(2n+1)}.$$

Thereupon $D_m = 0$, and $m = 2n+1$.

Insert expression (3) into the boundary condition (iii), then

$$(8)\qquad \frac{d}{dx}f_1(h_c) + \sum f_{3,m}(y)\cdot\frac{d}{dx}f_{2,m}(h_c) = \frac{\lambda_{c0}}{\sigma_c}\Big[T_0 - f_1(h_c) - \sum f_{3,m}f_{2,m}(h_c)\Big].$$

Now put

$$(9)\qquad \begin{cases} \frac{d}{dx}f_1(h_c) + \frac{\lambda_{c0}}{\sigma_c}f_1(h_c) = \frac{\lambda_{c0}}{\sigma_c}T_0, \\ \frac{d}{dx}f_{2,m}(h_c) = -\frac{\lambda_{c0}}{\sigma_c}f_{2,m}(h_c), \end{cases}$$

then equation (8) is satisfied.

Therefore inserting expression (6) into this equation, one obtains

$$\frac{B_m}{A_m} = \frac{1-\frac{\lambda_{c0}}{\sigma_c}\cdot\frac{\lambda_s}{2\pi(2n+1)}}{1+\frac{\lambda_{c,0}}{\sigma_c}\cdot\frac{\lambda_s}{2\pi(2n+1)}}e^{-\frac{4\pi}{\lambda_s}(2n+1)h_c}$$

As this amount is very small compared with 1, we can neglect B_m against A_m. Therefore $B_m = 0$. Hence

$$f_{2,m}(x) = A_m e^{-\frac{2\pi}{\lambda_s}(2n+1)x} \tag{10}$$

may be obtained.

Inserting expression (3) into the boundary condition (i), it follows

$$\sum\left[\frac{d}{dx}f_{2,m}(0)-\frac{\lambda_{s,c}}{\sigma_c}f_{2,m}(0)\right]f_{3,m}(y) = \left[\frac{\lambda_{s,c}}{\sigma_c}f_1(0)-\frac{d}{dx}f_1(0)\frac{\lambda_{s,c}}{\sigma_c}T'_p\right]$$

or

$$-\sum\left[\frac{2\pi}{\lambda_s}(2n+1)+\frac{\lambda_{s,c}}{\sigma_c}\right]\frac{4}{\pi}T_{c,d}\frac{\sin(2n+1)\frac{2\pi}{\lambda_s}y}{(2n+1)}$$
$$= \left[\frac{\lambda_{s,c}}{\sigma_c}f_1(0)-\frac{d}{dx}f_1(0)-\frac{\lambda_{s,c}}{\sigma_c}T'_p\right].$$

Multiplying both sides of the above equation by $\sin(2n+1)\frac{2\pi}{\lambda_s}y$ and integrating its results from zero to $\frac{\lambda_s}{2}$, then it follows

$$-T_{c,d}\left[\frac{2\pi}{\lambda_s}(2n+1)+\frac{\lambda_{s,c}}{\sigma_c}\right] = \left[\frac{\lambda_{s,c}}{\sigma_c}f_1(0)-\frac{d}{dx}f_1(0)-\frac{\lambda_{s,c}}{\sigma_c}T'_p\right]. \tag{11}$$

Again, insert expression (3) into the boundary condition (ii)

$$\frac{4}{\pi}T_{c,d}\sum\frac{\sin(2n+1)\frac{2\pi}{\lambda_s}y}{(2n+1)} = T''_p-f_1(0), \tag{12}$$

and multiplying both the sides by $\sin(2n+1)\frac{2\pi}{\lambda_s}y$ and integrating from $\lambda_s/2$ to λ_s.

$$-T_{c,d} = T''_p-f_1(0). \tag{13}$$

From (11) and (13),

$$\frac{\frac{\lambda_{s,c}}{\sigma_c}f_1(0)-\frac{d}{dx}f_1(0)-\frac{\lambda_{s,c}}{\sigma_c}T'_p}{-\frac{2\pi}{\lambda_s}(2n+1)-\frac{\lambda_{s,c}}{\sigma_c}} = f_1(0)-T''_p. \tag{14}$$

The iron loss in the core Q_c depends upon the induction in the core B_a and if the magnetic induction in the core indicates the dropping character in the radial direction and also if it can be assumed as follows

$$B_a = \frac{B_{a\,\max}}{h_c}[h_c - x]$$

where h_c is the radial length of the core, then the core losses $W_{h,a}$ and $W_{w,a}$ due to the hysteresis and the eddy current respectively can be written[1]

$$W_{h,a} = \sigma_h \left[\frac{f}{100}\right]\left[\frac{B_{a\,\max}}{1000}\right]^{1.6} \frac{1}{1000}\left[1-\frac{x}{h_c}\right]^{1.6} \text{watt/cm}^3 ,$$

$$W_{w,a} = \sigma_w \left[t_a\frac{f}{100}\right]^2\left[\frac{B_{a\,\max}}{1000}\right]^2 \frac{1}{1000}\left[1-\frac{x}{h_c}\right]^2 \text{watt/cm}^3 ,$$

where

σ_h = hysteresis constant
σ_w = constant depending on the eddy current
f = frequency per sec.
t_a = thickness of the sheet iron in mm.

Then $Q_c = W_{h,a} + W_{w,a}$ and

$$(15) \qquad Q_c = Q_h\left[1-\frac{x}{h_c}\right]^{1.6} + Q_w\left[1-\frac{x}{h_c}\right]^2 ,$$

where

$$Q_h = \sigma_h\left[\frac{f}{100}\right]\left[\frac{B_{a\,\max}}{1000}\right]^{1.6}\frac{1}{1000} ,$$

$$(15)' \qquad Q_w = \sigma_w\left[t_a\frac{f}{100}\right]^2\left[\frac{B_{a\,\max}}{1000}\right]^2\frac{1}{1000} .$$

Put this expression of Q_c into equation (4) and integrate it, then

$$(16) \qquad f_1(x) = \frac{Q_h}{\sigma_c}\frac{h_c^2}{2.6\times 3.6}\left[1-\frac{x}{h_c}\right]^{3.6} + \frac{Q_w}{\sigma_c}\frac{h_c^2}{12}\left[1-\frac{x}{h_c}\right]^4 + C_1x + C_2 .$$

If $f_1(x)$ is inserted into equations (8) and (14), in order to find the values of the unknown constants C_1 and C_2 contained in the function $f_1(x)$, then their values may be determined as follows

1) Arnold:—Wechselstrom Technik Bd. IV, S. 480-486.

$$C_1 = \frac{\Delta_1}{\Delta}, \qquad C_2 = \frac{\Delta_2}{\Delta}$$

$$\Delta = \left[\frac{2\pi}{\lambda_s} + 2\frac{\lambda_{s,c}}{\sigma_c}\right]\left[1 + \frac{\lambda_{c,0}}{\sigma_c} h_c\right] + \frac{\lambda_{c,0}}{\sigma_c}$$

$$\Delta_1 = \frac{\lambda_{c,0}}{\sigma_c} T_0 \left[\frac{2\pi}{\lambda_s} + 2\frac{\lambda_{s,c}}{\sigma_c}\right] + \frac{\lambda_{c,0}}{\sigma_c}\left[\frac{Q_h}{\sigma_c}\frac{h_c}{2.6} + \frac{Q_w}{\sigma_c}\frac{h_c}{3}\right] - \frac{\lambda_{c,0}}{\sigma_c}\frac{\lambda_{s,c}}{\sigma_c} T'_p$$

$$+ \frac{\lambda_{c,0}}{\sigma_c}\left[\frac{2\pi}{\lambda_s} - 2\frac{\lambda_{s,c}}{\sigma_c}\right]\left[\frac{Q_h}{\sigma_c}\frac{h_c^2}{2.6\times 3.6} + \frac{Q_w}{\sigma_c}\frac{h_c^2}{12}\right] - \frac{\lambda_{c,0}}{\sigma_c}\left[\frac{2\pi}{\lambda_s} - \frac{\lambda_{s,c}}{\sigma_c}\right] T''_p$$

$$\Delta_2 = -\left[1 + \frac{\lambda_{c,0}}{\sigma_c} h_c\right]\left[\frac{2\pi}{\lambda_s} + 2\frac{\lambda_{s,c}}{\sigma_c}\right]\left[\frac{Q_h}{\sigma_c}\frac{h_c^2}{2.6\times 3.6} + \frac{Q_w}{\sigma_c}\frac{h_c^2}{12}\right]$$

$$-\left(1 + \frac{\lambda_{c,0}}{\sigma_c} h_c\right)\left[\frac{Q_h}{\sigma_c}\frac{h_c}{2.6} + \frac{Q_w}{\sigma_c}\frac{h_c}{3}\right] + \left[1 + \frac{\lambda_{c,0}}{\sigma_c} h_c\right]\frac{\lambda_{s,c}}{\sigma_c} T'_p$$

$$+\left(1 + \frac{\lambda_{c,0}}{\sigma_c} h_c\right)\left[\frac{2\pi}{\lambda_s} + \frac{\lambda_{s,c}}{\sigma_c}\right] T''_p + \frac{\lambda_{c,0}}{\sigma_c} T_0 .$$

From equation (13)

$$(17) \qquad T_{c.d} = f_1(0) - T''_p = \frac{Q_h}{\sigma_c}\frac{h_c^2}{2.6\times 3.6} + \frac{Q_w}{\sigma_c}\frac{h_c^2}{12} + C_2 - T''_p .$$

If the cooling area of the iron core is considered to be small (compared with h_c) and if also the cooling device in the iron core is not effective to make the power loss flow away, then the coefficient $\lambda_{c,0}$ of Newton's law can be considered to be small, i.e. $\lambda_{c,0}/\sigma_c$ is small to be compared with the terms;

$$\left[\frac{2\pi}{\lambda_s} + 2\frac{\lambda_{s,c}}{\sigma_c}\right]\left[1 + \frac{\lambda_{c,0}}{\sigma_c} \cdot h_c\right],$$

so the term $\lambda_{c,0}/\sigma_c$ can be neglected. Thus one obtains

$$C_2 = -\frac{1}{\dfrac{2\pi}{\lambda_s} + 2\dfrac{\lambda_{s,c}}{\sigma_c}}\left[\left(\frac{Q_h}{\sigma_c}\frac{h_c}{2.6} + \frac{Q_w}{\sigma_c}\frac{h_c}{3}\right) + \frac{\lambda_{s,c}}{\sigma_c} T'_p\right]$$

$$-\left[\frac{Q_h}{\sigma_c}\frac{h_c^2}{2.6\times 3.6} + \frac{Q_w}{\sigma_c}\frac{h_c^2}{12}\right] + T''_p .$$

From this result, it can be ascertained that the temperature of the iron core is nearly independent of the temperature of the cooling medium and that when the larger Q_h, Q_w and h_c become, the less the temperature difference between the slot and the teeth influences the iron core.

On the contrary, if $\frac{\lambda_{c,o}}{\sigma_c}$ is comparatively large against $\left[\frac{2\pi}{\lambda_s}+2\frac{\lambda_{s,c}}{\sigma_c}\right]\left[1+\frac{\lambda_{c,o}}{\sigma_c}h_c\right]$ (as the cooling at the surface of iron core is very good)

$$C_1 = T_0\left[\frac{2\pi}{\lambda_s}+2\frac{\lambda_{s,c}}{\sigma_c}\right]+\left[\frac{Q_h}{\sigma_c}\frac{h_c}{2.6}+\frac{Q_w}{\sigma_c}\frac{h_c}{3}\right]-\frac{\lambda_{s,c}}{\sigma_c}T'_p$$
$$+\left[\frac{2\pi}{\lambda_s}-2\frac{\lambda_{s,c}}{\sigma_c}\right]\left[\frac{Q_h}{\sigma_c}\frac{h_c^2}{2.6\times 3.6}+\frac{Q_w}{\sigma_c}\frac{h_c^2}{12}\right]-\left[\frac{2\pi}{\lambda_s}+\frac{\lambda_{s,c}}{\sigma_c}\right]T''_p$$

may be obtained. From this result, the larger Q_w, Q_h and h_c become, the larger the temperature gradient in X-direction becomes.

The temperature in the iron core is given by the following equation;

$$(18)\qquad T_c = f_1(x)+\frac{4}{\pi}T_{c,d}\sum_{n=0}^{\infty}e^{-\frac{2n}{\lambda_s}(2n+1)x}\frac{\sin(2n+1)\frac{2\pi}{\lambda_s}y}{(2n+1)}.$$

The first term $f_1(x)$ indicates the mean temperature and the latter term indicates the temperature fluctuation of Y-direction. Therefore the mean temperature is

$$(19)\qquad T_{c,m} = \frac{Q_h}{\sigma_c}\frac{h_c^2}{2.6\times 3.6}\left(1-\frac{x}{h_c}\right)^{3.6}+\frac{Q_w}{\sigma_c}\frac{h_c^2}{12}\left(1-\frac{x}{h_c}\right)^4+C_1x+C_2,$$

and the temperature fluctuation is described as follows;

$$(20)\qquad T_{c,f} = \frac{4}{\pi}T_{c,d}\sum_{n=0}^{\infty}e^{-\frac{2\pi}{\lambda_s}(2n+1)x}\frac{\sin(2n+1)\frac{2\pi}{\lambda_s}y}{2n+1}.$$

As both the formulae (19) and (20) contain the temperatures of the slot and the teeth T'_p, T''_p respectively, the temperatures T'_p and T''_p might be obtained inversely from the two formulae, if the mean temperature $T_{c,m}(h_c)$ and the fluctuated temperature $T_{c,f}(h_c)$ at the surface $x=h_c$ are obtained from the experiment. However, the

fluctuated temperature at the surface $x = h_c$ is very small, because $f_2(x)$ is very rapidly converged into zero with increasing x, since the thermal conductivity of the iron core is fairly large in the direction of the radius. Therefore only the mean temperature of the slot and the teeth at $x = h_c$ is obtained.

(2) TEMPERATURE OF TEETH.

If the temperature T_t and the power loss Q_t in the teeth are expressed with the subindex t, the fundamental equation in the teeth may be described in a similar manner as that of the iron core.

$$\frac{\partial^2 T_t}{\partial x^2}+\frac{\partial^2 T_t}{\partial y^2} = \frac{Q_t}{\sigma_t} \tag{21}$$

The temperature T_t is solved so as to be satisfied by the following boundary conditions (i), (ii) and (iii); the temperature must be continuous at the boundary between the iron core and the bottom of the teeth, and also the boundary condition (iv) is satisfied from the relation shown in Fig. 2. The boundary conditions to be satisfied are;

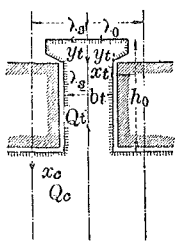

Fig. 2.

(i) at $y = \pm\frac{b_t}{2}$,

$$\left[\frac{\partial T_t}{\partial y}\right]_{y=\pm\frac{b_t}{2}} = \frac{\lambda_{s,t}}{\sigma_t}[T_s - T_t]_{y=\pm\frac{b_t}{2}} .$$

By the boundary condition (i) it is meant that the heat flow exists at the boundary surface between the slot and the teeth. T_s is the temperature of the slot and $\lambda_{,t}$ is the constant in reference to the heat delivery between them.

(ii) at $y = 0$,

$$\left[\frac{\partial T_t}{\partial y}\right]_{y=0} = 0$$

(iii) at $x = 0$,

$$\left[\frac{\partial T_t}{\partial x}\right]_{x=0} = \frac{\lambda_{t,0}}{\sigma_t}[T_t - T_0]_{x=0} .$$

Condition (iii) expresses the heat transmission due to Newton's cooling

law at the boundary surface facing the air gap. T_0 is the temperature and $\lambda_{t,0}$ the cooling coefficient in the cooling medium.

(iv) at $x_t = h_t$ or $x_c = 0$,

$$\left[\frac{\partial T_t}{\partial x}\right]_{x_t=h_t} = \left[\frac{\partial T_c}{\partial x}\right]_{x_c=0}$$

and

$$[T_t]_{x_t=h_t} = [T_c]_{x_c=0}$$

h_t is the height of the teeth in cm.

By putting

$$\tau_t = T_t - T_s \,, \tag{22}$$

the fundamental equation is written again

$$\frac{\partial^2 \tau_t}{\partial x_t^2} + \frac{\partial^2 \tau_t}{\partial y_t^2} = \frac{Q_t}{\sigma_t} \tag{23}$$

and the form of solution may be assumed as follows

$$\tau_t = F_1(x) + U(x, y) \tag{24}$$

where $$F_1(x) = \frac{1}{2}\frac{Q_t}{\sigma_t} x_t^2 \,.$$

Let us consider the function $\psi_i(y)$ to be satisfied by the condition

$$\int_{-\frac{1}{2}b_t}^{+\frac{1}{2}b_t} \psi_i(y)dy = 1 \,,$$

and the equation

$$\frac{d^2\psi_i}{dy^2} + \nu^2\psi_i = 0 \,.$$

If $U(x, y)$ is expanded by the functions $\psi_i(y)$, then

$$U(x, y) = \sum_i \psi_i(y) \int_{-\frac{1}{2}b_t}^{+\frac{1}{2}b_t} U(x, \lambda)\psi_i(\lambda)d\lambda \,. \tag{25}$$

Therefore expanding $\frac{\partial^2 U(x, y)}{\partial y^2}$ the same as the above mentioned,

$$
(26)\quad \begin{cases} \dfrac{\partial^2 U(x,y)}{\partial y^2} = \sum\limits_i \psi_i(y) \displaystyle\int_{-\frac{1}{2}b_t}^{+\frac{1}{2}b_t} \frac{\partial^2 U(x,\lambda)}{\partial \lambda^2} \psi_i(\lambda) d\lambda \\ = \sum\limits_i \psi_i(y) \Big[\dfrac{\partial U\left(x, \frac{1}{2}b_t\right)}{\partial \lambda} \psi_i\left(\frac{1}{2}b_t\right) - \dfrac{\partial U\left(x, -\frac{1}{2}b_t\right)}{\partial \lambda} \psi_i\left(-\frac{1}{2}b_t\right) \\ - U\left(x, \frac{1}{2}b_t\right) \dfrac{\partial \psi_i\left(\frac{1}{2}b_t\right)}{\partial \lambda} + U\left(x, -\frac{1}{2}b_t\right) \dfrac{\partial \psi_i\left(-\frac{1}{2}b_t\right)}{\partial \lambda} \\ + \displaystyle\int_{-\frac{1}{2}b_t}^{+\frac{1}{2}b_t} U(x,\lambda) \frac{\partial^2 \psi_i(\lambda)}{\partial \lambda^2} d\lambda \Big] \end{cases}
$$

and
$$
\frac{\partial^2 U}{\partial x^2} = \sum_i \psi_i(y) \int_{-\frac{1}{2}b_t}^{+\frac{1}{2}b_t} \frac{\partial^2 U(x,\lambda)}{\partial x^2} \psi_i(\lambda) d\lambda \,.
$$

These functions are considered as even functions with respect to y.

Therefore

$$
\psi_i\left(\frac{1}{2}b_t\right) = \psi_i\left(-\frac{1}{2}b_t\right), \qquad \frac{\partial \psi_i\left(\frac{1}{2}b_t\right)}{\partial \lambda} = -\frac{\partial \psi_i\left(-\frac{1}{2}b_t\right)}{\partial \lambda},
$$

$$
\frac{\partial U\left(x, \frac{1}{2}b_t\right)}{\partial \lambda} = -\frac{\partial U\left(x, -\frac{1}{2}b_t\right)}{\partial \lambda}, \quad U\left(x, \frac{1}{2}b_t\right) = U\left(x, -\frac{1}{2}b_t\right).
$$

Concluding from the above results,

$$
(27)\quad \begin{cases} \dfrac{\partial^2 U}{\partial x^2} + \dfrac{\partial^2 U}{\partial y^2} = \sum\limits_i \psi_i(y) \Big[\displaystyle\int_{-\frac{1}{2}b_t}^{+\frac{1}{2}b_t} \frac{\partial^2 U(x,\lambda)}{\partial x^2} \psi_i(\lambda) d\lambda \\ + 2 \dfrac{\partial U\left(x, \frac{1}{2}b_t\right)}{\partial \lambda} \psi_i\left(\frac{1}{2}b_t\right) - 2U\left(x, \frac{1}{2}b_t\right) \dfrac{\partial \psi_i\left(\frac{1}{2}b_t\right)}{\partial \lambda} \\ + \displaystyle\int_{-\frac{1}{2}b_t}^{+\frac{1}{2}b_t} U(x,\lambda) \frac{\partial^2 \psi_i(\lambda)}{\partial \lambda^2} d\lambda \Big] = 0 \,. \end{cases}
$$

However as the particular function ψ_i must satisfy the equation

$$\frac{d^2\psi_i}{dy^2}+\nu^2\psi_i=0\,,$$

hence

$$\int_{-\frac{1}{2}b_t}^{+\frac{1}{2}b_t} U(x,\lambda)\frac{d^2\psi_i}{d\lambda^2}\,d\lambda=-\nu^2\int_{-\frac{1}{2}b_t}^{+\frac{1}{2}b_t} U(x,\lambda)\psi_i(\lambda)d\lambda\,.$$

Substitute both the equation and the equation deduced from the boundary condition (i),

$$\frac{\partial U\left(x,\frac{1}{2}b_t\right)}{\partial\lambda}=-\frac{\lambda_{s,t}}{\sigma_t}\left[U\left(x,\frac{1}{2}b_t\right)+F_1(x)\right]$$

into the above equation (27), and one obtains

$$\frac{d^2\phi_i(x)}{dx^2}-\nu^2\phi_i(x)-2\frac{\lambda_{s,t}}{\sigma_t}F_1(x)\psi_i\left(\frac{1}{2}b_t\right)=0\,, \tag{28}$$

where

$$\phi_i(x)=\int_{-\frac{1}{2}b_t}^{+\frac{1}{2}b_t} U(x,\lambda)\psi_i(\lambda)d\lambda\,,\qquad \frac{d\psi_i\left(\frac{1}{2}b_t\right)}{d\lambda}=-\frac{\lambda_{s,t}}{\sigma_t}\psi_i\left(\frac{1}{2}b_t\right).$$

If $F_1(x)=0$, one obtains from the equation

$$\frac{d^2\phi_i(x)}{dx^2}-\nu^2\phi_i(x)=0\,,$$

the solution

$$\phi_i=A_\nu\phi_1+B_\nu\phi_2\,.$$

However, if $F_1(x)$ exist, the general solution in this case can be written

$$\phi_i=A_\nu\phi_1+B_\nu\phi_2+2\frac{\lambda_{s,t}}{\sigma_t}\psi_i\left(\frac{1}{2}b_t\right)\int_0^x F_1(\xi)\frac{\begin{vmatrix}\phi_1(x) & \phi_2(x)\\ \phi_1(\xi) & \phi_2(\xi)\end{vmatrix}}{\begin{vmatrix}\phi_1'(\xi) & \phi_2'(\xi)\\ \phi_1(\xi) & \phi_2(\xi)\end{vmatrix}}d\xi\,.$$

where

$$\phi_1 = e^{-\nu h_t\left(1-\frac{x}{h_t}\right)}, \quad \phi_2 = e^{-\nu h_t \frac{x}{h_t}} .$$

Therefore

$$\phi_i = A_\nu e^{-\nu h_t\left(1-\frac{x}{h_t}\right)} + B_\nu e^{-\nu h_t \frac{x}{h_t}} \tag{29}$$
$$-\frac{\lambda_{s,t}}{\sigma_t}\frac{1}{\nu^2}\frac{Q_t}{\sigma_t}\psi_i\left(\frac{1}{2}b_t\right)\left[x^2+\frac{2}{\nu^2}-\frac{1}{\nu^2}(e^{\nu x}+e^{-\nu x})\right].$$

Therefore from (25)

$$U(x, y) = \sum_i \psi_i(y)\,\phi_i(x) . \tag{30}$$

Next the particular function ψ_i is determined from

$$\frac{d^2\psi_i}{dy^2}+\nu^2\psi_i = 0$$

where

$$\nu = \mu\frac{2\pi}{b_t}$$

and by the boundary condition (ii),

$$\psi_i = A\cos\mu\frac{2\pi}{b_t}y = A\cos\nu y .$$

From

$$\int_{-\frac{1}{2}b_t}^{+\frac{1}{2}b_t}\psi_i^2(y)\,dy = 1 ,$$

one obtains

$$A = \frac{2}{b_t}\sqrt{\frac{1}{1+\frac{\sin 2\mu\pi}{2\mu\pi}}} ,$$

and from

$$\frac{\partial^2\psi_i\left(\frac{1}{2}b_t\right)}{\partial\lambda^2}+\frac{\lambda_{s,t}}{\sigma_t}\psi_i\left(\frac{1}{2}b_t\right) = 0 ,$$

it follows

$$\mu_\pi \tan \mu_\pi = \frac{\lambda_{s,t}}{\sigma_t}\frac{b_t}{2} . \tag{30'}$$

If the roots μ of (30′) are written by μ_1, μ_2, μ_3, ..., $\psi_i(y)$ can be written as follows;

$$\psi_i(y) = A_i \cos \mu_i \frac{2\pi}{b_t} y . \tag{31}$$

From this it is clear that the temperature difference between the sides and center of the teeth becomes smaller with an increase of the width of teeth b_t as all A is nearly equal to $\frac{2}{b_t}$.

In order to determine the constants A_ν and B_ν from the boundary condition (iii)

$$\left[\frac{\partial \tau_t}{\partial x}\right]_{x=0} = \frac{\lambda_{t,0}}{\sigma_t}[\tau_t]_{x=0} + \frac{\lambda_{t,0}}{\sigma_t}[T_s - T_0] , \tag{32}$$

the equation

$$\sum_i \psi_i(y)\left[\frac{d\phi_i(0)}{dx} - \frac{\lambda_{t,0}}{\sigma_t}\phi_i(0)\right] = \frac{\lambda_{t,0}}{\sigma_t}[F_1(0) + T_s - T_0] - \frac{dF_1(0)}{dx}$$

is obtained. Multiplying both sides of this equation by ψ_i, and integrating from $-\frac{1}{2}b_t$ to $+\frac{1}{2}b_t$, from the orthogonal condition, the expression

$$\frac{d\phi_i(0)}{dx} - \frac{\lambda_{t,0}}{\sigma_t}\phi_i(0) = \int_{-\frac{1}{2}b_t}^{+\frac{1}{2}b_t} \psi_i\left[\frac{\lambda_{t,0}}{\sigma_t}\right\} F_1(0) + T_s - T_0\left.\right\} - \frac{dF_1(0)}{dx}\Bigg] dx \tag{33}$$

is obtained.

From the boundary condition (iv)

$$[\tau_t]_{x_t = h_t} + T_s = [T_c]_{x_c = 0} ,$$

the expression

$$\phi_i(h_t) = \left[(T_c)_{x_c=0} - T_s - F_1(h_t)\right] \int_{-\frac{1}{2}b_t}^{+\frac{1}{2}b_t} \psi_i(\lambda) d\lambda \tag{34}$$

is obtained.

From these equations constants A_ν and B_ν are obtained

$$
(35)\quad \begin{cases} A_\nu = \dfrac{K_1 e^{-\nu h_t} + K_2\left[\nu + \dfrac{\lambda_{t,0}}{\sigma_t}\right]}{\left[\nu - \dfrac{\lambda_{t,0}}{\sigma_t}\right] e^{-2\nu h_t} + \left[\nu + \dfrac{\lambda_{t,0}}{\sigma_t}\right]}, \quad B_\nu = \dfrac{K_2\left[\nu - \dfrac{\lambda_{t,0}}{\sigma_t}\right] e^{-\nu h_t} - K_1}{\left[\nu - \dfrac{\lambda_{t,0}}{\sigma_t}\right] e^{-2\nu h_t} + \left[\nu + \dfrac{\lambda_{t,0}}{\sigma_t}\right]}, \\ K_1 = \dfrac{b_t}{\mu\pi}\dfrac{\lambda_{t,0}}{\sigma_t}[T_s - T_0]\sin\mu\pi\sqrt{\dfrac{\dfrac{2}{b_t}}{1+\dfrac{\sin 2\mu\pi}{2\mu\pi}}}, \\ K_2 = \left[\dfrac{\lambda_{s,t}}{\sigma_t}\dfrac{1}{\nu^2}\dfrac{Q_t}{\sigma_t}\left\{h_t^2 + \dfrac{2}{\nu^2} - \dfrac{1}{\nu^2}(e^{\nu h_t} + e^{-\nu h_t})\right\}\cos\mu\pi \right. \\ \qquad \left. + \dfrac{b_t}{\mu\pi}\left\{[T_c]_{x_c=0} - T_s - \dfrac{Q_t}{\sigma_t}\dfrac{h_t^2}{2}\right\}\sin\mu\pi\right]\sqrt{\dfrac{\dfrac{2}{b_t}}{1+\dfrac{\sin 2\mu\pi}{2\mu\pi}}}. \end{cases}
$$

Put

$$
(36)\quad \begin{cases} A_\nu = A_{1\nu}\, T_s + A_{2\nu}[T_c]_{x_c=0} + A_{3\nu}, \\ B_\nu = B_{1\nu}\, T_s + B_{2\nu}[T_c]_{x_c=0} + B_{3\nu}, \end{cases}
$$

where

$$
A_{1\nu} = \sqrt{\frac{2}{b_t}}\frac{b_t}{\mu\pi}\frac{\sin\mu\pi}{\left[\nu - \dfrac{\lambda_{t,0}}{\sigma_t}\right] e^{-2\nu h_t} + \left[\nu + \dfrac{\lambda_{t,0}}{\sigma_t}\right]}\left[\frac{\lambda_{t,0}}{\sigma_t} e^{-\nu h_t} - \nu - \frac{\lambda_{t,0}}{\sigma_t}\right],
$$

$$
A_{2\nu} = \sqrt{\frac{2}{b_t}}\frac{b_t}{\mu\pi}\left[\nu + \frac{\lambda_{t,0}}{\sigma_t}\right]\frac{\sin\mu\pi}{\left[\nu - \dfrac{\lambda_{t,0}}{\sigma_t}\right] e^{-2\nu h_t} + \left[\nu + \dfrac{\lambda_{t,0}}{\sigma_t}\right]},
$$

$$
B_{1\nu} = \sqrt{\frac{2}{b_t}}\frac{b_t}{\mu\pi}\frac{\sin\mu\pi}{\left[\nu - \dfrac{\lambda_{t,0}}{\sigma_t}\right] e^{-2\nu h_t} + \left[\nu + \dfrac{\lambda_{t,0}}{\sigma_t}\right]}\left[\left(\frac{\lambda_{t,0}}{\sigma_t} - \nu\right) e^{-\nu h_t} - \frac{\lambda_{t,0}}{\sigma_t}\right],
$$

$$
B_{2\nu} = \sqrt{\frac{2}{b_t}}\frac{b_t}{\mu\pi}\left[\nu - \frac{\lambda_{t,0}}{\sigma_t}\right] e^{-\nu h_t}\frac{\sin\mu\pi}{\left[\nu - \dfrac{\lambda_{t,0}}{\sigma_t}\right] e^{-2\nu h_t} + \left[\nu + \dfrac{\lambda_{t,0}}{\sigma_t}\right]}.
$$

If $\lambda_{s,t}$ is small and also b_t is small, equation (30′) may be written as

$$\mu\pi \tan \mu\pi = 0 ,$$

or

$$\sin \mu\pi = 0 .$$

Hence

$$A_{1\nu} = 0 , \qquad B_{1\nu} = 0 , \qquad A_{2\nu} = 0 , \qquad B_{2\nu} = 0 .$$

From this assumption, if the width of the teeth is narrow and the materials of the electric insulation at the circumference of the slot have small thermal conductivity, then the temperature of the teeth should not depend upon the temperature of the iron core and the slot, i.e. :—the heat developed in the teeth themselves due to the power loss might be diffused into the air gap by Newton's cooling law.

In such a case, it follows

$$K_1 = 0 , \qquad K_2 = \sqrt{\frac{2}{b_t}} \frac{\lambda_{s,t}}{\sigma_t} \frac{1}{\nu^2} \frac{Q_t}{\sigma_t} \left[h_t^2 + \frac{2}{\nu^2} - \frac{1}{\nu^2} (e^{\nu h_t} + e^{-\nu h_t}) \right] \cos \mu\pi ,$$

$$A_\nu = K_2 , \qquad B_\nu = K_2 e^{-\nu h_t} \frac{\left[\nu - \frac{\lambda_{t,0}}{\sigma_t} \right]}{\left[\nu + \frac{\lambda_{t,0}}{\sigma_t} \right]}$$

and the temperature at $x = 0$, $y = 0$ is given as follows;

$$\tau_{t00} = \frac{2}{b_t} \frac{\lambda_{s,t}}{\sigma_t} \frac{Q_t}{\sigma_t} \sum_\nu \frac{1}{\nu^2} \frac{2\nu}{\nu + \frac{\lambda_{t,0}}{\sigma_t}} \left[\left(h_t^2 + \frac{2}{\nu^2} \right) e^{-\nu h_t} - \frac{1}{\nu^2} \right] \cos \mu\pi .$$

The temperature will become higher at the surface of the teeth facing the air gap, if Q_t and $\lambda_{t,0}$ become larger and σ_t becomes smaller. However its temperature is independent of the temperature in the iron core.

If h_t and $\lambda_{t,0}$ are large, then $A_{1\nu}$ and $B_{1\nu}$ are large, so the temperature of the teeth is higher than the others due to the fact that the heat developed in the slot is flowing into the teeth. In other words, the fact that h_t is larger, is favourable to cool the slot winding.

(3) HEAT FLOW CONDUCTED THROUGH THE ROTATING AXLE.

Referring to the rotating armature of the electric machine, the rotor is connected directly or indirectly to the rotating axle of the machine. In such a case, if the armature has several air ducts penetrating through the iron core, the large amount of the heat developed in the armature might be carried away through the air ducts, however even in such a case the heat which escapes from the surface of the axle, bearing and other parts can not be neglected.

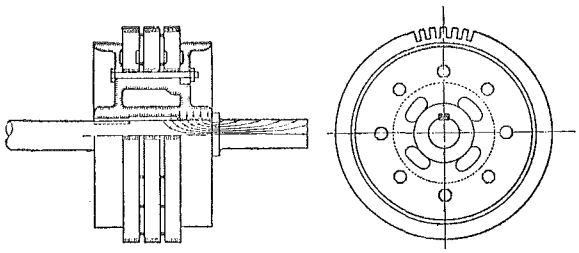

Fig. 3.

The heat carried away through the rotating axle is considered to flow into the axle, to bend in the direction of the axle and to diffuse from the surface facing the outer cooling medium as shown in Fig. 3. In this case, the temperature of the rotating axle surrounded by the iron core may be assumed to be constant.

The coordinate axis of z from the end of the iron core being taken as shown in Fig. 4, the fundamental equation of the heat conduction

$$\frac{\partial^2 T_w}{\partial x^2}+\frac{\partial^2 T_w}{\partial y^2}+\frac{\partial^2 T_w}{\partial z^2}=0 \tag{37}$$

can be written.

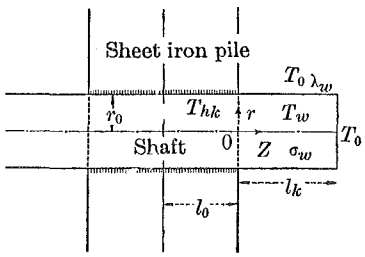

Fig. 4.

Neglecting the power loss in the rotating axle and putting

$$\tau_w = T_w - T_0 , \tag{38}$$

the equation is transformed by making use of the cylindrical coordinate r, θ, z into

$$\frac{\partial^2 \tau_w}{\partial r^2}+\frac{1}{r}\frac{\partial \tau_w}{\partial r}+\frac{\partial^2 \tau_w}{\partial z^2}=0 \tag{39}$$

where τ_w is independent of θ.

Substituting $\tau_w = R(r)Z(z)$ into equation (39), one obtains

$$\left[\frac{d^2R}{dr^2}+\frac{1}{r}\frac{dR}{dr}\right]\frac{1}{R}+p^2=0, \qquad \frac{1}{z}\frac{d^2z}{dz}=p^2. \tag{40}$$

From the two expressions R and Z, the solutions

$$\begin{cases} R(r)=\sum_p [C_p J_0(pr)+D_p Y_0(pr)] \\ Z(z)=\sum_p [A_p e^{-pz}+B_p e^{+pz}] \end{cases} \tag{41}$$

are obtained.

As Y_0 becomes infinitely great at the limit of $r=0$, D_p must be zero

$$\tau_w=\sum_p A_p J_0(pr)[e^{-pz}+B_p e^{+pz}]. \tag{42}$$

Newton's cooling law is established at the peripheral surface of the rotating axle $r=r_0$,

$$\frac{\partial \tau_w}{\partial r}+\frac{\lambda_w}{\sigma_w}\tau_w=0$$

where λ_w is Newton's constant at the peripheral surface $r=r_0$ and σ_w is the thermal conductivity in the axle.

If the Newton's cooling equation at the surface $r=r_0$ is established with respect to τ_w, the expression

$$(pr_0)J_1(pr_0)=\frac{\lambda_w}{\sigma_w}r_0 J_0(pr_0) \tag{43}$$

may be obtained. Roots of this equation are found as follows:—

$$p=p_1,\ p_2,\ p_3,\ \ldots\ldots,\ p_n,\ \ldots\ldots .$$

Next, at $Z=lk$,

$$\frac{d\tau_w}{dz}+\frac{\lambda_w}{\sigma_w}\tau_w=0. \tag{44}$$

From this

$$B_n = \frac{p_n - \frac{\lambda_w}{\sigma_w}}{p_n + \frac{\lambda_w}{\sigma_w}} e^{-2p_n l k} . \tag{45}$$

A_n is obtained from the condition that the temperature distribution is uniform at the section $z = 0$, and therefore $\tau_w = \tau_{h_c}$. If the constant τ_{h_c} is expanded by the Bessel function $J_0(p_n x)$ in the range $r = 0 \rightarrow r = r_0$, then $\tau_{h_c} = \sum_{n=1}^{\infty} K_n J_0(p_n x)$.

$$\begin{cases} K_n = \dfrac{2p_n^2}{\left[\left(\dfrac{\lambda_w}{\sigma_w}\right)^2 + p_n^2\right] J_0(p_n r_0)} \displaystyle\int_0^{r_0} \frac{x}{r_0} \tau_{h_k} J_0(p_n x) \frac{dx}{r_0} \\ A_n = \dfrac{2}{r_0^2} \tau_{h_c} \dfrac{1}{\left[\left(\dfrac{\lambda_w}{\sigma_w}\right) + p_n^2\right](1 + B_n) J_0(p_n r_0)} . \end{cases} \tag{46}$$

Then the solution (42) is written

$$\tau_w = \sum_n A_n J_0(p_n r) [e^{-p_n z} + B_n e^{+p_n z}] . \tag{47}$$

As the value of B_n is small compared with the other terms, it can be neglected. The temperature of the axle has a decreasing character in reference to z direction according to the exponential curve and the larger l_k becomes, the smaller the mean temperature becomes. This fact is easily understood by the fact that the larger l_k becomes, the larger the cooling surface is.

Putting $p_n r = \xi_n$, the formula

$$\xi_n J_1(\xi_n) = \frac{\lambda_w}{\sigma_w} r_0 J_0(\xi_n) \tag{48}$$

is obtained, where λ_w has complicated value in the practical case because the shaft is surrounded by the cooling medium directly and sometimes not. But σ_w might be nearly constant referring to the machine already constructed. The radius of the axle r_0 is determined from the consideration of the mechanical strength, and also of the radial heat flow.

Denote the temperature at the surface r_0 by $\tau_w r_0$. The mean value of the temperature in the direction z is

$$\tau_{wr_0\,\mathrm{mean}} = \frac{1}{l_c}\int_0^{l_c} \tau_{wr_0}\, dz \ . \tag{49}$$

Therefore the heat quantity $2\pi r_0 h_c \lambda_w \tau_{wr_0\mathrm{mean}}$ flows away from the surface of the rotating axle and in the case where the iron core is not connected to the axle, but surrounded by the cooling medium directly, the flowing heat quantity is $2\pi r_0 l_0 \lambda \tau_{h_c}$.

If the heat quantities described above are equal to each other referring to two cases where one is conducted through the rotating axle and the other is directly diffused into the cooling medium, the formula can be written as follows;

$$\lambda = \frac{\tau_{wr_0\,\mathrm{mean}}}{\tau_{h_c}} \frac{h_k}{l_0} \lambda_w \ . \tag{50}$$

The temperature of the armature with Newton's constant λ above mentioned could be calculated as if the armature were not connected to the shaft, even in the case where the armature is connected to the shaft directly or indirectly.

(4) EFFECT OF VENTILATING DUCTS.

Up to present, the heat flow to be conducted radially to the armature core only is considered, though there is the heat flow axially conducted. Therefore the effect of the axial heat flow exerted upon the radial heat flow must be calculated.

The axial temperature gradient causes the axial heat flow which is conducted perpendicularly to the sheet iron pile and is diffused from the ventilating ducts. At the middle part in the sheet A in Fig. 5 of the machine core the temperature is the highest. The radial and axial heat flows of A are considered to be as shown in Fig. 6(a) and (b).

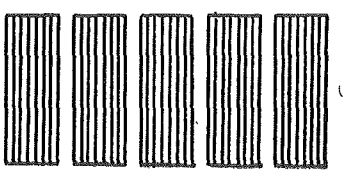

Fig. 5.

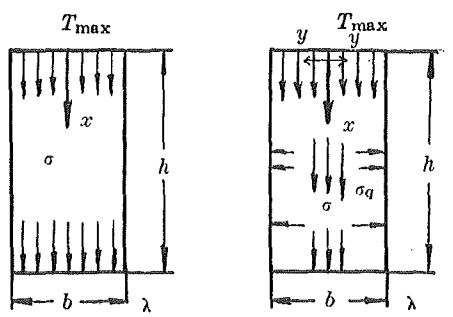

Fig. 6.

λ = Newton's constant.
σ = thermal conductivity of the sheet iron.
σ_q = thermal conductivity in the direction forward the sheet iron piles.
T = temperature in the sheet iron pile.

Referring to the heat flow shown in Fig. 6(a), the equation becomes

$$\frac{\partial^2 T}{\partial x^2} = 0 .$$

The boundary conditions are such that

$$\text{at} \quad x = 0 , \quad T = T_{\max}$$

and

$$x = h , \quad \frac{\partial T}{\partial x} = \frac{\lambda}{\sigma}(T_0 - T) .$$

Therefore the temperature distribution in the radial direction

$$T = \frac{\frac{\lambda}{\sigma}(T_0 - T_{\max})}{1 + \frac{\lambda}{\sigma} h} x + T_{\max} .$$

Referring to the heat flow shown in Fig. 6(b), the equation becomes

$$\frac{\partial^2 T}{\partial x^2} + \frac{\partial^2 T}{\partial y^2} = 0 ,$$

and boundary conditions are

(i) $$\text{at} \quad x = x , \quad y = \pm \frac{1}{2} b ,$$

$$\mp \frac{\partial \tau}{\partial y} = \frac{\lambda}{\sigma_q} \tau ,$$

(ii) $$\text{at} \quad x = 0 , \quad y = y ,$$

$$T = T_{\max} ,$$

where $\tau = T - T_0$

From the above boundary conditions, the equation is solved as follows

$$T = (T_{\max} - T_0)\, e^{-2n_\nu \frac{h}{b} \frac{x}{h}} \cos n_\nu \frac{2}{b} y + T_0$$

$$n_\nu \tan n_\nu = \frac{\lambda}{\sigma_q}\frac{b}{2}$$

$$n_\nu = n_1,\ n_2,\ n_3,\ \ldots\ldots\ .$$

This formula represents the radial temperature distribution where the axial heat flow exists only in the sheet iron pile.

The temperature gradient

$$\frac{T_{\max}-[T]_{x=h}}{h} \qquad \text{at} \qquad y=0\ ,$$

is deduced from the formula for the radial or axial heat flow only. Referring to the radial heat flow, the formula is obtained

$$(T_{\max}-T_0)\frac{\lambda}{\sigma}\frac{1}{1+\frac{\lambda}{\sigma}h} \qquad \ldots\ldots\ldots\ldots\ldots\ldots\ldots\ldots\ (a)$$

and to the axial heat flow,

$$(T_{\max}-T_0)\frac{1}{h}e^{-2n_\nu\frac{h}{b}}\ . \qquad \ldots\ldots\ \ldots\ldots\ldots\ldots\ (b)$$

The temperature gradient (a) is larger than (b) because the formula (a) represents the radial heat flow and the formula (b) represents the axial heat flow, therefore, if both heat flows exist, the temperature gradient may be described as follows :—

$$(T_{\max}-T_0)\left[\frac{\frac{\lambda}{\sigma}}{1+\frac{\lambda}{\sigma}h}+\frac{e^{-2n_\nu\frac{h}{b}}}{h}\right]. \qquad \ldots\ldots\ldots\ldots\ (c)$$

Formula (c) represents the temperature gradient where the radial and axial heat flows exist in the sheet iron pile. The ratio of the formulae (a) and (c) is

$$f_1 = \frac{1}{1+\frac{1+\frac{\lambda}{\sigma}h}{\frac{\lambda}{\sigma}h}e^{-2n_\nu\frac{h}{b}}}$$

f_1 is the factor of the ventilating ducts.

Example

$\lambda_1 = 0.004$ watt/cm², °C
$\sigma = 0.466$ watt/cm, °C
$\sigma_q = 0.0245$,, } for M-sheet
$b = 4.5$ cm $\lambda = 0.006$ watt/cm², °C.

$$n_\nu \tan n_\nu = 0.368$$
$$n_\nu \fallingdotseq 0.61$$
$$f_1 \fallingdotseq 0.9$$

(5) NUMERICAL EXAMPLE.

Synchronous alternator at the hydro-electric power station for railway service.

phase	3
capacity	31,000 kVA
voltage	11,000 V
revolution	150 r.p.m.
frequency	50 cycle/sec.
rotor peripheral speed	54.5 m/sec.

Loss at each part of the machine.

iron loss of stator	200 kW
copper loss of stator	155 kW
copper loss of rotor	133 kW
stray load loss	50 kW

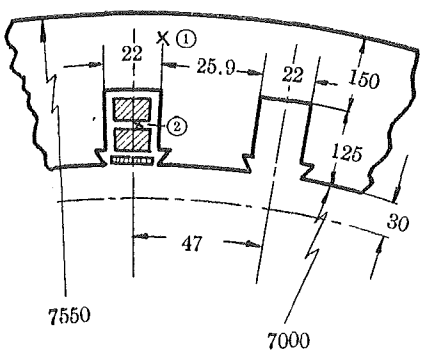

Stator dimenson.

Fig. 7.

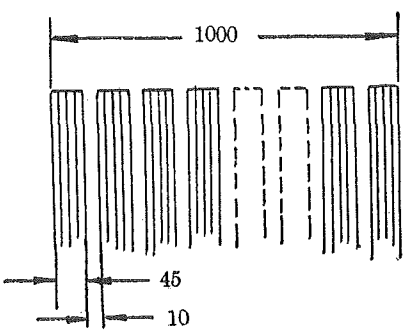

Fig. 8.

[A] TEMPERATURE OF CORE.

slot pitch	$\lambda_s = 4.7$ cm
core height	$h_c = 15$ cm

Temperatures at each part :—

$$T_0 = 20°C \qquad T'_p = 75°C \qquad T''_p = 68°C$$

Although the base temperature adopted by the International Committee is 40°C, one takes for the base temperature $T_0 = 20°C$ at which the measurement is carried out practically. The temperature rise of slot at the spot marked with ② in Fig. 7 measured 50°C by means of the search coil resistance method which is considered to give the temperature 5°C lower than the real one. Therefore the temperature of slot T'_p was estimated at 75°C. Also, the temperature rise of core at the spot marked with ① in Fig. 7 measured 27~28°C by means of mercury thermometer through which correction of +10°C is wanted. Therefore one estimates the temperature of core marked ① at 57~58°C. These experimental results being compared with the calculated results, one finds a quite good coincidence.

Newton's constant at the slot insulation is deduced from the curve as shown in Fig. 9 which represents the relation between the thermal

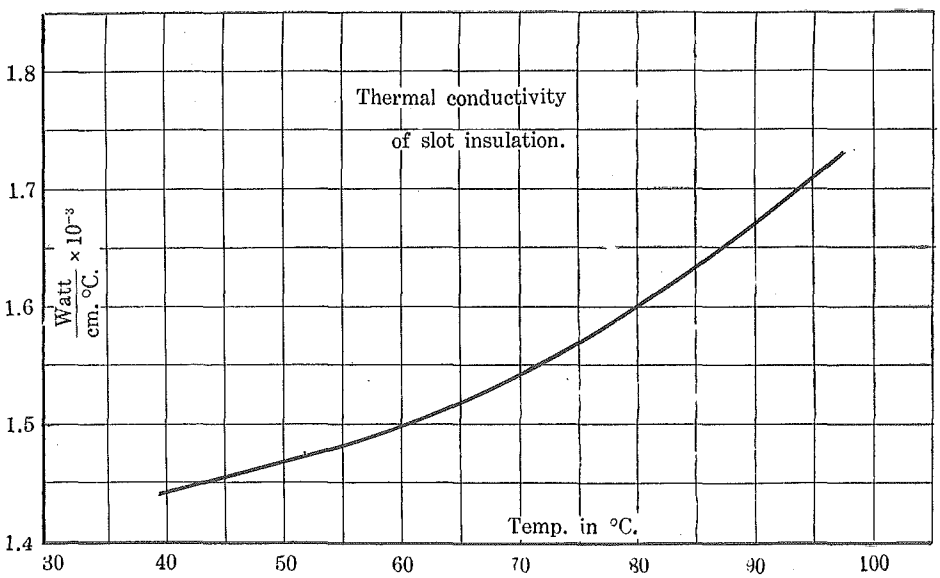

Fig. 9.

conductivity of the slot insulating material and the temperature of the slot conductors. From the curve, Newton's constant at the slot insulation is taken as follows :—

(thickness of slot insulation = 10 mm)

$$\lambda_{s,c} = 1.57 \times 10^{-3} \text{ watt/cm}^2, \ ^\circ\text{C}.$$

Referring to the circumference of the slot, the Newton's constant is

$$1.57 \times 10^{-3} \times (12.5 \times 2 + 2.2) = 4.32 \times 10^{-2} \text{ watt/cm}^2, \ ^\circ\text{C}.$$

The thermal conductivity of the core-sheet (class *M*-sheet) is taken as

$$\sigma_c = 0.466 \text{ watt/cm}, \ ^\circ\text{C}.$$

which is the value taken in the radial direction, and the sheet iron is painted twice with insulating varnish (class A-varnish). The back surface of the stator core directly faces the air and the end surface of the sheet iron packet is in contact with the air through the varnish layer which is coated on the sheet iron. Therefore the heat development in the core is considered to diffuse radially in the core and dissipate in the air from the core back surface.

Newton's constant is taken at the core back surface

$$\lambda_{c,0} = 0.006 \quad \text{watt/cm}^2, \ ^\circ\text{C}.$$

The magnetic flux density is designed as

$$B_{\text{core}} = 12{,}000 \quad \text{lines/cm}^2,$$
$$B_{\text{teeth}} = 16{,}000 \quad \text{lines/cm}^2.$$

Therefore, the ratio of the iron loss is approximately expressed by

$$1.2^{1.6} : 1.6^{1.6} = 1.34 : 2.12 \ .$$

The volume ratio of the slot and teeth is

$$22 : 25.9 \ .$$

Now it is assumed approximately that the density of the iron loss in the teeth is twice larger than that of the iron core, because the volumes of the teeth and the slot are nearly equal to each other, and the no-load losses are considered to be uniformly distributed in the total volume of the armature containing the teeth and slot.

The net volume of armature

$$\frac{4}{\pi}(755^2-700^2)4.5\times 18\times 0.8 = 4\times 10^6\,\mathrm{cm}^3$$

The total iron loss in the stator is measured at the rotating machine factory after the machine is fully constructed and its value is

$$200\ \mathrm{kW}$$

so the loss density in the core is

$$0.05\ \mathrm{watt}/\mathrm{cm}^3$$

$$C_1 = -0.5 \qquad C_2 = 65$$

$$f_1(x) = 2\left(1-\frac{x}{15}\right)^{3.6}-0.5x+6.5\ .$$

The mean temperature distribution in the radial direction is described in Fig. 10.

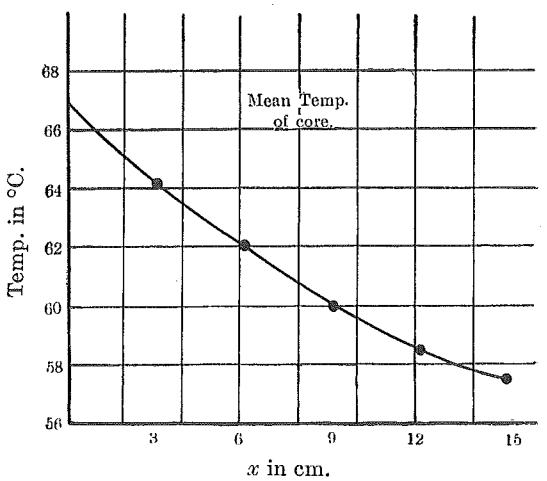

Fig. 10.

Next, the term of the temperature fluctuation $T_{c,f}$ which corresponds to the temperatures of slot and teeth can be calculated from the formula (20).

From the formula (17)

$$T_{c,d} = 2+65-68 = -1°\mathrm{C}.$$

Then,

$$T_{c,f} = \frac{4}{\pi} \sum e^{-1.34(2n+1)x} \frac{\sin 1.34(2n+1)y}{(2n+1)} .$$

From the above formula, the fluctuated temperature is obtained as shown in Fig. 11 which represent the percentage temperature.

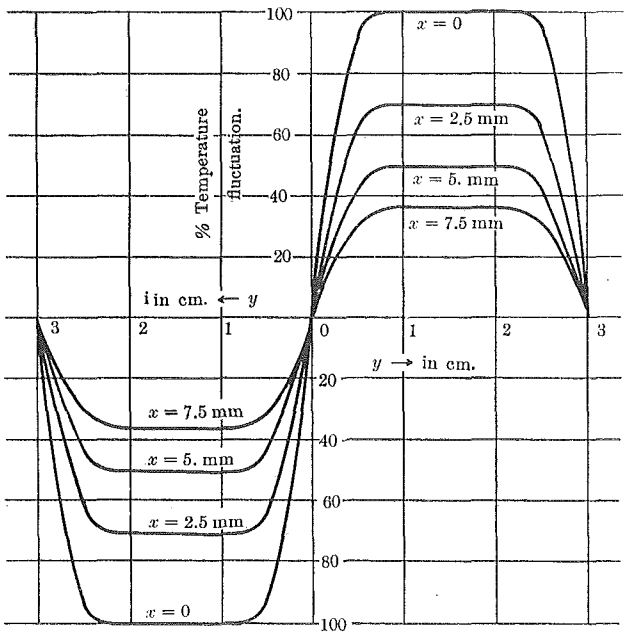

Fig. 11.

[B] THE TEMPERATURE OF TEETH.

$$h_t = 12.5 \text{ cm} , \qquad b_t = 2.6 \text{ cm} ,$$

$$\sigma_t = 0.466 \text{ . watt/cm, C°.}$$

$$\lambda_{s,t} = 1.57 \times 10^{-3} \quad \text{watt/cm}^2, \ ^\circ\text{C.}$$

Newton's constant $\lambda_{t,0}$, facing the air gap is taken to be

$$\lambda_{t,0} = 0.007 \quad \text{watt/cm}^2 , \ ^\circ\text{C.}$$

which is taken in the case where the peripheral speed of the rator is 54.5 m/sec.

$$[T_c]_{x=0} = 67°\text{C.}, \qquad T_p' = 75°\text{C.},$$

$$Q_t = 0.1 \quad \text{watt/cm}^3,$$

$$\mu\pi \tan \mu\pi = \frac{1.57 \times 10^{-3}}{0.466 \times 0.9} \times \frac{2.6}{2} = 4.86 \times 10^{-3},$$

$$\mu\pi \fallingdotseq 0.07,$$

$$\mu = 0.0223, \qquad \nu = 0.0538,$$

$$A = 0.545.$$

K_1 and K_2 are calculated from the above constants;

$$K_1 = 1.33, \qquad K_2 = 0.8.$$

Hence, the constants A_ν and B_ν are

$$A_\nu = 9.3 \qquad B_\nu = -16.7$$

From the above numerical values, the functions $F_1(x)$, $\phi_i(x)$ and $\psi_i(y)$ may be calculated as shown in Fig. 12 the temperature distribution in the teeth is described in Fig. 12 with a curve which is increasing with x.

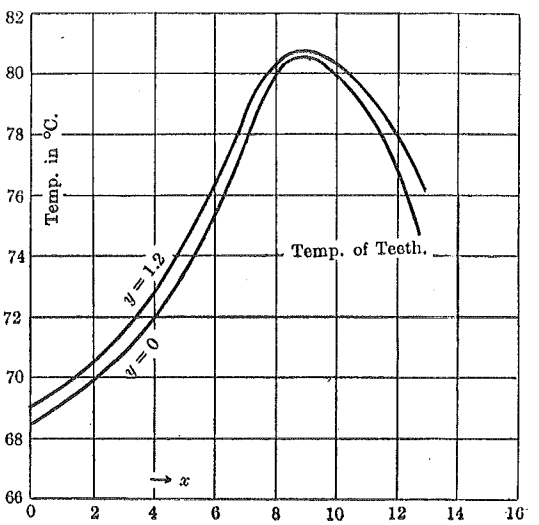

Fig. 12.

CHAPTER III.

TEMPERATURE DISTRIBUTION IN THE AXIAL DIRECTION.

In the preceding chapter the radial heat flow in the armature alone has been treated. As the end of the armature faces directly or indirectly toward the cooling medium, the inner temperature of the armature must be estimated taking into consideration both the radial and the axial heat flows.

Since the laminated sheet irons by means of which the iron core of the armature is constructed, are piled up in the direction of the axle, the thermal conductivity of the iron core in the axial direction is lower than that of the radial direction. However, referring to the copper conductors inserted into the slot, the thermal conductivity of the slot conductors in the axial direction is higher than that in the radial direction, because the insulating materials by which the slot conductors are surrounded, disturb the radial heat flow. Therefore if the two kinds of radial and axial heat flows are compared with each other, the slot temperature estimated only from the radial flow may be too much higher; on the contrary the temperature of the teeth and the iron core similarly estimated may be too much lower than that only from the axial flow.

(1) MATHEMATICAL TREATMENT.

In the calculation of the axial heat flow, the following notations are used:—

q = sectional area in cm^2,
u = peripheral length in cm,
Q = power loss in $watt/cm^3$,
α = temperature coefficient of the slot conductor in $°C^{-1}$,
σ = thermal conductivity in watt/cm, °C.

The slot conductor is expressed with the suffix s, the end connector with e, the teeth with t, and the iron core with c. Thus the temperature of the slot conductor is denoted by T_s, that of the teeth by T_t, that of the iron core by T_c, and the end connector by T_e. Then the relations about the heat flow between the four parts of the machine are expressed by the four equations (1), (2), (3) and (4).

With reference to the slot conductor, it follows

$$(1)\qquad Q_s q_s(1+\alpha T_s)+\sigma_s q_s\frac{d^2T_s}{dz^2}=\lambda_{s,t}u_{s,t}(T_s-T_t)+\lambda_{s,c}u_{s,c}(T_s-T_c)+\lambda_{s,0}u_{s,0}(T_s-T_0)\,.$$

The first and the second terms in the left hand of the equation indicate the heat developed and the heat conducted in the slot respectively, and the first, the second and the third terms of the right hand of the equation indicate the heat flow over the boundaries between the slot and the teeth, the slot and the core, and also the slot and the outer cooling medium respectively.

Similarly equations (2), (3) and (4) are written in the similar manner as shown in expression (1),

$$(2)\qquad Q_t q_t+\lambda_{s,t}u_{s,t}(T_t-T_s)+\sigma_q q_t\frac{d^2T_t}{dz^2}=b_t\lambda_{t,c}(T_t-T_c)+\lambda_{t,0}u_{t,0}(T_t-T_0)$$

$$(3)\qquad Q_c q_c+\lambda_{s,c}u_{s,c}(T_c-T_s)+\sigma_q q_c\frac{d^2T_c}{dz^2}+\lambda_{t,c}u_{t,c}(T_c-T_t)=\lambda_{c,0}u_{c,0}(T_c-T_0)$$

$$(4)\qquad Q_e q_e(1+\alpha T_e)+\sigma_e q_e\frac{d^2T_e}{dz^2}=\lambda_{e,0}u_{e,0}(T_e-T_0)$$

where

σ_q = thermal conductivity of iron core in the direction perpendicular to the plane of sheet iron,
$u_{s,t}$ = boundary surface between the slot and the teeth,
$u_{s,c}$ = boundary surface between the slot and the iron core,
$u_{s,0}$ = boundary surface between the slot and the cooling air.

These notations are shown in the section of armature axis shown in Fig. 13.

In order to simplify the equation, put

$$(5)\qquad \begin{cases} u_s=u_e=u_{s,t}+u_{s,c}+u_{s,0}\,, \\ \tau_s=T_s-T_0\,, \qquad \tau_t=T_t-T_0\,, \\ \tau_c=T_c-T_0\,, \qquad \tau_e=T_e-T_0\,, \end{cases}$$

and

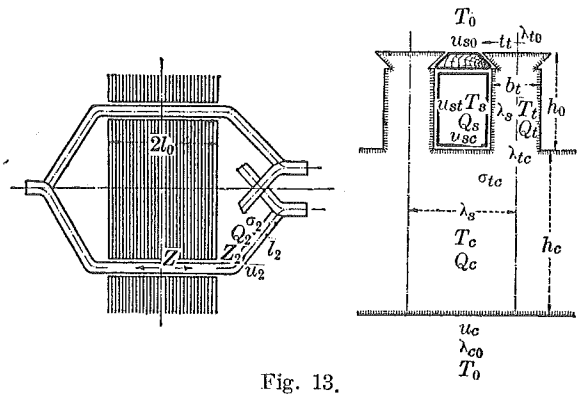

Fig. 13.

$$
(6)\quad
\begin{cases}
a_s^2 = \dfrac{\lambda_s u_s - Q_s q_s \alpha}{\sigma_s q_s}\,, \qquad b_s = \dfrac{\lambda_s u_{s,t}}{\sigma_s q_s}\,, \qquad c_s = \dfrac{\lambda_s u_{s,c}}{\sigma_s q_s} \\
d_s = \dfrac{Q_s}{\sigma_s}(1+\alpha T_0)\,, \\
a_t^2 = \dfrac{-\lambda_s u_{s,t} + \lambda_{t,c} b_t + \lambda_{t,0} u_{t,0}}{\sigma_q q_t}\,, \qquad b_t = \dfrac{-\lambda_s u_{s,t}}{\sigma_q q_t}\,, \\
c_t = \dfrac{\lambda_{t,c} u_{t,c}}{\sigma_q q_t}\,, \qquad d_t = \dfrac{Q_t}{\sigma_q}\,, \\
a_c^2 = \dfrac{-\lambda_s u_{s,c} - \lambda_{t,c} u_{t,c} + \lambda_{c,0} u_{c,0}}{\sigma_q q_c}\,, \qquad b_c = \dfrac{-\lambda_s u_{s,c}}{\sigma_q q_c}\,, \\
c_c = \dfrac{-\lambda_{t,c} u_{t,c}}{\sigma_q q_c}\,, \qquad d_c = \dfrac{Q_c}{\sigma_q}\,.
\end{cases}
$$

Then equations (1), (2), (3) and (4) reduce to the following,

$$
(7)\quad \frac{d^2\tau_s}{dz^2} - a_s^2\tau_s = -f_s(z)\,, \qquad f_s(z) = b_s\tau_t + c_s\tau_c + d_s\,,
$$

$$
(8)\quad \frac{d^2\tau_t}{dz^2} - a_t^2\tau_t = -f_t(z)\,, \qquad f_t(z) = b_t\tau_s + c_t\tau_c + d_t\,,
$$

$$
(9)\quad \frac{d^2\tau_c}{dz^2} - a_c^2\tau_c = -f_c(z)\,, \qquad f_c(z) = b_c\sigma_s + c_c\tau_t + d_c\,.
$$

To solve equations (7), (8) and (9), take as the first approximation the following equation;

$$
\frac{d^2\tau_s}{dz^2} - a_s^2\tau_s = 0\,,
$$

$$\frac{d^2\tau_t}{dz^2}-a_t^2\tau_t=0\ ,$$

$$\frac{d^2\tau_c}{dz^2}-a_c^2\tau_c=0\ ,$$

then the solution is

$$\text{(10)}\qquad \begin{cases} \tau_s = A_s e^{a_s z}+B_s e^{-a_s z}\ , \\ \tau_t = A_t e^{a_t z}+B_t e^{-a_t z}\ , \\ \tau_c = A_c e^{a_c z}+B_c e^{-a_c z}\ . \end{cases}$$

The differential equations (7), (8) and (9) can be transformed into Volterra's integral equations by making use of the first approximations.[1)]

$$\text{(11)}\qquad \tau_s = \frac{d_s}{a_s^2}+\left(A_s-\frac{d_s}{2a_s^2}\right)e^{a_s z}+\left(B_s-\frac{d_s}{2a_s^2}\right)e^{-a_s z}$$
$$-\int_0^z \frac{b_s}{2a}\left[e^{a_s(z-\xi)}-e^{-a_s(z-\xi)}\right]\tau_t(\xi)\,d\xi$$
$$-\int_0^z \frac{c_s}{2a_s}\left[e^{a_s(z-\xi)}-e^{-a_s(z-\xi)}\right]\tau_c(\xi)\,d\xi\ ,$$

$$\text{(12)}\qquad \tau_t = \frac{d_t}{a_t^2}+\left(A_t-\frac{d_t}{2a_t^2}\right)e^{a_t z}+\left(B_t-\frac{d_t}{2a_t^2}\right)e^{-a_t z}$$
$$-\int_0^z \frac{b_t}{2a_t}\left[e^{a_t(z-\xi)}-e^{-a_t(z-\xi)}\right]\tau_s(\xi)\,d\xi$$
$$-\int_0^z \frac{c_t}{2a_t}\left[e^{a_t(z-\xi)}-e^{-a_t(z-\xi)}\right]\tau_c(\xi)\,d\xi\ ,$$

$$\text{(13)}\qquad \tau_c = \frac{d_c}{a_c^2}+\left(A_c-\frac{d_c}{2a_c^2}\right)e^{a_c z}+\left(B_c-\frac{d_c}{2a_c^2}\right)e^{-a_c z}$$
$$-\int_0^z \frac{b_c}{2a_c}\left[e^{a_c(z-\xi)}-e^{-a_c(z-\xi)}\right]\tau_s(\xi)\,d\xi$$
$$-\int_0^z \frac{c_c}{2a_c}\left[e^{a_c(z-\xi)}-e^{-a_c(z-\xi)}\right]\tau_t(\xi)\,d\xi\ .$$

1) Yosirô Ikeda: Memoirs of Faculty of Engineering, Hokkaidô Imperial University, Vol. 1. (1928) pp. 193-209.

Put

$$\varphi_s(z) = \frac{d_s}{a_s^2} + A_s' \cosh a_s z\,, \qquad A_s' = A_s - \frac{d_s}{2a_s^2}\,, \tag{14}$$

$$\varphi_t(z) = \frac{d_t}{a_t^2} + A_t' \cosh a_t z\,, \qquad A_t' = A_t - \frac{d_t}{2a_t^2}\,, \tag{15}$$

$$\varphi_c(z) = \frac{d_c}{a_c^2} + A_c' \cosh a_c z\,, \qquad A_c' = A_c - \frac{d_c}{2a_c^2}\,. \tag{16}$$

As A and B are symmetrical to each other, $A = B$.

Putting

$$\left\{\begin{aligned}
K_{s,t}(z,\xi) &= -\frac{b_s}{2a_s}\left[e^{a_s(z-\xi)} - e^{-a_s(z-\xi)}\right],\\
K_{s,c}(z,\xi) &= -\frac{c_s}{2a_s}\left[e^{a_s(z-\xi)} - e^{-a_s(z-\xi)}\right],\\
K_{t,s}(z,\xi) &= -\frac{b_t}{2a_t}\left[e^{a_t(z-\xi)} - e^{-a_t(z-\xi)}\right],\\
K_{t,c}(z,\xi) &= -\frac{c_t}{2a_t}\left[e^{a_t(z-\xi)} - e^{-a_t(z-\xi)}\right],\\
K_{c,s}(z,\xi) &= -\frac{b_c}{2a_c}\left[e^{a_c(z-\xi)} - e^{-a_c(z-\xi)}\right],\\
K_{c,t}(z,\xi) &= -\frac{c_c}{2a_c}\left[e^{a_c(z-\xi)} - e^{-a_c(z-\xi)}\right],
\end{aligned}\right. \tag{17}$$

the following integral equations will be written

$$\tau_s = \varphi_s(z) + \int_0^z K_{s,t}(z,\xi)\tau_t(\xi)\,d\xi + \int_0^z K_{s,c}(z,\xi)\tau_c(\xi)\,d\xi\,, \tag{18}$$

$$\tau_t = \varphi_t(z) + \int_0^z K_{t,s}(z,\xi)\tau_s(\xi)\,d\xi + \int_0^z K_{t,c}(z,\xi)\tau_c(\xi)\,d\xi\,, \tag{19}$$

$$\tau_c = \varphi_c(z) + \int_0^z K_{c,s}(z,\xi)\tau_s(\xi)\,d\xi + \int_0^z K_{c,t}(z,\xi)\tau_t(\xi)\,d\xi\,. \tag{20}$$

If the resolvents $S_{s,s}$, $S_{s,t}$, $S_{s,c}$, ... of the kernels, $K_{s,s}$, $K_{s,t}$, ... are known respectively, the solutions will be

$$\begin{aligned}\tau_s = \varphi_s(z) &- \int_0^z S_{t,s}(z,\xi)\varphi_t(\xi)\,d\xi - \int_0^z S_{c,s}(z,\xi)\varphi_c(\xi)\,d\xi\\ &- \int_0^z S_{s,s}(z,\xi)\varphi_s(\xi)\,d\xi\,,\end{aligned} \tag{21}$$

$$(22)\qquad \tau_t = \varphi_t(z) - \int_0^z S_{t,t}(z,\xi)\varphi_t(\xi)d\xi - \int_0^z S_{c,t}(z,\xi)\varphi_c(\xi)d\xi - \int_0^z S_{s,t}(z,\xi)\varphi_s(\xi)d\xi ,$$

$$(23)\qquad \tau_c = \varphi_c(z) - \int_0^z S_{t,c}(z,\xi)\varphi_t(\xi)d\xi - \int_0^z S_{c,c}(z,\xi)\varphi_c(\xi)d\xi - \int_0^z S_{s,c}(z,\xi)\varphi_s(\xi)d\xi .$$

Though the solutions are very complicated, terms necessary for the practical application can be easily obtained.

For example, if the first order is taken as

$$S_{t,t} = 0 , \qquad S_{c,c} = 0 , \qquad S_{s,s} = 0 ,$$

$$S_{t,c} = \frac{c_t}{a_t}\sinh a_t(z-\xi) , \qquad S_{c,t} = \frac{c_c}{a_c}\sinh a_c(z-\xi) ,$$

$$S_{s,t} = \frac{b_s}{a_s}\sinh a_s(z-\xi) , \qquad S_{t,s} = \frac{b_t}{a_t}\sinh a_t(z-\xi) ,$$

$$S_{c,s} = \frac{b_c}{a_c}\sinh a_c(z-\xi) , \qquad S_{s,c} = \frac{c_s}{a_s}\sinh a_s(z-\xi) ,$$

the solutions will be

$$(24)\qquad \tau_s = \frac{d_s}{a_s^2} + \frac{d_t}{a_t^2}\frac{b_t}{a_t^2}(1-\cosh a_t z) - \frac{d_c}{a_c^2}\frac{b_c}{a_c^2}(1-\cosh a_c z) + A_s' \cosh a_s z - A_t'\frac{b_t}{2a_t} z\sinh a_t z - A_c'\frac{b_c}{2a_c} z\sinh a_c z ,$$

$$(25)\qquad \tau_t = \frac{d_t}{a_t^2} + \frac{d_s}{a_s^2}\frac{b_s}{a_s^2}(1-\cosh a_s z) + \frac{d_c}{a_c^2}\frac{c_c}{a_c^2}(1-\cosh a_c z) + A_t' \cosh a_t z - A_s'\frac{b_s}{2a_s} z\sinh a_s z - A_c'\frac{c_c}{2a_c} z\sinh a_c z ,$$

$$\tau_c = \frac{d_c}{a_c^2} + \frac{d_s}{a_s^2}\frac{c_s}{a_s^2}(1-\cosh a_s z) \tag{26}$$

$$+\frac{d_t}{a_t^2}\frac{c_t}{a_t^2}(1-\cosh a_t z)+A_c' \cosh a_c z$$

$$-A_s'\frac{c_s}{2a_s} z \sinh a_s z - A_t'\frac{c_t}{2a_t} z \sinh a_t z \ .$$

(2) BOUNDARY CONDITIONS.

Integration constants A_s', A_t' and A_c' are determined from the boundary conditions, τ_s, τ_t and τ_c consist of six terms, in which the first three terms do not depend on the boundary conditions, but on three kinds of heat source, in the slot, the teeth and the iron core respectively, while the latter three terms depend on the boundary conditions i.e. :— their values are determined from the cooling conditions at the boundaries.

The temperature of the end connector τ_e can be solved as it depends on the slot temperature τ_s alone at the boundary. Therefore from (4), the equation is obtained :—

$$\frac{d^2\tau_e}{dz^2} = a_e^2 \tau_e - d_e \ , \tag{27}$$

and the solution of (27) is

$$\tau_e = \frac{d_e}{a_e^2} + A_e \cosh a_e z + B_e \sinh a_e z \ , \tag{28}$$

where

$$a_e^2 = \frac{\lambda_e u_e - Q_e q_e \alpha}{\sigma_e q_e} \ , \qquad d_e = \frac{Q_e}{\sigma_e}(1+\alpha T_0) \ . \tag{29}$$

Since the temperature of the end connector should be minimum at the middle part of the end connector, the condition

$$\left[\frac{d\tau_e}{dz}\right]_{z=l_e} = 0$$

is established. Therefore

$$B_e = -A_e \tanh a_e l_e \ .$$

Substitute B_e in (28), then

$$\tau_e = \frac{d_e}{a_e^2} + A_e[\cosh a_e z - \tanh a_e l_e \sinh a_e z] \tag{30}$$

Constants A_s', A_t', A_c' and A_e are determined from the following boundary conditions.

(i) at $z = \pm l_0$ $\quad \frac{d\tau_t}{dz} \pm \frac{\lambda_{t,z}}{\sigma_q}\tau_t = 0$,

where l_0 means half axial length of the armature.

(ii) at $z = \pm l_0$ $\quad \frac{d\tau_0}{dz} \pm \frac{\lambda_{c,z}}{\sigma_q}\tau_t = 0$.

By these conditions it means that Newton's cooling law holds at the side surface of the armature.

(iii) $$\left[\frac{d\tau_s}{dz}\right]_{z_s=l_0} = \left[\frac{d\tau_e}{dz}\right]_{z_e=0} .$$

(iv) $$[\tau_s]_{z_s=l_0} = [\tau_e]_{z_e=0} .$$

Boundary conditions (iii) and (iv) hold at the boundary surface between the slot conductor and the end connector.

Four unknown constants are determined from the four boundary conditions above described.

For expressing the values of the constants A_s', A_t', A_c' and A_e in simple forms, the following notations are used

$$D_1 = \frac{\lambda_{t,z}}{\sigma_q}\left[\frac{d_t}{a_t^2} + \frac{d_s}{a_s^2}\frac{b_s}{a_s^2}(1-\cosh a_s l_0) + \frac{d_c}{a_c^2}\frac{c_c}{a_c^2}(1-\cosh a_c l_0)\right]$$
$$- \frac{d_s}{a_s^2}\frac{b_s}{a_s^2} a_s \sinh a_s l_0 - \frac{d_c}{a_c^2}\frac{c_c}{a_c^2} a_c \sinh a_c l_0 ,$$

$$D_2 = \frac{\lambda_{c,z}}{\sigma_q}\left[\frac{d_c}{a_c^2} + \frac{d_s}{a_s^2}\frac{c_s}{a_s^2}(1-\cosh a_s l_0) + \frac{d_t}{a_t^2}\frac{c_t}{a_t^2}(1-\cosh a_t l_0)\right]$$
$$- \frac{d_s}{a_s^2}\frac{c_s}{a_s^2} a_s \sinh a_s l_0 - \frac{d_t}{a_t^2}\frac{c_t}{a_t^2} a_t \sinh a_t l_0 ,$$

$$D_3 = \frac{d_t}{a_t^2}\frac{b_t}{a_t^2} a_t \sinh a_t l_0 + \frac{d_c}{a_c^2}\frac{b_c}{a_c^2} a_c \sinh a_c l_0 ,$$

$$D_4 = \frac{d_s}{a_s^2}+\frac{d_t}{a_t^2}\frac{b_t}{a_t^2}(1-\cosh a_t l_0)+\frac{d_c}{a_c}\frac{b_c}{a_c^2}(1-\cosh a_c l_0)-\frac{d_e}{a_e^2},$$

$$B_{t,t} = \frac{\lambda_{t,z}}{\sigma_q}\cosh a_t l_0 + a_t \sinh a_t l_0 ,$$

$$B_{t,c} = \frac{\lambda_{t,z}}{\sigma_q}\frac{c_c}{a_c^2} l_0 \sinh a_c l_0 + \frac{c_c}{2a_c}(\sinh a_c l_0 + a_c l_0 \cosh a_c l_0) ,$$

$$B_{t,s} = \frac{\lambda_{t,z}}{\sigma_q}\frac{b_s}{2a_s^2} l_0 \sinh a_s l_0 + \frac{b_s}{2a_s}(\sinh a_s l_0 + a_s l_0 \cosh a_c l_0) ,$$

$$B_{c,t} = \frac{\lambda_{c,z}}{\sigma_q}\frac{c_t}{2a_t} l_0 \sinh a_t l_0 + \frac{c_t}{2a_t}(\sinh a_t l_0 + a_t l_0 \cosh a_t l_0) ,$$

$$B_{c,c} = \frac{\lambda_{c,z}}{\sigma_q}\cosh a_c l_0 + a_c \sinh a_c l_0 ,$$

$$B_{c,s} = \frac{\lambda_{c,z}}{\sigma_q}\frac{c_s}{2a_s} l_0 \sinh a_s l_0 + \frac{c_s}{2a_s}(\sinh a_s l_0 + a_s l_0 \cosh a_s l_0) ,$$

$$B_{s,t} = \frac{b_t}{2a_t}(\sinh a_t l_0 + a_t l_0 \cosh a_t l_0) , \qquad B_{s,s} = a_s \sinh a_s l_0 ,$$

$$B_{s,c} = \frac{b_c}{2a_c}(\sinh a_c l_0 + a_c l_0 \cosh a_c l_0) , \qquad B_{s,e} = a_e \tanh a_e l_0 ,$$

$$B_{e,t} = \frac{b_t}{2a_t} l_0 \sinh a_t l_0 , \qquad B_{e,c} = \frac{b_c}{2a_c} l_0 \sinh a_c l_0 ,$$

$$B_{e,s} = \cosh a_s l_0 .$$

Further put

$$\begin{aligned}\Delta &= (B_{t,c}B_{c,t}-B_{t,t}B_{c,c})(B_{s,s}+B_{e,s}B_{s,e})\\ &\quad +(B_{t,s}B_{c,t}+B_{t,t}B_{c,s})(B_{s,c}+B_{s,e}B_{e,c})\\ &\quad +(B_{t,c}B_{c,s}+B_{t,s}B_{c,c})(B_{s,t}+B_{e,t}B_{s,e}) ,\end{aligned}$$

$$\begin{aligned}\Delta_t &= D_1[B_{c,c}(B_{s,s}+B_{s,e}B_{e,s})-B_{c,s}(B_{s,c}+B_{s,e}B_{e,c})]\\ &\quad +D_2[B_{t,c}(B_{s,s}+B_{s,e}B_{e,s})+B_{t,s}(B_{s,c}+B_{e,c}B_{s,e})]\\ &\quad +D_3[B_{t,c}B_{c,s}+B_{t,s}B_{c,c}]+D_4[B_{t,c}B_{c,s}+B_{t,s}B_{c,c}]B_{s,e} ,\end{aligned}$$

$$\begin{aligned}\Delta_c &= D_1[B_{c,t}(B_{s,e}+B_{s,e}B_{e,s})+B_{c,s}(B_{s,t}+B_{s,e}B_{e,t})]\\ &\quad +D_2[B_{t,t}(B_{s,s}+B_{s,e}B_{e,s})-B_{t,s}(B_{s,t}+B_{s,e}B_{e,t})]\\ &\quad +D_3(B_{t,t}B_{c,s}+B_{t,s}B_{c,t})+D_4(B_{t,t}B_{c,s}+B_{t,s}B_{c,t})B_{s,c} ,\end{aligned}$$

$$
\begin{aligned}
\Delta_s = {} & D_1[B_{c,c}(B_{s,t}+B_{s,e}B_{e,t})+B_{c,t}(B_{s,c}+B_{s,e}B_{e,c})] \\
& +D_2[B_{t,c}(B_{s,t}+B_{s,e}B_{e,t})+B_{t,t}(B_{s,c}+B_{s,e}B_{e,c})] \\
& -D_3[B_{t,c}B_{c,t}+B_{t,t}B_{c,c}]+D_4[B_{t,t}B_{c,c}-B_{t,c}B_{c,t}]B_{s,e}\ , \\
\Delta_e = {} & D_1[B_{c,c}(B_{s,t}B_{e,s}-B_{s,s}B_{e,t})+B_{c,s}(B_{s,c}B_{e,t}-B_{s,t}B_{e,c}) \\
& +B_{c,t}(B_{s,c}B_{e,s}-B_{s,s}B_{e,c})] \\
& +D_2[B_{t,c}(B_{s,t}B_{e,s}-B_{s,s}B_{e,t})+B_{t,s}(B_{e,c}-B_{s,c}B_{e,t}) \\
& +B_{t,t}(B_{s,c}B_{e,s}-B_{s,s}B_{e,c})] \\
& +D_3[B_{t,c}(B_{c,s}B_{e,t}+B_{e,s}B_{c,t})+B_{t,s}(B_{c,c}B_{e,t}+B_{e,c}B_{c,t}) \\
& +B_{t,t}(B_{c,s}B_{e,c}-B_{c,c}B_{c,s})] \\
& +D_4[B_{t,c}(B_{c,s}B_{s,t}+B_{s,s}B_{c,t})+B_{t,s}(B_{c,c}B_{s,t}+B_{c,t}B_{s,c}) \\
& +B_{t,t}(-B_{c,c}B_{s,s}+B_{s,c}B_{c,s})]\ .
\end{aligned}
$$

Lastly from the four boundary conditions:— (i), (ii), (iii) and (iv), by making use of these constants, it follows

$$
(31) \qquad \begin{cases} A'_s = \dfrac{\Delta_s}{\Delta}\ , & A'_t = \dfrac{\Delta_t}{\Delta}\ , \\ A'_c = \dfrac{\Delta_e}{\Delta}\ , & A'_e = \dfrac{\Delta_e}{\Delta}\ . \end{cases}
$$

(3) NO-LOAD AND SHORT CIRCUIT.

Four unknown constants have been found from the calculation above described. In the process of this calculation, constants D_1, D_2, D_3 and D_4 contain four kinds of heat source Q_t, Q_c, Q_s and Q_e. Again constants B, ... contain the thermal constant and the dimension of the armature.

In the case where the electric machine is running at no-load, the condition

$$d_s \fallingdotseq 0$$

may be established, because the copper loss in the slot conductor is approximately zero and the iron loss only exists in the teeth and the iron core. Thus it follows

$$(32)\quad \tau_s = \sigma_{t,1}\sigma_{t,2}(1-\cosh a_t z)+\sigma_{c,1}\sigma_{c,2}(1+\cosh a_c z)$$
$$+[A'_s]_{d_s=0}\cosh a_s z-[A'_t]_{d_s=0}\frac{\sigma_{t,2}}{2}a_t z\sinh a_t z$$
$$-[A'_c]_{d_s=0}\frac{\sigma_{c,2}}{2}a_c z\sinh a_c z\ ,$$

$$(33)\quad \tau_t = \sigma_{t,1}+\sigma_{c,1}\sigma_{c,3}(1-\cosh a_c z)$$
$$+[A'_t]_{d_s=0}\cosh a_t z-[A'_s]_{d_s=0}\frac{\sigma_{s,2}}{2}a_s z\sinh a_s z$$
$$-[A'_c]_{d_s=0}\frac{\sigma_{c,3}}{2}a_c z\sinh a_c z\ ,$$

$$(34)\quad \tau_c = \sigma_{c,1}+\sigma_{t,1}\sigma_{t,3}(1-\cosh a_t z)$$
$$+[A'_c]_{d_s=0}\cosh a_c z-[A'_s]_{d_s=0}\frac{\sigma_{s,3}}{2}a_s z\sinh a_s z$$
$$-[A'_t]_{d_s=0}\frac{\sigma_{t,3}}{2}a_t z\sinh a_t z\ ,$$

where

$$(35)\quad \begin{cases} \sigma_{s,1}=\dfrac{d_s}{a_s^2}\ , & \sigma_{t,1}=\dfrac{d_t}{a_t^2}\ , & \sigma_{c,1}=\dfrac{d_c}{a_c^2}\ , \\ \sigma_{t,2}=\dfrac{b_t}{a_t^2}\ , & \sigma_{c,2}=\dfrac{b_c}{a_c^2}\ , & \sigma_{s,2}=\dfrac{b_s}{a_s^2}\ , \\ \sigma_{c,3}=\dfrac{c_c}{a_c^2}\ , & \sigma_{s,3}=\dfrac{c_s}{a_s^2}\ , & \sigma_{t,3}=\dfrac{c_t}{a_t^2}\ . \end{cases}$$

$\sigma_{s,1}$, $\sigma_{t,1}$, and $\sigma_{c,1}$ are the functions referring to the heat sources Q_s, Q_t and Q_c respectively, which are also expressed by the terms d_s, d_t and d_c. $\sigma_{t,2}$, $\sigma_{t,3}$, $\sigma_{c,2}$, $\sigma_{c,3}$, $\sigma_{s,2}$ and $\sigma_{s,3}$ are constants referring to the thermal constants and the dimensions of the electric machine. $[A'_s]_{d_s=0}$, $[A'_t]_{d_s=0}$ and $[A'_c]_{d_s=0}$ are determined from the boundary conditions and might also contain the four kinds of heat source Q_s, Q_t, Q_c and Q_e.

In case of the short circuit where the iron losses are minimum in the iron core and the teeth, then

$$d_t \fallingdotseq 0\ , \qquad d_c \fallingdotseq 0\ , \qquad \therefore\ \ \sigma_{t,1}\fallingdotseq 0 \ \text{ and } \ \sigma_{c,1}\fallingdotseq 0\ .$$

Therefore

$$(36)\quad \tau_s = \sigma_{s,1} + [A'_s]_{\substack{d_t=0\\d_c=0}} \cosh a_s z - [A'_t]_{\substack{d_t=0\\d_c=0}} \frac{\sigma_{t,2}}{2} a_t z \sinh a_t z - [A'_c]_{\substack{d_t=0\\d_c=0}} \frac{\sigma_{c,2}}{2} a_c z \sinh a_c z ,$$

$$(37)\quad \tau_t = \sigma_{s,1}\sigma_{s,2}(1-\cosh a_s z) + [A'_t]_{\substack{d_t=0\\d_c=0}} \cosh a_t z - [A'_s]_{\substack{d_t=0\\d_c=0}} \frac{\sigma_{s,2}}{2} a_s z \sinh a_s z - [A'_c]_{\substack{d_t=0\\d_c=0}} \frac{\sigma_{c,3}}{2} a_c z \sinh a_c z ,$$

$$(38)\quad \tau_c = \sigma_{s,1}\sigma_{s,3}(1-\cosh a_s z) + [A'_c]_{\substack{d_t=0\\d_c=0}} \cosh a_c z - [A'_s]_{\substack{d_t=0\\d_c=0}} \frac{\sigma_{s,3}}{2} a_s z \sinh a_s z - [A'_t]_{\substack{d_t=0\\d_c=0}} \frac{\sigma_{t,3}}{2} a_t z \sinh a_t z .$$

Temperatures in the plane perpendicular to the axis and passing through the center of the axis are found by putting $z = 0$ into the equations τ_s, τ_t and τ_c. Thus

$$(39)\quad \tau_s = \sigma_{s,1} = \frac{d_s}{a_s^2} , \qquad \tau_t = \sigma_{t,1} = \frac{d_t}{a_t^2} , \qquad \tau_c = \sigma_{c,1} = \frac{d_c}{a_c^2} .$$

Temperatures in this plane have already been investigated in chapter II where the radial heat flow in the armature is treated. Therefore the temperatures in the parts of the armature are corresponding to $\sigma_{s,1}$, $\sigma_{t,1}$ and $\sigma_{c,1}$ respectively.

The axial temperature distributions are expressed in formulae (32), (33) and (34) in the case where the machine runs at no-load. Again the axial temperature distributions in the short circuit case are expressed in formulae (36), (37) and (38).

Expressing the formulae of the axial distribution with $[\tau_s]_{d_s=0}$, $[\tau_t]_{d_s=0}$ and $[\tau_c]_{d_s=0}$ with reference to the temperatures of the slot, the teeth and the iron core in the case of no-load and expressing them with $[\tau_s]_{\substack{d_t=0\\d_c=0}}$, $[\tau_t]_{\substack{d_t=0\\d_c=0}}$ and $[\tau_c]_{\substack{d_t=0\\d_c=0}}$ with reference to the temperatures of the slot, the teeth and the iron core in the case of the short circuit, then the expressions τ_s, τ_t and τ_c at an arbitary load can be given in the following form;

$$(40)\qquad \begin{cases} \tau_s = [\tau_s]_{d_s=0} + [\tau_s]_{\substack{d_t=0 \\ d_c=0}}, \\ \tau_t = [\tau_t]_{d_s=0} + [\tau_t]_{\substack{d_t=0 \\ d_c=0}}, \\ \tau_c = [\tau_c]_{d_s=0} + [\tau_c]_{\substack{d_t=0 \\ d_c=0}}. \end{cases}$$

If the temperature distribution is found from the experiment or the mathematical calculation at no-load under the rated voltage and the temperature distribution is found from the experiment or the mathematical calculation at short circuit referring to any value of current passing through the armature winding, then the temperature distribution at any load may be easily obtained by means of the summation of two cases where one is no-load and the other is short circuit by taking the values Q_s, Q_t and Q_c, i.e., d_s, d_t and d_c to be suitable.

Temperature gradient in the axial direction depends upon a_s, a_t, a_c and a_e at every part of the machine where a_s means to refer to the slot conductor only existing in the problem and also a_t, a_c or a_e means to refer to the teeth, the iron core or the end connector respectively, similar as in the slot conductor.

It can be concluded that the larger the thermal conductivity is, the less a_s becomes. Therefore the temperature gradient in the slot is very small compared with the other parts, because the thermal conductivity is larger in the slot than in the other parts.

On the contrary, a_t and a_c are very large and then the temperature gradients are large in the iron core and the teeth, because the laminated sheet iron pile has a small thermal conductivity in the direction of its pile compared with that in its plane.

In general, $Q_t > Q_c$ must be kept in ordinary running, therefore $a_t > a_c$ may be held at all times. a_e is nearly equal to a_s, however, a_e is slightly greater than a_s.

(4) THE EFFECT OF THE VENTILATING DUCTS.

The cooling effects of the radial and axial ventilating ducts are not directly treated in this chapter, but these effects of the existence of the radial and axial ventilating ducts may be indirectly calculated by using the equivalent constant that is the increment of the cooling area in the core back and the air gap.

Fig. 14 shows the half part of the machine core whith piling up the sheet iron in the axial direction.

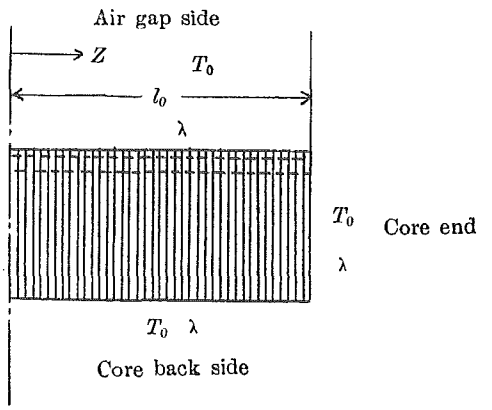

Fig. 14.

If the iron core has no loss and the heat developed in the other part of the machine passes through the core and diffuses in and from the surface of the core back alone, then the core temperature will be linearly distributed in the axial direction.

However, in the case where the core loss Q is uniformly distributed, the temperature of the core can be obtained by superposing it on the above linear distribution:

$$\frac{Q}{\sigma_q} l_0 \left(1-\frac{z}{l_0}\right)^2 + \frac{Q}{\sigma_q} l_0 \left(1-\frac{z}{l_0}\right) + c$$

as shown by curve A in Fig. 15.

Curve A in Fig. 15 indicates the temperature when the core loss Q is distributed uniformly and the cooling surface exists only at the core end. However, the heat developed in the core diffuses not only from the core end, but also it flows in a radial direction and dissipates from the core back and the air gap. Curve B indicates the temperature in the case where the heat dissipates at the core back, air gap and the core end.

In the calculation of the axial temperature of the machine treated in chapter III, the heat dissipation is considered to occur through the three kinds of cooling surfaces above described. The temperature of the machine curve C in Fig. 15 in practical cases is lower than the above ones, because it has ventilating ducts radially and axially as shown in Fig. 16. The difference of the curves B and C corresponds to the heat amount diffused from these ventilating ducts.

The axial ventilating ducts may be considered to be equivalent with the increment of the core back-surface and also the radial ventilating ducts may be considered to be the same as the axial ventilating ducts; because the sheet iron pack has a small thickness and the heat conduction is very small in the direction of the sheet-piling. There-

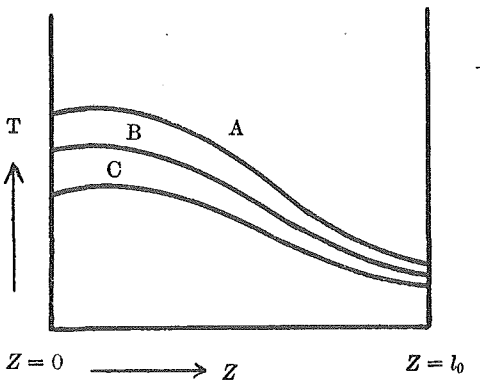

Fig. 15.

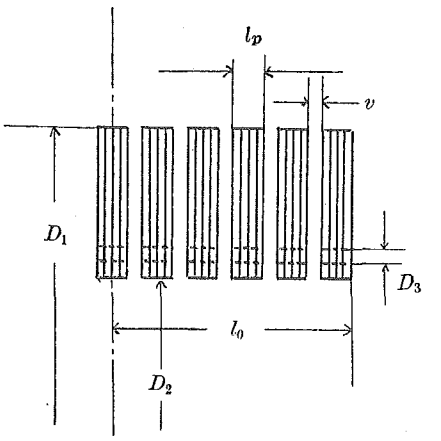

Fig. 16.

fore the difference of the curves B and A is the same as the difference of C and B. The effect of the ventilating ducts may be equal to that of the increase of the radial cooling surface.

The effect of the ventilating ducts will be as follows:—

The cooling area of the radial ventilating ducts:—

$$\frac{\pi}{4}(D_1^2-D_2^2)\,2n_{v_1}$$

where n_{v_1} = total number of the radial ventilating ducts.
D_1 = outer diameter of core in cm.
D_2 = inner diameter of core in cm.

The cooling area of the axial ventilating ducts:—

$$D_3\pi n_{v_2}(2l_0-v n_{v_1})$$

where D_3 = diameter of axial ventilating ducts
n_{v_2} = total number of the axial ventilating ducts
$2l_0$ = axial length of armature core
v = air gap of radial ventilating ducts.

Therefore, the equivalent area of the core back may be described as follows:—

$$\frac{\pi}{2}(D_1^2-D_2^2)n_{v_1}\frac{\lambda_{v_1}}{\lambda_B}\frac{\sigma_q}{\sigma_r}+D_3\pi n_{v_2}(2l_0-v n_{v_1})\frac{\lambda_{v_2}}{\lambda_B}$$

where λv_1 = Newton's constant at the surface of the radial ventilating ducts
λv_2 = Newton's constant at the surface of the axial ventilating ducts
σ_q = thermal conductivity of the core in the direction of sheet-piling
σ_r = thermal conductivity of the core in the radial direction.

By using the above value of the cooling area, the temperature of the core with the radial and axial ventilating ducts can be calculated.

These constants may be taken about

$\lambda v_1 = 0.002$ watt/cm², °C
$\lambda v_2 = 0.004$ watt/cm², °C
$\sigma_r = 0.466$ watt/cm, °C
$\sigma_q = 0.0245$ watt/cm, °C
} For M-sheet

(5) EXAMPLE.

Turbo-generator for steam power plant service,

Capacity	50,000 kVA
Voltage	11,000 V

Losses at each part of machine.

Iron loss in the stator	310 kW.
Copper loss in the stator	75 kW.
Stray load loss in the stator	200 kW.

Total number of the radial ventilating ducts

$$n_{v_1} = 69 .$$

Cooling surface of the radial ventilating ducts

$$\frac{\pi}{4}(245^2 - 145.6^2) \times 2 \times 69 = 4.21 \times 10^6 \text{ cm}^2 .$$

Total number of the axial ventilating ducts

$$n_{v_2} = 18 .$$

Axial length of the armature

$$2l_0 = 390 \text{ cm} .$$

Net value of the axial length of the sheet iron-pile of the armature

$$390 - 1.3 \times 69 \fallingdotseq 300 \text{ cm} .$$

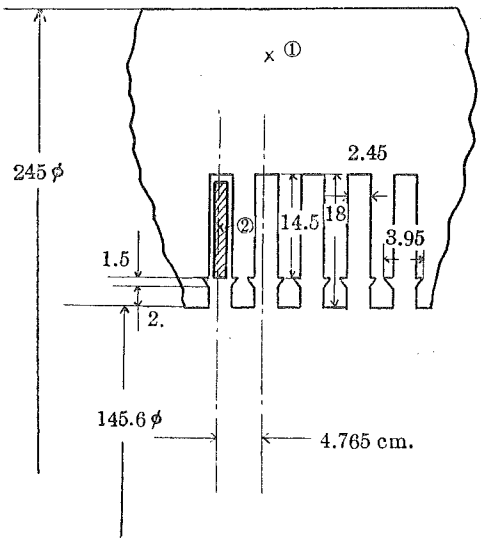

Fig. 17 (a).

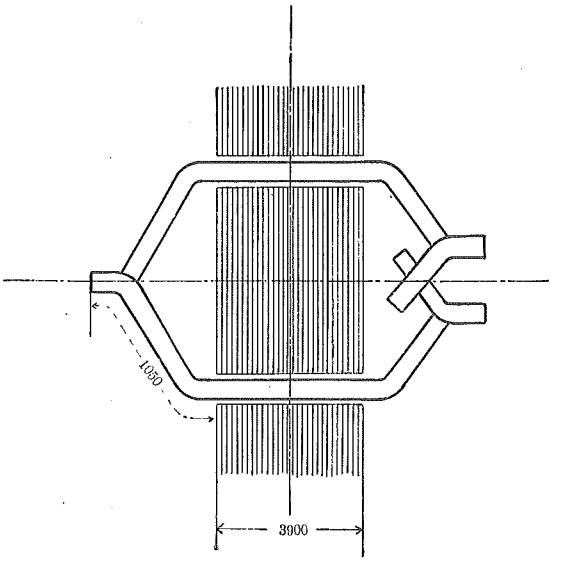

Fig. 17 (b).

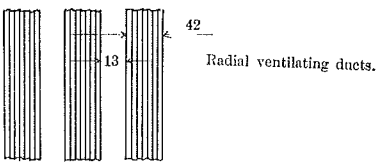

Fig. 17 (c).

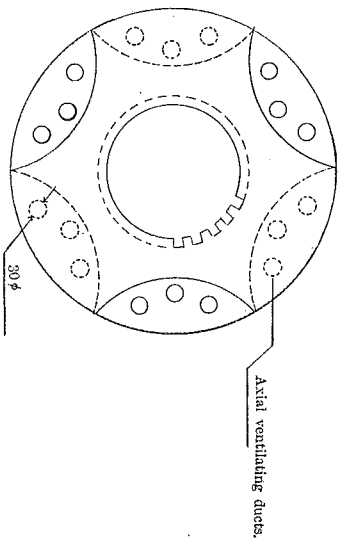

Fig. 17 (d).

Total area of the axial ventilating ducts

$$3\pi \times 18(390-1.3\times 69) = 5.1\times 10^4 \text{ cm}^2 .$$

Newton's constants at the surface of the radial and the axial ventilating ducts

$$\lambda_{v_1} = 0.003 \text{ watt/cm}^2, ^\circ\text{C}$$

$$\lambda_{v_2} = 0.004 \text{ watt/cm}^2, ^\circ\text{C}$$

and thermal conductivities in the direction of the radial and the axial direction in the iron core

$$\sigma_r = 0.466 \text{ watt/cm}, ^\circ\text{C}$$

$$\sigma_q = 0.024 \text{ watt/cm}, ^\circ\text{C} .$$

Newton's constant at the core back

$$\lambda_B = 0.006 \text{ watt/cm}^2, ^\circ\text{C} .$$

The area of the core back equivalent to the radial and the axial ventilating ducts

$$4.21\times 10^6 \times \frac{0.003}{0.006}\,\frac{0.024}{0.466} + 5.1\times 10^4 \times \frac{0.004}{0.006}$$

$$= 1.08\times 10^5 + 3.4\times 10^4 = 1.42\times 10^5 \text{ cm}^2 .$$

Area of the core back

$$245\pi(390-1.3\times 69) = 2.31\times 10^5 \text{ cm}^2 .$$

Equivalent Newton's constant

$$0.006\times\frac{2.31+1.42}{2.31} = 0.0097 \text{ watt/cm}^2, ^\circ\text{C} .$$

The radial and axial ventilating ducts have twice larger heat dissipating capacity of the armature than in case of one without them. Therefore if two times Newton's constant at the core back, is not taken the thermal conductivity in the copper conductor and sheet iron would be twice larger than the true value.

$$\sigma_s = 3.8\times 2 = 7.6 \text{ watt/cm}, ^\circ\text{C}$$

$$\sigma_r = 0.932 \quad ,,$$

$$\sigma_q = 0.048 \quad ,, \quad .$$

The slot insulation and the conductor arrangement in the slot are shown in Fig. 18.

Newton's constant at the slot insulation is taken

$$\lambda = 1.57 \times 10^{-3} \text{ watt/cm}^2, \text{ °C}.$$

Losses in the armature are shown:—

Iron loss
in the stator = 310 kW

Copper loss
in the stator = 75 kW

Stray load loss
in the stator = 200 kW

Number of slots = 96.

Length of the coil = 600 cm.

Copper loss per unit length of coil

$$\frac{75000}{600 \times 2 \times 96} = 0.65 \text{ watt}.$$

Length of the coil inserting into the slot = 400 cm.

Stray loss per unit length of the stator coil inserting into the slot;

$$\frac{200000}{400 \times 2 \times 96} = 2.6 \text{ watt}.$$

Sectional area of the copper strip

$2.4 \times 6.4 = 14.8 \text{ mm}^2$.

Sectional area of one conductor

$14.8 \times 2 \times 21 = 6.22 \text{ cm}^2$.

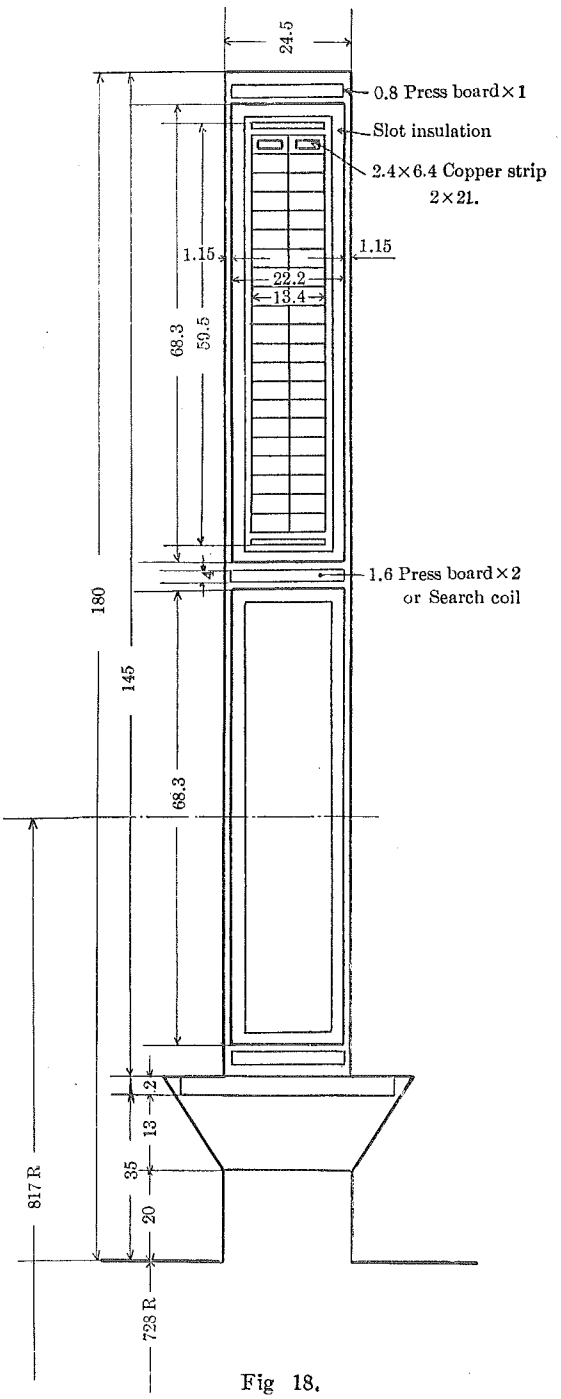

Fig 18.

Loss per unit volume in the slot conductor

$$Q_s = \frac{0.65+2.6}{6.22} = 0.522 \text{ watt/cm}^3 .$$

Loss per unit volume in the end connector

$$Q_e = \frac{0.65}{6.22} = 0.104 \text{ watt/cm}^3 .$$

Sectional area of the total slot conductor

$$q_s = 6.22 \times 2 = 12.44 \text{ cm}^2 .$$

Peripheral length of the slot conductor

$$u_s = (2.45+18) \times 2 \fallingdotseq 41 \text{ cm} .$$

Temperature coefficient of resistance of the copper strip

$$\alpha = 0.004 .$$

Magnetic induction in the core

$$B = 12{,}000 \text{ lines/cm}^2 .$$

Magnetic induction in the teeth

$$B = 16{,}000 \text{ lines/cm}^2 .$$

Volume of the core

$$\frac{\pi}{4}[245^2-181^2] \times 300 - 18 \times 300 \times 3\pi = 6.36 \times 10^6 \text{ cm}^3 .$$

Volume of the teeth

$$2.3 \times 18 \times 300 \times 96 = 1.19 \times 10^6 \text{ cm}^3 .$$

Ratio of iron loss of the teeth and the core,

$$2.12 : 1.34 .$$

Iron loss of the core per unit volume

$$Q_c = \frac{310000}{6.36 \times 10^6 + 1.19 \times \frac{2.12}{1.34} \times 10^6} = 0.0376 \text{ watt/cm}^3 .$$

Iron loss of the teeth per unit volume

$$Q_t = 0.0376 \times \frac{2.12}{1.34} = 0.0595 \text{ watt/cm}^3 ,$$

$$a_s = \sqrt{\frac{\lambda_s u_s - Q_s q_s \alpha}{\sigma_s q_s}} = \sqrt{\frac{1.57 \times 2 \times 41 \times 10^{-3} - 0.522 \times 12.44 \times 0.004}{3.8 \times 12.44}}$$

$$= 0.0466$$

$$\frac{d_s}{a_s^2} = \frac{Q_s(1+\alpha T_0) q_s}{\lambda_s u_s - Q_s q_s \alpha} = \frac{0.522 \times (1+0.004 \times 20) \times 12.44}{1.57 \times 2 \times 41 \times 10^{-3} - 0.522 \times 12.44 \times 0.004} = 68.3$$

$$a_t = \sqrt{\frac{-\lambda_s u_{s,t} + \lambda_{t,c} b_t + \lambda_{t,0} b_s}{\sigma_q q_t}}$$

$$= \sqrt{\frac{-1.57 \times 2 \times 36 \times 10^{-3} + 0.056 \times 2.4 + 0.008 \times 2.3}{0.024 \times 41.4}} = 0.201$$

$$\frac{d_t}{a_t^2} = \frac{0.0591 \times 41.4}{0.04} = 61.1$$

$$a_c = \sqrt{\frac{-\lambda_s u_{s,c} - \lambda_{t,c} b_t + \lambda_{c,0} u_c}{\sigma_q q_c}}$$

$$= \sqrt{\frac{-1.57 \times 2 \times 2.45 \times 10^{-3} - 0.056 \times 2.4 + 0.006 \times 73.17}{0.024 \times 3.04 \times 10^2}}$$

$$= \sqrt{\frac{0.2983}{0.024 \times 3.04 \times 10^2}} = 0.203$$

$$\frac{d_c}{a_c^2} = 38$$

$$a_e = \sqrt{\frac{\lambda_e u_e - Q_e q_e \alpha}{\sigma_e q_e}} = \sqrt{\frac{1.57 \times 2 \times 41 \times 10^{-3} - 0.104 \times 12.44 \times 0.004}{3.8 \times 12.44}}$$

$$= 0.0512$$

$$d_e = \frac{Q_e}{\sigma_e}(1+\alpha T_0) = \frac{0.104}{3.8}(1+0.004 \times 20) = 0.0295$$

$$\frac{d_e}{a_e^2} = 11.3$$

$$A_s = -0.305\,, \qquad A_t = -1.9 \times 10^{-12}\,,$$

$$A_c = -467 \times 10^{-12}\,, \qquad A_e = 31.2\,.$$

The calculated results are expressed in the curves of Fig. 19. These calculated results coincide with the experimental data.

According to experimental results, the temperature of the spot marked ① in Fig. 17 (a) is

> 21°C (measured temperature rise)+10°C (correction for the thermometer method) + 20°C (room temperature) = 51°C,

and the temperature of the spot marked ② in Fig. 17 (a) is

> 40°C (measured temperature rise)+5°C (correction for the search coil method) + 20°C (room temperature) = 65°C.

Again, from calculated results, the temperature rise of spot ①, and that of spot ② are 18°C and 42.5°C respectively. Thus these calculated results coincide rather well with the experimental results.

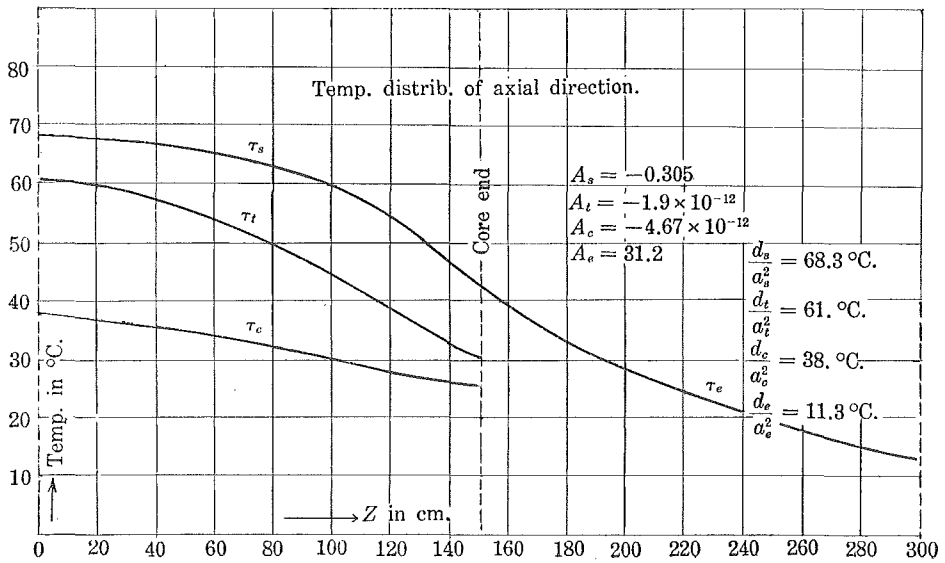

Fig. 19.

CHAPTER IV.

CURRENT DISTRIBUTION IN THE SLOT AND "ALTERNATING CURRENT RESISTANCE".

When the direct current passes through the conductor inserted into the slot of the electric machine, the current density is uniform in the section of the conductor. However, in the case of the alternating current, it is well known that the distribution of the current is not uniform and this non-uniformity increases with the frequency, for the current passing through the slot conductor produces a leakage flux in the teeth and in the iron core and consequently the counter electromotive force is induced in the slot conductor. The distribution depends upon the dimensions of the slot and the conductors and the arrangement of the conductor.

In this chapter, the problem of the distribution of the current is treated as a two dimensional one and the current distributions are calculated. Lastly "the alternating current resistance" is discussed in order to calculate the problem of the temperature rise of the slot conductor due to power losses.

(1) CURRENT AND LEAKAGE FIELD.

A single conductor with section as shown in Fig. 20 is inserted into the slot and the rectangular path with width dx at distance x from the bottom of the slot is investigated.

If the magnetic field is integrated along the rectangular path, then the following equation from the fundamental equation of Maxwell is obtained

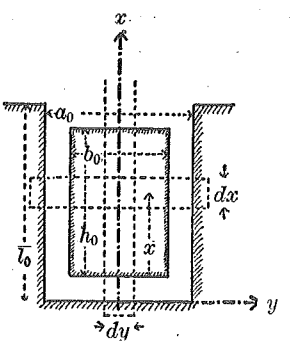

Fig. 20.

$$(1) \qquad \int_{-\frac{1}{2}a_0}^{+\frac{1}{2}a_0} H_{y_{(x+dx)}}\,dy + \frac{B_x}{\mu}\,dx + \int_{+\frac{1}{2}a_0}^{-\frac{1}{2}a_0} H_{y_{(x)}}\,dy + \frac{B_x}{\mu}\,dx$$

$$= 0.4\pi\left[\int_{-\frac{1}{2}b_0}^{+\frac{1}{2}b_0} i\,dy\right]dx$$

and also if the magnetic field is integrated along the rectangular path with the width dy and surrounding the x-axis, then one obtains equation (2),

$$(2) \qquad \int_0^x H_{x\,(y=dy)}\,dx+2H_{y\,(x=x)}+\int_x^0 H_{x\,(y=dy)}\,dx+2\frac{B_{y(x=0)}}{\mu}\,dy$$

$$=0.8\pi\left[\int_{d_2}^{x} i\,dx\right]dy$$

where H_x and H_y are the components of the field intensities referring to the directions of x and y respectively. B_x and B_y are the components of the magnetic induction in the sheet iron referring to the directions x and y respectively. i is the current density in the slot conductor,

a_0 = width of the slot in cm,
l_0 = height of the slot in cm,
b_0 = width of the conductor in cm,
h_0 = height of the conductor in cm.

Now the rectangular path having the widths dx and dy in the planes perpendicular to the y- and x-axes respectively is considered. From consideration of the relation between the voltage drop along the integrating path and total flux interlinkage, equations (3) and (4) are written from the second equation of Maxwell,

$$(3) \qquad \rho[i_{x+dx}-i_x]=\frac{\partial H_y}{\partial t}\,dx\,10^{-8}\,,$$

$$(4) \qquad \rho[i_{y+dy}-i_y]=\frac{\partial H_x}{\partial t}\,dy\,10^{-8}\,.$$

Equations (3) and (4) express the relation between the current density and the magnetic field, where ρ is the specific resistivity of the copper conductor. Since the permeability μ of the sheet iron is very large, the approximate equtions are obtained,

$$B_y\frac{1}{\mu}\fallingdotseq 0\,, \qquad B_x\frac{1}{\mu}\fallingdotseq 0\,.$$

Putting

$$i=I(x,y)\,e^{j\omega t}$$

into equations (1) and (2),

$$\int_0^{\frac{1}{2}a_0} \frac{\partial^2 I}{\partial x^2}\, dy = j\omega \frac{0.4\pi}{\rho} 10^{-8} \int_0^{\frac{1}{2}b_0} I dy\ ,$$

$$\frac{\partial^2 I}{\partial x^2} + \frac{\partial^2 I}{\partial y^2} = j\omega \frac{0.4\pi}{\rho} 10^{-8} I\ .$$

Similarly from equations (3) and (4)

$$H_y = \frac{\rho}{j\omega} 10^{+8} \frac{\partial I}{\partial x} \qquad \text{and} \qquad H_x = \frac{\rho}{j\omega} 10^{+8} \frac{\partial I}{\partial y}\ ,$$

are obtained.

Assuming the current I as

$$I = u(x)\, v(y)\ ,$$

it follows;

$$(5) \qquad \frac{d^2u}{dx^2} = j\omega \frac{0.4\pi}{\rho} 10^{-8} \frac{\int_0^{\frac{1}{2}b_0} v(y)\, dy}{\int_0^{\frac{1}{2}a_0} v(y)\, dy} u(x)$$

$$(6) \qquad \frac{d^2u}{dx^2}\frac{1}{u(x)} + \frac{d^2v}{dy^2}\frac{1}{v(y)} = j\omega \frac{0.4\pi}{\rho} 10^{-8}\ .$$

Put

$$(7) \qquad \alpha_v^2 = 2\pi\omega \frac{10^{-9}}{\rho} \left[\frac{\int_0^{\frac{1}{2}b_0} v(y)\, dy}{\int_0^{\frac{1}{2}a_0} v(y)\, dy} \right],$$

equation (5) will be written

$$(8) \qquad \frac{d^2u}{dx^2} = 2j\alpha_v^2 u(x)\ .$$

Again put

$$(9) \qquad \beta_v^2 = 2\pi\omega \frac{10^{-9}}{\rho} \left[1 - \frac{\int_0^{\frac{1}{2}b_0} v(y)\, dy}{\int_0^{\frac{1}{2}a_0} v(y)\, dy} \right]$$

and substitute (8) and (9) in (6), then it follows

$$\frac{d^2v}{dy^2} = 2j\beta_\nu^2 v(y) \,. \tag{10}$$

If equations (7) and (9) are added, the relation is obtained.

$$\alpha_\nu^2+\beta_\nu^2 = 2\pi\omega\frac{10^{-9}}{\rho} \,.$$

Therefore the solutions of $u(x)$ and $v(y)$ are

$$u(x) = A_{1\nu}e^{\alpha_\nu(1+j)x}+B_{1\nu}e^{-\alpha_\nu(1+j)x} \,, \tag{11}$$

$$v(y) = A_{2\nu}e^{\beta_\nu(1+j)y}+B_{2\nu}e^{-\beta_\nu(1+j)y} \,. \tag{12}$$

From equation (7), by putting $a_0 = b_0+\varepsilon$, the formula

$$\left(\alpha_\nu^2 2\pi\omega\frac{10^{-9}}{\rho}\right)\int_0^{\frac{1}{2}b_0} v(y)\,dy = -\alpha_\nu^2\int_{+\frac{1}{2}b_0}^{+\frac{1}{2}(b_0+\varepsilon)} v(y)\,dy \tag{13}$$

is obtained.

If the integral

$$\int_{\frac{1}{2}b_0}^{+\frac{1}{2}(b_0+\varepsilon)} v(y)\,dy$$

is expanded by the ascending power series with ε, then

$$\int_{\frac{1}{2}b_0}^{\frac{1}{2}(b_0+\varepsilon)} v(y)dy = A_{2\nu}e^{\beta_\nu(1+j)\frac{1}{2}b_0}\ \frac{1}{2}\varepsilon\left[1+\frac{1}{4}\varepsilon\beta_\nu(1+j)+\frac{1}{12}\varepsilon^2\beta_\nu^2(1+j)^2+\cdots\cdot\right]$$

$$+B_{2\nu}e^{-\beta_\nu(1+j)\frac{1}{2}b_0}\ \frac{1}{2}\varepsilon\left[1-\frac{1}{4}\varepsilon\beta_\nu(1+j)+\frac{1}{12}\varepsilon^2\beta_\nu^2(1+j)^2+\cdots\cdot\right]$$

is obtained.

Since the function $v(y)$ is symmetrical with respect to the x-axis, it follows that $A_{2\nu} = B_{2\nu}$. Hence this condition is inserted into the above equation,

$$\int_{\frac{1}{2}b_0}^{\frac{1}{2}a_0} v(y)\,dy = A_{2\nu}\frac{\epsilon}{2}\left[e^{\beta_\nu(1+j)\frac{1}{2}b_0}+e^{-\beta_\nu(1+j)\frac{1}{2}b_0}\right]$$

$$+A_{2\nu}\frac{\epsilon^2}{8}\beta_\nu(1+j)\left[e^{\beta_\nu(1+j)\frac{1}{2}b_0}-e^{-\beta_\nu(1+j)\frac{1}{2}b_0}\right]$$

$$+A_{2\nu}\frac{\epsilon^3}{24}\beta_\nu^2(1+j)^2\left[e^{\beta_\nu(1+j)\frac{1}{2}b_0}+e^{-\beta_\nu(1+j)\frac{1}{2}b_0}\right]+\cdots\cdots .$$

If only the first term of this expanding formula is taken and it is inserted into equation (13), then from the relation

$$\alpha_\nu^2+\beta_\nu^2 = 2\pi\omega\frac{10^{-9}}{\rho}$$

the values of α_ν and β_ν can be obtained:

$$(14)\qquad \alpha_{\nu_1}^2 = \frac{b_0}{a_0}2\pi\omega\frac{10^{-9}}{\rho}, \qquad \beta_{\nu_1}^2 = \frac{a_0-b_0}{a_0}2\pi\omega\frac{10^{-9}}{\rho}.$$

If this approximation is used, α_ν and β_ν are independent of the subindex ν and therefore the subindex is given up here-after. Again

$$(15)\qquad \alpha = 2\pi\sqrt{\frac{f}{\rho}\frac{b_0}{a_0}10^{-9}}, \qquad \beta = 2\pi\sqrt{\frac{f}{\rho}\frac{a_0-b_0}{a_0}10^{-9}}.$$

The constants α and β are the characteristic ones to determine the distributions of current referring to the directions of x- and y-axes respectively. They have various values according to the ratio $\lambda_0 = \frac{b_0}{a_0}$, where b_0 is the width of the conductor and a_0 that of the slot. α may become smaller in accordance with λ_0 which tends from 1 to 1/2. On the contrary, constants β may become larger from the same reason. At last both constants α and β may become equal to each other when λ_0 attains to 1/2. If $\lambda_0 = 1$, then $\beta = 0$, and there appears uniform distribution with reference to the direction of y-axis.

The variations of α and β referring to λ_0 are shown in Fig. 21 (a) where the specific resistivity of copper is calculated as

$$\rho = 2\times 10^{-6}\ \text{ohm cm}.$$

From Fig. 21a it is found that the rate of increase of β is larger than that of the decrease of α, and that both α and β increase with the frequency f. The variations of α and β referring to the frequency f are shown in Fig. 21 (b) and from this curve, it is found that α is larger than β, and the curve in Fig. 21 (b) is obtained by putting $\lambda_0 = 0.9$. In this case, constants are

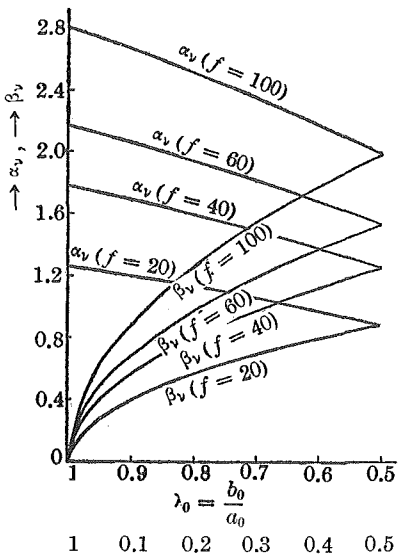

Fig. 21 (a).

$$\alpha = 0.1335\sqrt{f}$$

$$\beta = 0.0445\sqrt{f}\ .$$

Let us carry on this calculation taking only the first order with respect to the function $u(x)$ and $v(y)$, so

$$(16)\quad i = [A\{e^{(1+j)(\alpha x+\beta y)} + e^{(1+j)(\alpha x-\beta y)}\} + B\{e^{-(1+j)(\alpha x-\beta y)} + e^{-(1+j)(\alpha x+\beta y)}\}]\, e^{j\omega t},$$

the above equation is established. Now

$$(17)\quad A = a+jb\ ,\quad B = c+jd\ ,\quad \delta_1 = \sqrt{a^2+b^2}\ ,\quad \delta_2 = \sqrt{c^2+d^2}\ ,$$

$$(18)\quad \tan\beta_1 = \frac{1-\frac{a}{b}}{1+\frac{a}{b}}\ ,\qquad \tan\beta_2 = \frac{1-\frac{c}{d}}{1+\frac{c}{d}}\ .$$

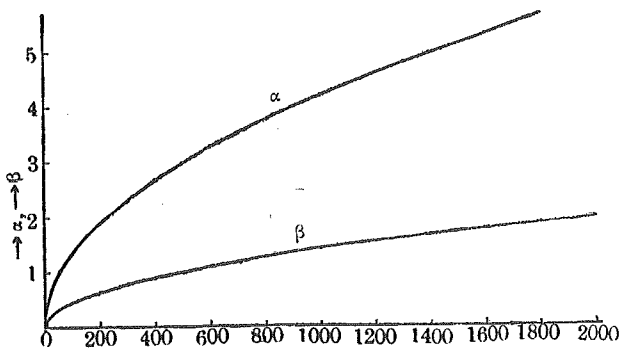

Fig. 21 (b).

The equations may be written again as follows :—

$$(19)\quad \begin{cases} i = \delta_1 e^{\alpha x+\beta y}\sin\left[\omega t+\alpha x+\beta y+\beta_1+\dfrac{\pi}{4}\right] \\ \quad +\delta_1 e^{\alpha x-\beta y}\sin\left[\omega t+\alpha x-\beta y+\beta_1+\dfrac{\pi}{4}\right] \\ \quad +\delta_2 e^{-\alpha x+\beta y}\sin\left[\omega t-\alpha x+\beta y+\beta_2+\dfrac{\pi}{4}\right] \\ \quad +\delta_2 e^{-\alpha x-\beta y}\sin\left[\omega t-\alpha x-\beta y+\beta_2+\dfrac{\pi}{4}\right]. \end{cases}$$

(2) SHAPE OF SLOT.

The type of slot, especially the slot-opening, can be classified into the open slot, semi-open slot, slightly opened slot and totally enclosed slot which correspond to (A), (B), (C) and (D) respectively in Fig. 21 (c).

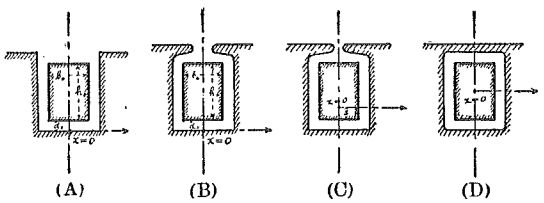

Fig. 21 (c).

In the case of the open or semi-open slot, as the condition $H_y = 0$ is satisfied at the bottom of the slot, it is useful to choose the bottom of the slot for the origin of x-axis. In the case of totally enclosed slot, as the condition $H_y = 0$ is satisfied at the middle height of conductor, so the origin of x-axis is taken as at this point and in the case of slightly opened slot, the condition $H_y = 0$ may be satisfied at some point between the middle point and the bottom of the slot. This point can be found approximately by taking some distance from the middle point of the slot downward, whose distance is determined by the value obtained by dividing the electromotive force at the slot opening by the permeability μ of the sheet iron, but the magneto-motive force is consumed considerably at the slot opening so the origin is taken at the bottom, for the slot has a larger opening than the semi-open slot.

If the origin is thus determined, then $H_y = 0$ and $x = 0$ may be established at this point. From these reasons, put $H_y = 0$ in the following equation.

$$H_y = \rho\, 10^{+8} \int_0^t \frac{\partial i}{\partial x}\, dt \,, \tag{20}$$

then the equation

$$\frac{\partial i}{\partial x} = 0$$

may be obtained.

From the two conditions above described,

$$\delta_1 = \delta_2 \quad \text{and} \quad \beta_1 = \beta_2 \,.$$

Put

$$\delta_1 = \delta_2 = \delta_0 \quad \text{and} \quad \beta_1 = \beta_2 = \beta_0 \,. \tag{21}$$

In the next paragraph the constants δ_0 and β_0 are to be calculated.

(A) OPEN AND SEMI-OPEN SLOT.

In this case, the origin is taken at the bottom of slot. The total current becomes

$$2 \int_{d_0}^{d_0+h_0} \int_0^{\frac{1}{2}b_0} i\, dx\, dy = I_0 \sin \omega t \,. \tag{22}$$

From equation (19) it follows

$$\tan \beta_0 = -\frac{d(a-b)+c(a+b)}{d(a+b)-c(b-a)} \,.$$

where

$$a = \sin \frac{1}{2}\beta b_0 \cosh \frac{1}{2}\beta b_0 \,, \qquad b = \cos \frac{1}{2}\beta b_0 \sinh \frac{1}{2}\beta b_0 \,,$$

$$c = \sin \alpha h_0 \cosh \alpha h_0 \,, \qquad d = \cos \alpha h_0 \sinh \alpha h_0 \,.$$

Since β is small, the next assumption may be fulfilled

$$\sin \frac{1}{2}\beta b_0 \cosh \frac{1}{2}\beta b_0 \fallingdotseq \cos \frac{1}{2}\beta b_0 \sinh \frac{1}{2}\beta b_0 \,,$$

Thus

$$\delta_0 = \frac{I_0 \alpha\beta}{2\sqrt{(\cosh 2\alpha h_0 - \cos 2\alpha h_0)(\cosh \beta b_0 - \cos \beta b_0)}} \tag{23}$$

is obtained.

Again equation (19) is written as the following form

$$i = -\sqrt{2}\,\delta_0 A \sin(\omega t - \theta_0 + \varphi)\,, \tag{24}$$

where $\beta_0 = \pi - \theta_0$ and

$$A = \sqrt{2}\sqrt{(\cosh 2\alpha x + \cos 2\alpha x)(\cosh 2\beta y + \cos 2\beta y)} \tag{25}$$

$$\tan\varphi = \frac{\cos\alpha x \cosh\alpha x + \sin\alpha x \sinh\alpha x}{\cos\alpha x \cosh\alpha x - \sin\alpha x \sinh\alpha x}\,, \tag{26}$$

or

$$\begin{aligned} i = I_0 \alpha\beta \frac{\sqrt{(\cosh 2\alpha x + \cos 2\alpha x)(\cosh 2\beta y + \cos 2\beta y)}}{\sqrt{(\cosh 2\alpha h_0 - \cos 2\alpha h_0)(\cosh \beta h_0 - \cos \beta b_0)}} \\ \times \sin\Bigg[\omega t - \arctan\frac{\sin\alpha h_0 \cosh\alpha h_0}{\cos\alpha h_0 \sinh\alpha h_0} \\ + \arctan\frac{\cos\alpha x \cosh\alpha x + \sin\alpha x \sinh\alpha x}{\cos\alpha x \cosh\alpha x - \sin\alpha x \sinh\alpha x}\Bigg]. \end{aligned} \tag{27}$$

The mean current density I_d is indicated as $I_0 = I_d b_0 h_0$ and the amplitude of the current i is constituted of the terms containing x and y respectively :—

$$\alpha h_0 \sqrt{\frac{\cosh 2\alpha x + \cos 2\alpha x}{\cosh 2\alpha h_0 - \cos 2\alpha h_0}} \tag{28}$$

and

$$\beta b_0 \sqrt{\frac{\cosh 2\beta y + \cos 2\beta y}{\cosh \beta b_0 - \cos \beta b_0}}\,. \tag{29}$$

These two terms depend upon the temperature distribution referred to x- or y-axis respectively and from the first term, assuming the height of the conductor as $h_0 = 10$ cm, the curve is obtained as shown in Fig. 21(d) with respect to the frequency f. From this figure it is

found that the current does not pass at the bottom but passes through only at the upper part of the conductor and this phenomenon may become intensive with the increase of the frequency.

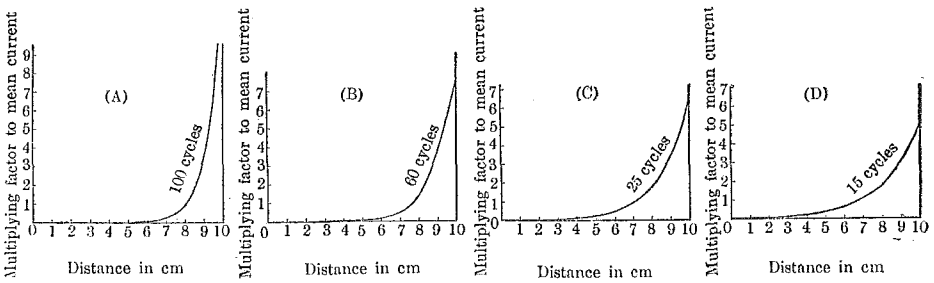

Fig. 21 (d).

Current densities at $x = h_0$ are expressed in Fig. 21 (e) referring to the various dimensions of the conductor. From this result, the distri-

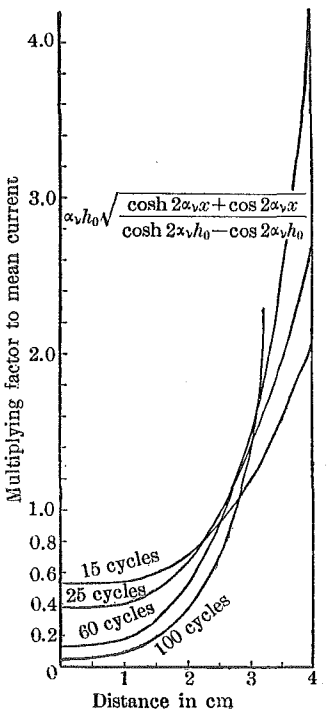

Fig. 21 (e).

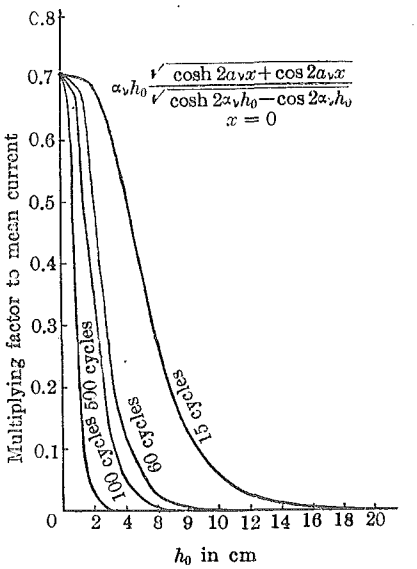

Fig. 21 (f).

bution is almost uniform when the height of the conductor attains to $h_0 = 1$ cm and then the current density suddenly increases at the

upper part of the conductor if its height increases over this limit $h_0 = 1\,\text{cm}$. On the other hand, current densities at $x = 0$ are as expressed in Fig. 21(f) which shows extensive dropping characters in accordance with the height h_0.

The distribution in the direction of y-axis is shown in Fig. 21(g) assuming the ratio λ_0 as 0.9 and observing on these curves, it is found that the current densities are almost uniform so far as its frequency attains to about 60 cycles/sec, but the variation of distribution appears at the higher frequency more than 60 cycles : —especially at 500~1000 cycles as shown in Fig. 21(g).

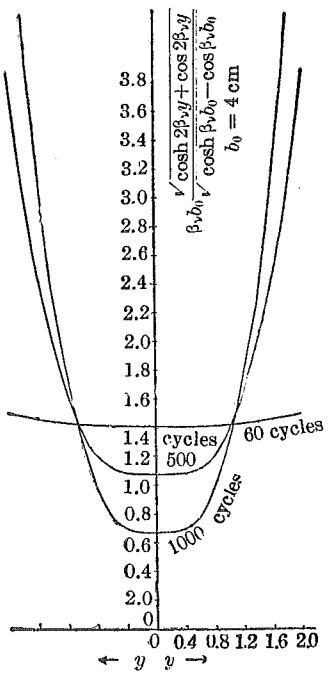

Fig. 21 (g).

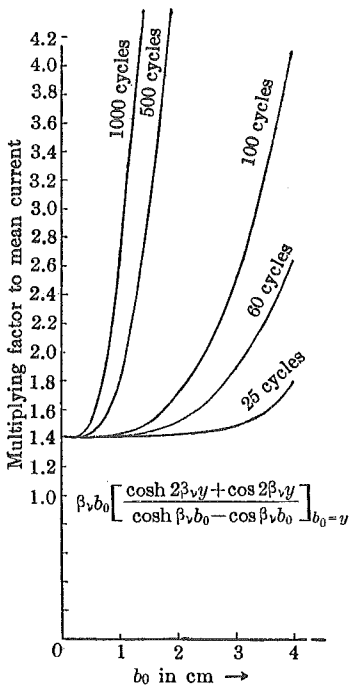

Fig. 21 (h).

The variation of distribution due to the change of the width of the conductor is shown in Figs. 21(h) and 22, corresponding to two cases where one is taken at $y = \frac{b_0}{2}$ and the other is taken at $y = 0$.

The shifting of phase due to the variation of h_0 is expressed in Fig. 23 and that due to the variation along x-axis is expressed in Fig. 24. Both shiftings of phase along become larger with the enlargement of h_0 and x.

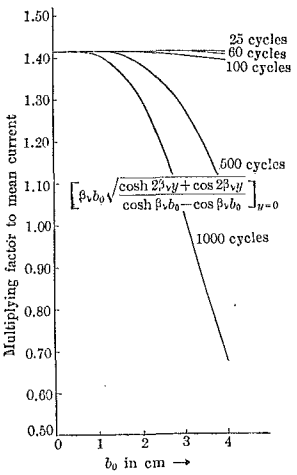

Fig. 22.

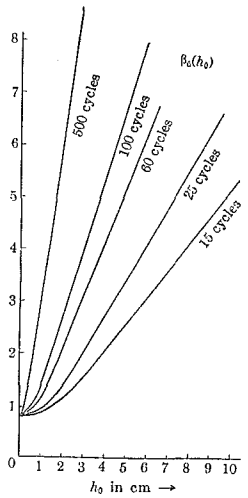

Fig. 23.

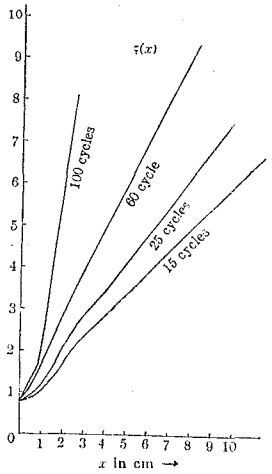

Fig. 24.

(B) TOTALLY ENCLOSED SLOT.

In this case, the current distribution is symmetrical with reference to the center of the section of slot, so the current is symmetrical with reference to x-axis and also y-axis, then the total current is

$$4\int_0^{\frac{1}{2}h_0}\int_0^{\frac{1}{2}b_0} i\,dx\,dy = I_0 \sin \omega t\ . \tag{30}$$

From this equation, the constants δ_0 and θ_0 are determined.

$$\delta_0 = \frac{-I_0\alpha\beta}{\nu(\cosh \alpha h_0 - \cos \alpha h_0)(\cosh \beta b_0 - \cos \beta b_0)} \tag{31}$$

and

$$\tan \theta_0 = \frac{\tan \frac{1}{2}\alpha h_0}{\tanh \frac{1}{2}\alpha h_0}\ . \tag{32}$$

Therefore, the current is expressed by the equation as follows

$$i = -\nu\sqrt{2}\,\delta_0 A \sin(\omega t - \theta_0 + \varphi)\ . \tag{33}$$

(C) SLIGHTLY OPENED SLOT.

The point at which $H_y = 0$ is assumed at the distance s from the bottom. If this distance s is estimated to be a suitable value from the consideration of the magnetomotive force at the slot opening as shown in Fig. 16 (c), the total current is

$$2\int_s^{h_0-s}\int_0^{\frac{1}{2}b_0} i\,dx\,dy = I_0 \sin\omega t\,. \tag{34}$$

Similarly calculating as above

$$\delta_0 = \frac{I_0\,\alpha\beta}{2\nu\sqrt{\{\cosh\beta b_0 - \cos\beta b_0\}\{\cosh 2\alpha(h_0-s) - \cos 2\alpha(h_0-s) + \cosh 2\alpha s}} \tag{35}$$

$$\overline{-\cos 2\alpha s + 2\cos\alpha h_0 \cosh\alpha(h_0-2s) - 2\cos\alpha(h_0-2s)\cosh\alpha h_0\}}$$

and

$$\tan\theta_0 = \frac{\sin\alpha(h_0-s)\cosh\alpha(h_0-s) - \sin\alpha s\cosh\alpha s}{\cos\alpha(h_0-s)\sinh\alpha(h_0-s) - \cos\alpha s\sinh\alpha s}\,. \tag{36}$$

The current distributions are expressed in Fig. 25 at the equal time interval of $\frac{\pi}{4\omega}$ with the schedule of (a), (b), (c) and (d), taking the distance as abscissa, where the height of the conductor is taken as $h_0 = 4$ cm.

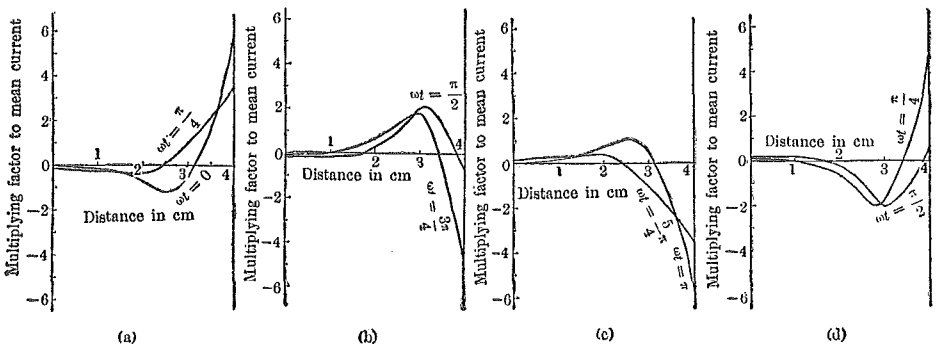

Fig. 25.

Next, referring to formula (29) which expresses only the distribution of y-axis, if βb_0 is so small as to be calculated by the first order, then the formula may be simplified as follows

$$\beta b_0 \sqrt{\frac{\cosh 2\beta y + \cos 2\beta y}{\cosh \beta b_0 - \cos \beta b_0}} \fallingdotseq \sqrt{2}$$

which coincides with the calculation performed by Rogowski and Field. Put $\beta = 0.345$ and $b_0 = 2$ cm in formula (29), and compare the values at two points, one is calculated at the center of the conductor, and the other at the side of conductor, then the difference of them for 60 cycles does not exceed 0.5% between two values, but the difference may attain to 26% in the case of $f = 500$ cycles and also the latter may attain to 12 times the former in the case of $f = 5000$ cycles. I is the amplitude of i.

Since the expression

$$(37) \qquad \frac{I}{I_d} = \beta b_0 \sqrt{\frac{\cosh 2\beta y + \cos 2\beta y}{\cosh \beta b_0 - \cos \beta b_0}} \, \alpha h_0 \sqrt{\frac{\cosh 2\alpha x + \cos 2\alpha x}{\cosh 2\alpha h_0 - \cos 2\alpha h_0}}$$

is complicated, this formula is expanded with respect to $\cosh \beta b_0$ and $\cos \beta b_0$,

$$(38) \qquad \frac{\beta b_0}{\sqrt{\cosh \beta b_0 - \cos \beta b_0}} \fallingdotseq 1 ,$$

and similarly the above formula is expanded with respect to $\cos 2\alpha h_0$ and $\cos 2\alpha h_0$,

$$(39) \qquad \frac{\alpha h_0}{\sqrt{\cosh 2\alpha h_0 - \cos 2\alpha h_0}} \fallingdotseq \frac{1}{2} .$$

Table I.

($\rho = 2 \times 10^{-6}$, $\lambda = 0.9$)

f	15	25	40	50	60	100	500	1000	5000
α_ν	0.517	0.667	0.845	0.944	1.035	1.335	2.985	4.22	9.44
β_ν	0.172	0.222	0.282	0.314	0.345	0.445	0.995	1.408	3.14

This formula (38) may be used in practice, if $\beta b_0 \leqq 2$, because there exists error by 2.15% in the case, $\beta b_0 = 2$. If the amount of (39) is taken to be equal to 1/2, and if $\alpha h_0 \leqq 1$, then the error is

about the same as 2.15%. Therefore, in the case of $\beta b_0 \leqq 2$ and $\alpha h_0 \leqq 1$, the expression

$$\frac{I}{I_d} = \sqrt{\cosh 2\alpha x + \cos 2\alpha x}\sqrt{\cosh 2\beta y + \cos 2\beta y} \tag{40}$$

may be always available. Table II expresses the range given by the above simplifying formula, where the errors referred to x and y do not exceed 2.15%.

Table II.

f	15	25	40	50	60	100	500	1000	5000
b_0(cm)	11.6	9.0	7.1	6.37	5.8	4.5	2.0	1.40	0.637
h_0(cm)	1.93	1.5	1.18	1.06	0.96	0.75			

In the range $\alpha h_0 \geqq 2$, the next formula is available

$$\frac{\alpha h_0}{\sqrt{\cosh 2\alpha h_0 - \cos 2\alpha h_0}} \fallingdotseq \sqrt{2}\,\alpha h_0\, e^{-\alpha h_0}. \tag{41}$$

In this case the error is about 1.19%.

(3) IN THE CASE WHERE MANY CONDUCTORS ARE INSERTED INTO THE SLOT FORMING A SINGLE LONGITUDINAL ROW.

If many conductors are inserted into the slot and are arranged as a single longitudinal row in the direction of x-axis and if the total current is the same in every conductor, then the equation may be obtained on account of symmetry of the current to x-axis,

$$\begin{aligned} i = {} & 2\delta_1 e^{\alpha x}\left[\cosh\beta y\cos\beta y\sin\left(\omega t+\alpha x+\beta_1+\frac{\pi}{4}\right)\right. \\ & \left.+\sinh\beta y\sin\beta y\cos\left(\omega t+\alpha x+\beta_1+\frac{\pi}{4}\right)\right] \\ & +2\delta_2 e^{-\alpha x}\left[\cosh\beta y\cos\beta y\sin\left(\omega t-\alpha x+\beta_2+\frac{\pi}{4}\right)\right. \\ & \left.+\sinh\beta y\sin\beta y\cos\left(\omega t-\alpha x+\beta_2+\frac{\pi}{4}\right)\right]. \end{aligned} \tag{42}$$

The origin of coordinate (x, y) is taken at the bottom of every conductor as shown in Fig. 26. Referring to the p-th conductor counting from those placing at the bottom of the slot, the relation between the field intensity H_y at $x=0$ and the total current I_0 passing through the whole section of the conductor is described as follows:—

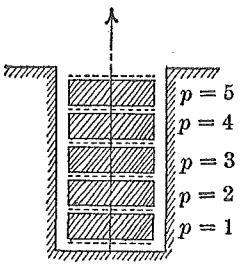

Fig. 26.

$$2\int_0^{\frac{1}{2}a_0} H_{y_{(x=0)}}\,dy = (p-1)0.4\pi I_0 \sin\omega t\,. \tag{43}$$

The relation between the magnetic field in the direction of y-axis and the current is expressed as follows

$$\frac{\partial i}{\partial x}\rho\,10^{-8} = \frac{\partial H_y}{\partial t}\,.$$

Referring to the current passing through each conductor, the equation is

$$2\int_0^{\frac{1}{2}b_0}\int_0^{h_0} i\,dx\,dy = I_0 \sin\omega t\,. \tag{44}$$

Put

$$\begin{cases}
a = \cosh\frac{1}{2}\beta a_0 \sin\frac{1}{2}\beta a_0\,, & a' = \cosh\frac{1}{2}\beta b_0 \sin\frac{1}{2}\beta b_0\,,\\
b = \sinh\frac{1}{2}\beta a_0 \cos\frac{1}{2}\beta a_0\,, & b' = \sinh\frac{1}{2}\beta b_0 \cos\frac{1}{2}\beta b_0\,,\\
c = e^{\alpha h_0}\cos\alpha h_0 - 1\,, & d = e^{-\alpha h_0}\cos\alpha h_0 - 1\,,\\
e = e^{\alpha h_0}\sin\alpha h_0\,, & f = -e^{-\alpha h_0}\sin\alpha h_0\,,\\
(a'^2+b'^2) \fallingdotseq (a^2+b^2)\,,\\
r_1 = b' - \frac{p-1}{\lambda_0}(af+bd)\,, & r_2 = a' - \frac{p-1}{\lambda_0}(ad-bf)\,,\\
r_3 = b' - \frac{p-1}{\lambda_0}(af+bc)\,, & r_4 = a' - \frac{p-1}{\lambda_0}(ad-be)\,,\\
r_5 = b' - \frac{p-1}{\lambda_0}(cb+ae)\,, & r_6 = a' - \frac{p-1}{\lambda_0}(ac-be)\,.
\end{cases} \tag{45}$$

The constants appeared in equation (42) are determined from the conditions (43) and (44),

$$(46)\quad \begin{cases} \tan\left(\beta_1+\dfrac{\pi}{4}\right)=\dfrac{-(e-f)r_2+(c-d)r_1}{(e-f)r_3+(c-d)r_4}\,, \\ \tan\left(\beta_2+\dfrac{\pi}{4}\right)=\dfrac{-(e-f)r_4+(c-d)r_3}{(e-f)r_5+(c-d)r_6}\,. \\ \delta_1=\dfrac{\alpha h_0\beta b_0}{2}I_d\dfrac{(c-d)r_4+(e-f)r_3}{(a'^2+b'^2)\{(d-c)^2+(f-e)^2\}}\sqrt{1+\left[\dfrac{(c-d)r_1-(e-f)r_2}{(c-d)r_4+(e-f)r_3}\right]^2}, \\ \delta_2=\dfrac{\alpha h_0\beta b_0}{2}I_d\dfrac{(c-d)r_6+(e-f)r_5}{(a'^2+b'^2)\{(d-c)^2+(f-e)^2\}}\sqrt{1+\left[\dfrac{(c-d)r_3-(e-f)r_4}{(c-d)r_6+(e-f)r_5}\right]^2}. \end{cases}$$

Simplifying the above formulae,

$$(47)\quad \begin{cases} \tan\left(\beta_1+\dfrac{\pi}{4}\right)=\dfrac{\dfrac{p-1}{\lambda_0}e^{\alpha h_0}\sin\alpha h_0}{1-\dfrac{p-1}{\lambda_0}(e^{\alpha h_0}\cos\alpha h_0-1)}\,, \\ \tan\left(\beta_2+\dfrac{\pi}{4}\right)=\dfrac{-\dfrac{p-1}{\lambda_0}e^{-\alpha h_0}\sin\alpha h_0}{1-\dfrac{p-1}{\lambda_0}(e^{-\alpha h_0}\cos\alpha h_0-1)}\,, \\ \delta_1\fallingdotseq\dfrac{2b}{a^2+b^2}\dfrac{\lambda_0}{\rho}\dfrac{\beta}{\alpha}\pi^2 f I_0 10^{-9}\dfrac{1-\dfrac{p-1}{\lambda_0}(e^{\alpha h_0}\cos h_0-1)}{e^{\alpha h_0}\sin 2\alpha h_0} \\ \delta_2\fallingdotseq\dfrac{2\lambda_0}{a^2+b^2}\dfrac{1}{\rho}\dfrac{\beta}{\alpha}\pi^2 f I_0 10^{-9}\dfrac{a\sin\alpha h_0+b\cos\alpha h_0}{e^{\alpha h_0}\sin 2\alpha h_0} \\ \qquad\times\left\{1-\dfrac{p-1}{\lambda_0}(e^{\alpha h_0}\cos\alpha h_0-1)\right\}. \end{cases}$$

$$A_1=\sqrt{2}\,e^{\alpha x}\sqrt{\cosh 2\beta y+\cos 2\beta y}\,,\quad A_2=\sqrt{2}\,e^{-\alpha x}\sqrt{\cosh 2\beta y+\cos 2\beta y}\,,$$

$$\tan\psi_1=\frac{\cosh\beta y\cos\beta y\sin\alpha x+\sinh\beta y\sin\beta y\cos\alpha x}{\cosh\beta y\cos\beta y\cos\alpha x-\sinh\beta y\sin\beta y\sin\alpha x}\,,$$

$$\tan\psi_2=\frac{\cosh\beta y\cos\beta y\sin\alpha x-\sinh\beta y\sin\beta y\cos\alpha x}{\cosh\beta y\cos\beta y\cos\alpha x+\sinh\beta y\sin\beta y\sin\alpha x}\,,$$

the equation of current is obtained

$$(48)\quad i=\delta_1 A_1 \sin\left(\omega t+\beta_1+\frac{\pi}{4}+\psi_1\right)+\delta_2 A_2 \sin\left(\omega t+\beta_2+\frac{\pi}{4}+\psi_2\right).$$

The values of δ_1 and δ_2 are tabulated in Table III referring to the frequency and number of the conductors.

Table III.

($h=2$ cm, $a_0=4$ cm, $p_m=5$)

f	δ_1 ($p=2$)	δ_2 ($p=2$)	δ_1 ($p=3$)	δ_2 ($p=3$)	δ_1 ($p=4$)	δ_2 ($p=4$)	δ_1 ($p=5$)	δ_2 ($p=5$)
15	0.0398	−0.00105	0.089	−0.075	−0.135	−0.122	−0.184	−0.17
25	0.0483	−0.025	0.085	−0.053	0.186	0.025	0.2015	−0.136
60	0.0628	−0.0288	0.154	−0.070	0.23	−0.108	0.305	−0.146
100	0.157	+0.032	0.305	+0.0536	0.454	0.077	0.602	−0.099
500	−0.282	+0.47	−0.562	−0.945	−0.85	1.42	−1.13	−1.888
1000	0.2165	+0.0499	0.434	+0.099	0.65	0.148	0.864	0.197

Phase angles $\tan\left(\beta_1+\frac{\pi}{4}\right)$ and $\tan\left(\beta_2+\frac{\pi}{4}\right)$ are similarly tabulated in Table IV and expressed graphically as shown in Fig. 27 (a) and (b).

Table IV.

$$\text{I.}\quad \tan\left(\beta_1+\frac{\pi}{4}\right)=\frac{\frac{p-1}{\lambda}e^{\alpha h}\sin\alpha h}{1-\frac{p-1}{\lambda}(e^{\alpha h}\cos\alpha h-1)},$$

$$h=2\,\text{cm},\quad \lambda=0.9,\quad p=1,\quad \tan\left(\beta_1+\frac{\pi}{4}\right)=0$$

$$\text{II.}\quad \tan\left(\beta_2+\frac{\pi}{4}\right)=\frac{-\frac{p-1}{\lambda}e^{-\alpha h}\sin\alpha h}{1-\frac{p-1}{\lambda}(e^{-\alpha h}\cos\alpha h-1)}$$

$$h=2\,\text{cm},\quad \lambda=0.9,\quad p=1,\quad \tan\left(\beta_2+\frac{\pi}{4}\right)=0$$

cycles	I				II			
	$p=2$	$p=3$	$p=4$	$p=5$	$p=2$	$p=3$	$p=4$	$p=5$
15	5.21	173	−17.8	−11.45	−0.1774	−0.24	−0.2745	−0.2925
25	3.665	6.59	0.901	11.0	−0.1396	−0.185	−0.2067	−0.2205
60	1.222	1.327	1.368	1.385	−0.0565	−0.07325	−0.0813	−0.0860
100	0.445	0.46	0.464	0.467	−0.0171	−0.02267	−0.0255	−0.0270
500	0.326	0.3245	0.324	0.324	+0.0004	+0.00045	+0.0006	+0.0064
1000	−1.64	−1.642	−1.645	−1.647	−0.0001	−0.00013	−0.00015	−0.00016

These curves rise together with the increase of h_0, however curve (b) reaches the saturated state.

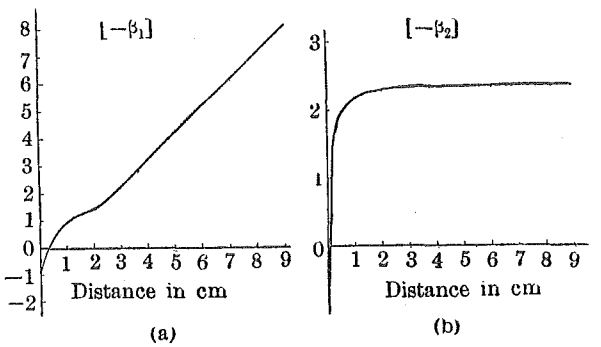

Fig. 27.

(4) IN THE CASE WHERE MANY CONDUCTORS ARE ARRANGED IN THE DIRECTION OF X- AND Y-AXES.

In the case where many conductors are inserted into the slot, p_0 conductors being laid in a row and $2q_0$ in a column as shown in Fig. 28, it must be suitable to apply the fundamental equation containing unknown constants δ_1, δ_2, δ_3, δ_4, β_1, β_2, β_3 and β_4. However, if the origin of x-axis is taken at the under part of every lateral row of conductors and the origin of y-axis is taken at the middle point of the width of the slot, then it is sufficient to determine four unknown constants δ_1, δ_2, β_1 and β_2, because there is symmetry to the x-axis in that case. Referring to the p-th conductor counting upward from those placed at the bottom of the slot, the expression

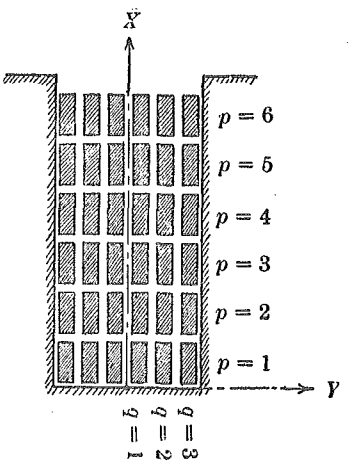

Fig. 28.

$$(49) \qquad 2\int_0^{\frac{1}{2}a_0} H_{y_{(x=0)}}\, dy = 2q_0(p-1)\times 0.4\pi I_0 \sin \omega t\ ,$$

may be obtained from the relation between the field intensity H_y at $x=0$ and the total current flowing in each of $2q_0$ conductors, where $2q_0$ is the total number of conductors in a lateral row and I_0 is the current passing through a single conductor.

Before the calculation is performed for the current and the field distribution at every conductor, one must give the number p-th and q-th to every conductor. The number p is given to every one counted from the bottom of the slot arranged in the lateral row. The number q is given to every one counted lateraly from the middle point of the width of slot.

In the case where the total number of conductors in the lateral row is even, the q-th conductor holds its position at the interval between $y=r=(q-1)b_0$ and $y=r+b_0$, while in the case of an odd number, it exists in the interval between $y=r=(q-1)b_0+\frac{1}{2}b_0=\left(q-\frac{1}{2}\right)b_0$ and $y=r+b_0$.

Therefore, referring to the p-th and q-th conductor, the next conditional equation about the total current may be obtained.

$$\int_r^{r+b_0}\int_0^{h_0} i\,dx\,dy = I_0 \sin\omega t\ . \tag{50}$$

Four constants δ_1, δ_2, β_1 and β_2 may be determined similarly formerly mentioned.

Putting

$$\begin{cases} a' = \cosh\beta(r+b_0)\sin\beta(r+b_0)-\cosh\beta r\sin\beta r\ , \\ b' = \sinh\beta(r+b_0)\cos\beta(r+b_0)-\sinh\beta r\cos\beta r\ , \\ g = \dfrac{a'^2+b'^2}{b'}\dfrac{b}{a^2+b^2}q_0(p-1)\dfrac{1}{\lambda_0}\ , \end{cases} \tag{51}$$

it follows

$$\tan\left(\beta_1+\frac{\pi}{4}\right)=\frac{eg}{1-gc}\ , \qquad \tan\left(\beta_2+\frac{\pi}{4}\right)=\frac{fg}{1-gd}\ ,$$

and

$$(52)\quad \begin{cases} \delta_1 = \dfrac{q_0}{a^2+b^2}\dfrac{p-1}{\rho}\dfrac{\beta}{\alpha}4\pi^2 f I_0 10^{-9}\dfrac{a\tan\left(\beta_2+\frac{\pi}{4}\right)-b}{\tan\left(\beta_2+\frac{\pi}{4}\right)-\tan\left(\beta_1+\frac{\pi}{4}\right)} \\ \qquad \times\sqrt{1+\tan^2\left(\beta_1+\frac{\pi}{4}\right)} \\ \delta_2 = \dfrac{q_0}{a^2+b^2}\dfrac{p-1}{\rho}\dfrac{\beta}{\alpha}4\pi^2 f I_0 10^{-9}\dfrac{a\tan\left(\beta_1+\frac{\pi}{4}\right)-b}{\tan\left(\beta_2+\frac{\pi}{4}\right)-\tan\left(\beta_1+\frac{\pi}{4}\right)} \\ \qquad \times\sqrt{1+\tan^2\left(\beta_2+\frac{\pi}{4}\right)}\,. \end{cases}$$

(5) SO-CALLED "ALTERNATING CURRENT RESISTANCE".

Joule's loss developed in the slot conductor is expressed by

$$(53)\qquad \frac{1}{2\pi}\int_0^{2\pi} i^2\rho\, d(\omega t) \qquad \text{watt / unit volume}$$

where i is the current across the section of unit area of the slot conductor. If the amplitude of the current density i is described by $\sqrt{2}I_{AC}$, then the power loss per unit volume may be expressed by $I_{AC}^2\rho$. It is sure that the power loss is the function of x and y because the current is not uniform in the section of conductor. The mean value of the A.C. intensity is defined as

$$\bar{I}_{AC} = \frac{\int I_{AC}\, ds}{\int ds}$$

where the integration with ds is performed all over the cross section.

Now the direct current density I_{DC} is used instead of $\bar{I}_{AC}$. Then the power loss per unit volume is expressed by $I_{DC}^2\rho$. If the ratio of power losses of A.C. against D.C. is denoted by k, one obtains

$$(54)\qquad k = \frac{I_{AC}^2\rho}{I_{DC}^2\rho} = \left(\frac{I_{AC}}{I_{DC}}\right)^2.$$

It is sure that this ratio k is generally expressed by the function of x, y in the case of non-uniform current distribution in the conductor

and it may be called "Alternating current resistance", because this ratio can be substituted for the increment of unit power loss due to non-uniform current distribution.

Now put

$$I_{AC\,\mathrm{mean}} = I_{DC} = \frac{I_0}{\sqrt{2}\,h_0 b_0}, \tag{55}$$

where I_0 is the amplitude of total current of A.C..

Therefore

$$k = 2(b_0 h_0)^2 \left(\frac{I_{AC}}{I_0}\right)^2 .$$

The expression

$$K = 2\left(\frac{b_0 h_0}{I_0}\right)^2 \int_0^{h_0}\int_0^{b_0} I_{AC}^2\, dx\, dy ,$$

denotes the increment of unit power loss referring to the whole section of conductor.

When the single conductor is inserted into the slot, the effective value of current is expressed by $\delta_0 A$ from the equation already mentioned. In this case, k is:

$$k = 2\delta_0 A^2 \left(\frac{b_0 h_0}{I}\right)^2 ,$$

$$k = (\alpha b_0 \beta b_0)^2 \frac{(\cosh 2\alpha x + \cos 2\alpha x)(\cosh 2\beta y + \cos 2\beta y)}{(\cosh 2\alpha h_0 - \cos 2\alpha h_0)(\cosh \beta b_0 - \cos \beta b_0)} , \tag{56}$$

"Alternating current resistance" referred to the whole section

$$K = \frac{1}{2}\alpha h_0 \beta b_0 \frac{(\sinh 2\alpha h_0 + \sin 2\alpha h_0)(\sinh \beta b_0 + \sin \beta b_0)}{(\cosh 2\alpha h_0 - \cos 2\alpha h_0)(\cosh \beta b_0 - \cos \beta b_0)} . \tag{57}$$

Now, neglecting $\cos 2\alpha x$ and $\cos 2\beta y$ with reference to $\cosh 2\alpha x$ and $\cosh 2\beta y$ respectively in formula (56), the reduced formula is obtained

$$k \fallingdotseq (\alpha h_0 \beta b_0)^2 \frac{\cosh 2\alpha x \cosh 2\beta y}{\cosh 2\alpha h_0 \cosh \beta b_0} . \tag{58}$$

At the curve where $k = 1$, the current density of every point on this curve is equal to the mean current density. For the purpose of

finding the locus $k=1$, the condition $k=1$ is inserted into formula (58), then the equation can be obtained as follows;

$$\cosh 2\alpha x \cosh 2\beta y = \frac{\cosh 2\alpha h_0 \cos \beta b_0}{\alpha^2 h_0^2 \beta^2 b_0^2} ,$$

and moreover, simplifying the equation, one obtains

$$\alpha x+\beta y = \alpha h_0+\frac{1}{2}\beta b_0-\log_e(\alpha h_0 \beta b_0) .$$

From this formula, it can be ascertained that x and y may keep the linear relation if f, h_0 and b_0 are taken to be constant. Since the gradient of this line is denoted by $\frac{\alpha}{\beta}$ and the term $\frac{\alpha}{\beta}$ contains no frequency terms, therefore it can be ascertained that the gradient of the line $x=f(y)$ is independent of the frequency of the source.

From (15), one obtains

$$\lambda_0 = \frac{b_0}{a_0} \qquad \text{and} \qquad \frac{\alpha}{\beta}\sqrt{\frac{\lambda_0}{1-\lambda_0}} .$$

Referred to the gradient of locus of mean current, it follows

$$\tan\theta = \frac{\alpha}{\beta} , \qquad \theta = \arctan\sqrt{\frac{\lambda_0}{1-\lambda_0}}$$

where θ is the angle between the straight line and x-axis.

By the condition $\lambda_0=1$, it is meant that there exists no side clearance between the conductor and the slot. In this case, $\theta=\frac{\pi}{2}$ means that the line is a horizontal straight line. However, if the side clearance between them is increased gradually, then θ decreases gradually till it attains to 0 in accordance with $\lambda_0 \to 0$.

To find the value of x at the point where the locus of $k=1$ intersects with the x-axis, $y=0$ is inserted into the above formula, then

$$x = h_0+\frac{1}{2}\frac{\beta}{\alpha}b_0-\frac{1}{\alpha}\log_e(\alpha h_0 \beta b_0) \tag{59}$$

may be obtained. The first and second terms of the right hand in the equation are independent of the frequency, but only the third term depends on the frequency. The second term depends on λ_0.

In order to discuss the relation between the frequency and the intersecting value to x-axis thus obtained, the following formula is used

$$(60) \qquad x = h_0 + \frac{1}{2}\frac{S}{h_0}\sqrt{\frac{1-\lambda_0}{\lambda_0}} - \frac{1}{2\pi}\sqrt{\frac{\rho}{f\lambda_0}}10^9 \times \log_e\left[4\pi^2\frac{f}{\rho}\sqrt{\lambda_0(1-\lambda_0)}S\,10^{-9}\right]$$

where the sectional area of the slot conductor is taken as constant such as:—

The first and second terms are the function of h_0, and x increases together with h_0 and also the third term contains the frequency f. Putting $S = 20$ cm^2, $\lambda_0 = 0.9$, $h_0 = 8$ cm and $\rho = 2\times10^{-6}$, the formula is reduced:—

$$x = 8.416 - 7.5\frac{1}{\sqrt{f}}\log_e 0.118f\ .$$

This formula is described graphically as shown in Fig. 29 where the intersecting point falls with the increase of the frequency f, but attains to the minimum point and then rises together with the increase of f.

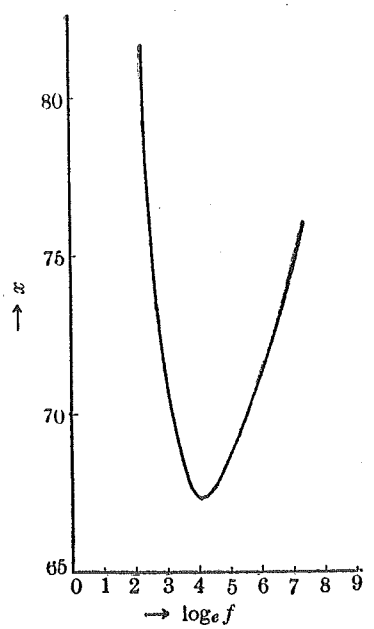

Fig. 29.

In order to obtain the minimum point due to the variation of the frequency, putting $\frac{dx}{df} = 0$, the formula is obtained

$$\log_e\left[4\pi^2\frac{f}{\rho}\sqrt{\lambda_0(1-\lambda_0)}S\,10^{-9}\right] = 2$$

and from that,

$$f = \frac{e^2}{4\pi^2\frac{1}{\rho}\sqrt{\lambda_0(1-\lambda_0)}S\,10^{-9}}\ .$$

The value of S corresponding to the minimum point may be given as follows;

$$x = h_0 + \frac{1}{2}\frac{S}{h_0}\sqrt{\frac{1-\lambda_0}{\lambda_0}} - 0.23\sqrt{S}\sqrt[4]{1-\lambda_0}\ .$$

Inserting the numerical values

$h_0 = 8$ cm, $\lambda_0 = 0.9$, $S = 20$ cm^2 and $\rho = 2\times 10^{-6}$ ohm, cm,

then one obtains $f = 62.3$ and $x = 7.837$ cm.

If $\frac{dx}{dh_0} = 0$ is inserted in the formula, to find the minimum value of x due to the variation of h_0 and if it is assumed that $S = \text{const.}$, then the expression may be obtained.

$$h_0 = \frac{1}{\sqrt{2}}S\sqrt[4]{\frac{1-\lambda_0}{\lambda_0}}\ .$$

In this case, from the formula

$$x = h_0 + \sqrt{\frac{S}{2}}\sqrt[4]{\frac{1-\lambda_0}{\lambda_0}} - \frac{1}{2\pi}\sqrt{\frac{\rho}{f\lambda_0}}10^9\log_e\left[4\pi^2\frac{f}{\rho}\sqrt{\lambda_0(1-\lambda_0)}S10^{-9}\right]$$

the minimum value referred to x at $h_0 = 1.825$ cm. can be found.

Next, referring to "Alternating current resistance" K about the whole section of conductor, the formula can be simplified as follows,

$$K \fallingdotseq \tanh 2\alpha h_0 \tanh \beta b_0 \frac{1}{2}\alpha h_0 \beta b_0\ .$$

K is determined from h, b, f and λ_0.

In the case where the area of the cross section of the conductor

$$S = h_0 b_0$$

is given, it is necessary for technical uses to find how one makes the "Alternating current resistance" to be minimum by selecting of the dimension of conductor h_0 and b_0.

Therefore put $\zeta = h_0 b_0 - S$. As K is expressed by the functions of x and y individually, the conditional formula is given as follows;

$$\delta K = \left[\frac{\partial K}{\partial h_0} - \lambda\frac{\partial \zeta}{\partial h_0}\right]\delta h_0 + \left[\frac{\partial K}{\partial b_0} + \lambda\frac{\partial \zeta}{\partial b_0}\right]\delta b_0 = 0\ .$$

From the above formula, two equations are obtained

$$\frac{\partial K}{\partial h_0}-\lambda\frac{\partial \zeta}{\partial h_0}=0\,,\qquad \frac{\partial K}{\partial b_0}+\lambda\frac{\partial \zeta}{\partial b_0}=0\,,$$

where λ is an arbitrary constant.

If the above two equations are inserted into K-formula and the arbitrary constant λ is eliminated, then

$$2\alpha h_0=\beta b_0 \qquad \text{and} \qquad h_0=\sqrt{\frac{1-\lambda_0}{\lambda_0}}\,\frac{b_0}{2}\,.$$

If the area of the cross section of the conductor is given, the relation between the dimensions h_0 and b_0 can be found under the condition of the minimum value of K. The formula denoting this relation, is applied to the ones having arbitrary frequency, because it contains no frequency. It must depend on λ_0 alone. λ_0 exists on the interval $0<\lambda_0<1$ and if the sectional area of conductor S is constant, h_0 may be smaller than b_0 with increasing of λ_0. If $\lambda_0=0.9$ is taken, then $h_0=b_0/6$. Hence it is ascertained that the height of the slot must keep to one-sixth of its width for the sake of the minimum "alternating current resistance".

The function K is expressed by the product of two functions which contain h_0 or b_0 respectively and therefore the limit of h_0 and b_0 is investigated in which K is considered to be constant.

Referring to the function containning h_0, formula (57) is written approximately,

$$\alpha h_0\,\frac{\sinh 2\alpha h_0+\sin 2\alpha h_0}{\cosh 2\alpha h_0-\cos 2\alpha h_0}\fallingdotseq \alpha h_0\tanh 2\alpha h_0\,.$$

The value of αh_0 keeping the condition $\alpha h_0\tanh 2\alpha h_0=1$, is found as follows

$$\tanh 2\alpha h_0\fallingdotseq 2\alpha h_0-\frac{8}{3}\alpha^3 h_0^3+\cdots\cdots$$

and neglecting the higher order than the second, one obtains

$$2\alpha^2 h_0^2=1 \qquad \text{and} \qquad \alpha h_0=\sqrt{\frac{1}{2}}=0.707.$$

Therefore, until $\alpha h_0=0.707$, the "Alternating current resistance" K is taken as a constant. Similarly, referring to βb_0,

$$\frac{1}{2}\beta b_0 \tanh \beta b_0 = 1 \qquad \text{and} \qquad \beta b_0 = \sqrt{2} = 1.414 .$$

Therefore K is taken as constant until $\beta b_0 = 1.414$. Thus

$$h_0 = 0.707 \frac{1}{2\pi} \sqrt{\frac{\rho}{f\lambda_0}\, 10^9} ,$$

$$b_0 = 1.414 \frac{1}{2\pi} \sqrt{\frac{\rho}{f(1-\lambda_0)}\, 10^9} .$$

If $f = 60$ cycles and $\lambda_0 = 0.9$, then $h_0 = 0.685$ and $b_0 = 2.9 \times 1.414 = 4.1$. In the case of arbitrary frequency,

$$h_0 = 0.685 \frac{1}{\sqrt{f}} \qquad \text{and} \qquad b_0 = 4.1 \frac{1}{\sqrt{f}}$$

that is:— they are inversely proportional to the square root of the frequency. If θ expresses the angle between these lines and the horizontal line, the formulae are given

$$\theta_{h_0} = \arctan \sqrt{2\pi \frac{f}{\rho} \lambda_0 10^{-9}} ,$$

$$\theta_{b_0} = \arctan \frac{\beta}{2} \fallingdotseq \arctan \pi \sqrt{\frac{f}{\rho}(1-\lambda_0) 10^{-9}} .$$

Putting $f = 50 \sim 60$ cycles, then one obtains $\theta_{h_0} = 45°$, $\theta_{b_0} = 9.55°$. Referring to any arbitrary frequency f, it follows

$$\theta_{h_0} = \arctan \sqrt{f} \qquad \text{and} \qquad \theta_{b_0} = \arctan \frac{1}{6} \sqrt{f} .$$

In the case where many conductors are ranged in the direction of x-axis, formula (48) about the current distribution is found already.

From (53)

$$\frac{1}{2\pi} \int_0^{2\pi} i^2 d(\omega t) = \frac{1}{2}\delta_1^2 A_1^2 + \frac{1}{2}\delta_2^2 A_2^2 + \frac{1}{2}\delta_1\delta_2 A_1 A_2 \cos(\beta_1 - \beta_2 + \psi_1 + \psi_2) .$$

Hence the "Alternating current resistance" may be given as follows

$$k = \frac{2(b_0 h_0)^2}{I_0^2} \frac{1}{2\pi} \int_0^{2\pi} i^2 \, d(\omega t) .$$

Putting

$$R_0 = (c-d)^2+(e-f)^2\,, \qquad R_1 = (c-d)r_1-(e-f)r_2\,,$$
$$R_2 = (c-d)r_3-(e-f)r_4\,, \qquad R_3 = (e-f)r_3+(c-d)r_4\,,$$
$$R_4 = (e-f)r_5+(c-d)r_6\,,$$

then

$$k = \frac{(\alpha h_0 \beta b_0)^2}{2}\frac{\cosh 2\beta y+\cos 2\beta y}{(a'^2+b'^2)R_0^2}\Big[(R_1^2+R_3^2)e^{2\alpha x}+(R_2^2+R_4^2)e^{-2\alpha x}$$
$$+2(R_3R_4+R_1R_2)\cos 2\alpha x-2(R_1R_4-R_2R_3)\sin 2\alpha x\Big]\,,$$

$$K = \frac{(\alpha h_0 \beta b_0)^2}{2}\frac{1}{2\alpha\beta}\frac{\sinh 2\beta b_0+\sin 2\beta b_0}{(a'^2+b'^2)}\frac{1}{R_0^2}\Big[(R_1^2+R_3^2)(e^{2\alpha h_0}-1)$$
$$+(R_2^2+R_4^2)(1-e^{-2\alpha h_0})+(R_3R_4+R_1R_2)\sin 2\alpha h_0$$
$$-(R_1R_4-R_2R_3)(1-\cos 2\alpha h_0)\Big]\,.$$

In the case where many conductors are ranged in the direction of x- and y-axes, put

$$R_1 = 1+\frac{b'}{a'^2+b'^2}\frac{a^2+b^2}{b}\frac{\lambda_0}{q_0(p-1)}-e^{\alpha h_0}\cos\alpha h_0\,,$$
$$R_2 = 1+\frac{b'}{a'^2+b'^2}\frac{a^2+b^2}{b}\frac{\lambda_0}{q_0(p-1)}-e^{-\alpha h_0}\cos\alpha h_0\,,$$
$$R_3 = e^{\alpha h}\sin\alpha h_0\,, \qquad R_4 = -e^{-\alpha h_0}\sin\alpha h_0\,,$$

then

$$k = 2(h_0 b_0)^2\frac{q_0^2}{(a^2+b^2)^2}\left(\frac{\beta}{\alpha}\right)^2\frac{\pi^2\omega^2}{\rho^2}10^{-18}\,.$$
$$\times\frac{\cosh 2\beta y+\cos 2\beta y}{\left\{2\left(p-1+\frac{b'}{a'^2+b'^2}\frac{a^2+b^2}{b^2}\frac{\lambda_0}{q_0}\right)\cosh\alpha h_0\sin\alpha h_0-(p-1)\sin 2\alpha h_0\right\}^2}$$
$$\times\Big[(aR_4-bR_2)^2(R_1^2+R_3^2)(p-1)^4(\cosh 2\alpha x+\sinh 2\alpha x)$$
$$+(aR_3-bR_1)^2(R_2^2+R_4^2)(p-1)^4(\cosh 2\alpha x-\sinh 2\alpha x)$$
$$+(aR_4-bR_2)(aR_3-bR_1)(R_1R_2+R_3R_4)(p-1)^4\cos 2\alpha x$$
$$+(aR_4-bR_2)(aR_3-bR_1)(R_2R_3-R_1R_4)(p-1)^4\sin 2\alpha x\Big]$$

and

$$K=\frac{h_0b_0}{2}\frac{q_0}{a^2+b^2}\frac{1}{\rho^2}\frac{\beta}{\alpha^3}\pi^2\omega^2 10^{-18}$$
$$\times\frac{\sinh 2\beta(r+b_0)-\sinh 2\beta r(r+b_0)\sin 2\beta r}{\left\{2\left(p-1+\frac{b'}{a'^2+b'^2}\frac{a^2+b^2}{b}\frac{\lambda_0}{q_0}\right)\cosh ah_0\sin ah_0-(p-1)\sin 2ah_0\right\}^2}$$
$$\times\Big[(aR_4-bR_2)^2(R_1^2+R_3^2)(p-1)^4(\sinh 2ah_0+\cosh 2ah_0-1)$$
$$+(aR_3-bR_1)^2(R_2^2+R_4^2)(p-1)^4(\sinh 2ah_0-\cosh 2ah_0+1)$$
$$+(aR_4-bR_2)(aR_3-bR_1)(R_1R_2+R_3R_4)(p-1)^4\sin 2ah_0$$
$$+(aR_4-bR_2)(aR_3-bR_1)(R_2R_3-R_1R_4)(p-1)_4(\cos 2ah_0-1)\Big].$$

(6) NUMERICAL EXAMPLE.

As the numerical example of the distribution of current in the slot conductor, the dimensions of the slot and slot conductors of a 31,000 kVA, 11,000 V synchronous alternator at a hydro-electric power station for railway service are shown in Fig. 30 and the numerical constants and dimensions are:—

$$a_0=2.2\text{ cm},\qquad b_0=1.04\text{ cm},\qquad h_0=1.3\text{ cm},$$
$$f=50\text{ cycles},\qquad \rho=2\times10^{-6}\,\Omega\text{ cm}.$$

From the above numerical values, the distribution coefficients may be obtained as follows:—

$$\alpha_\nu=0.683,$$
$$\beta_\nu=0.721.$$

α_ν is smaller and β_ν is larger than the examples before described, because the insulation thickness becomes thicker than the ones before described.

The distribution of the current density of each conductor ($p=1, 2, 3, \ldots, 6$) may be obtained by inserting these values into the formulae above described. The current distribution of

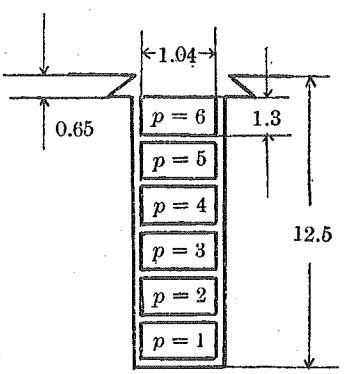

Fig. 30.

the conductor from $p = 1$ to $p = 6$ are shown in Fig. 31 as the results of the calculation.

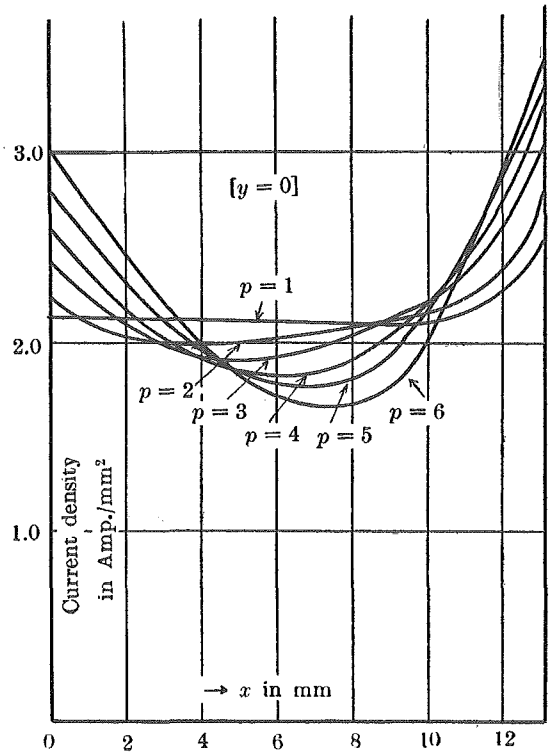

Fig. 31.

(7) EXPERIMENTAL INVESTIGATION.

It is difficult to measure the field and the current distribution in the slot conductor of an electric machine already constructed. Therefore the apparatus as shown in Fig. 32a is used, which forms one part of the armature constituted of the sheet iron, and this apparatus is made to resemble the armature as much as possible, having the slot in its surface and copper winding in it. The copper conductor has the dimensions 50 mm × 2 mm and is arranged laterally in the slot as shown in Fig. 32(b). As the disturbances due to the end effect in such a small apparatus, can not be eliminated, the experiment is performed only about the slot at the middle part of this apparatus.

For studying the density of the current and the intensity of the field along the x-axis continuously, a searching contactor or coil is

made as shown in Fig. 33 (a) and (b), and it is drawn up gradually from the bottom of the slot using a gear specially designed as shown in Fig. 33 (c).

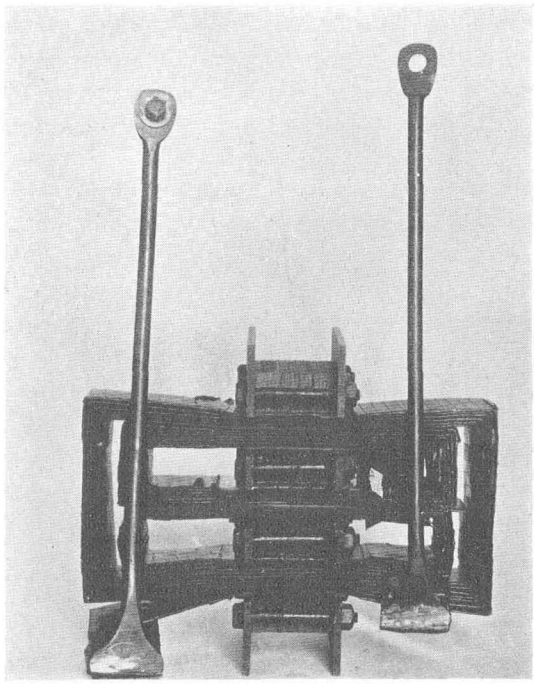

Fig. 32 (a).

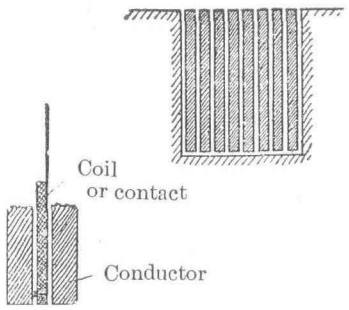

Fig. 32 (b).

The contactor shown in Fig. 33 (a) is made of a thin bakelite plate and contains two metal contact points. By this contactor, the voltage

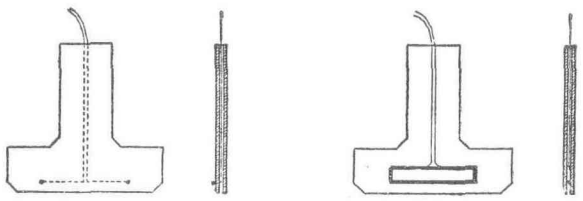

(a) (b)

Fig. 33.

drop along the two point contacts is observed or automatically recorded by an electric meter or oscillograph. The reading of the meter thus

obtained, is calibrated from several experiments by means of known density of direct current.

The search coil shown in Fig. 33 (b) is similarly made of the same materials as the above case, but it has a rectangular plane coil instead of two point contactors. By using this coil, the field intensity along the side surface of the slot conductor can be observed. Oscillograph and string galvanometer are suitable to record the current density and the field intensity automatically, if the search coil is made so as to be suitable to get the moderate deflection by adjustment of the number of turns in the coil.

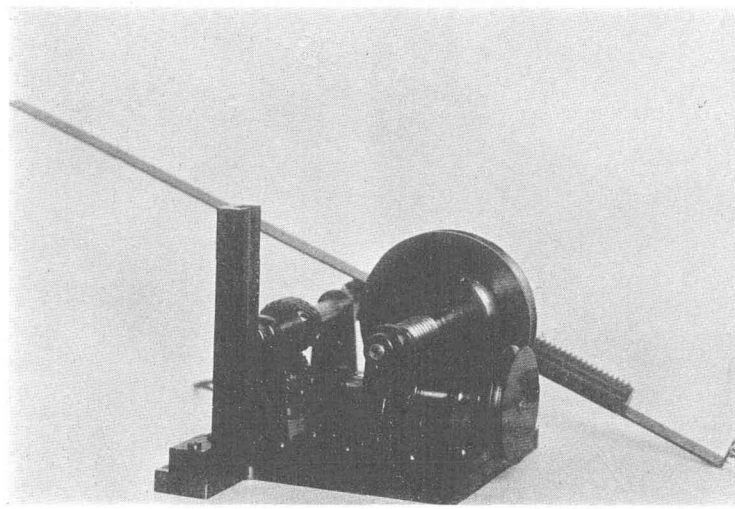

Fig. 33 (c).

When the distribution of current is measured by using the contactor, the voltage drop between the two contact points may be insufficient to drive the vibrating element of the oscillograph if the current is small. In such a case the string galvanometer is used.

In order to make the lateral scale of photographic paper correspond to the scale along the height of the slot conductor accurately, the apparatus is used for the gear coupling as shown in Fig. 33 (c). The rotation of drum carrying the photographic paper is transmitted to the linear motion drawing up the search contactor or coil by the gear coupling. If the drum carrying the photographic paper is rotated by a small motor and the deflection, i.e., the spot light of the oscillograph or string galvanometer is projected on the rotating drum passing through a cylindrical lens, then the current density corresponding to

every point along the height of the slot conductor is expressed by the deflection on the photographic paper.

(A) FIELD DISTRIBUTION IN THE CASE OF D.C.

Current density is uniform in the case of direct current and if the field intensity is measured with a ballistic galvanometer, then the

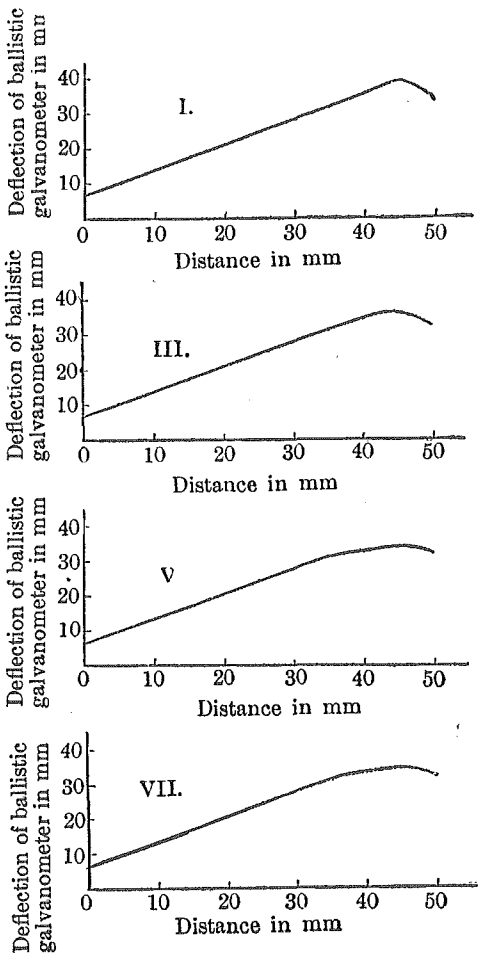

Operating current : D.C. 18 amps., Search coil: 350 turns

Fig. 34.

results may be obtained as shown in Fig. 34 where the number of turns of the search coil is 350 and a direct current of 18 amperes flows in each conductor.

The field distributions as shown in Fig. 35 are obtained from the experiments with the conductor placed at the central position in the case where the currents are 40, 60, 76 and 96 amperes respectively. From these experimental results, it is ascertained that the field intensity rises linearly with the height of the slot conductor.

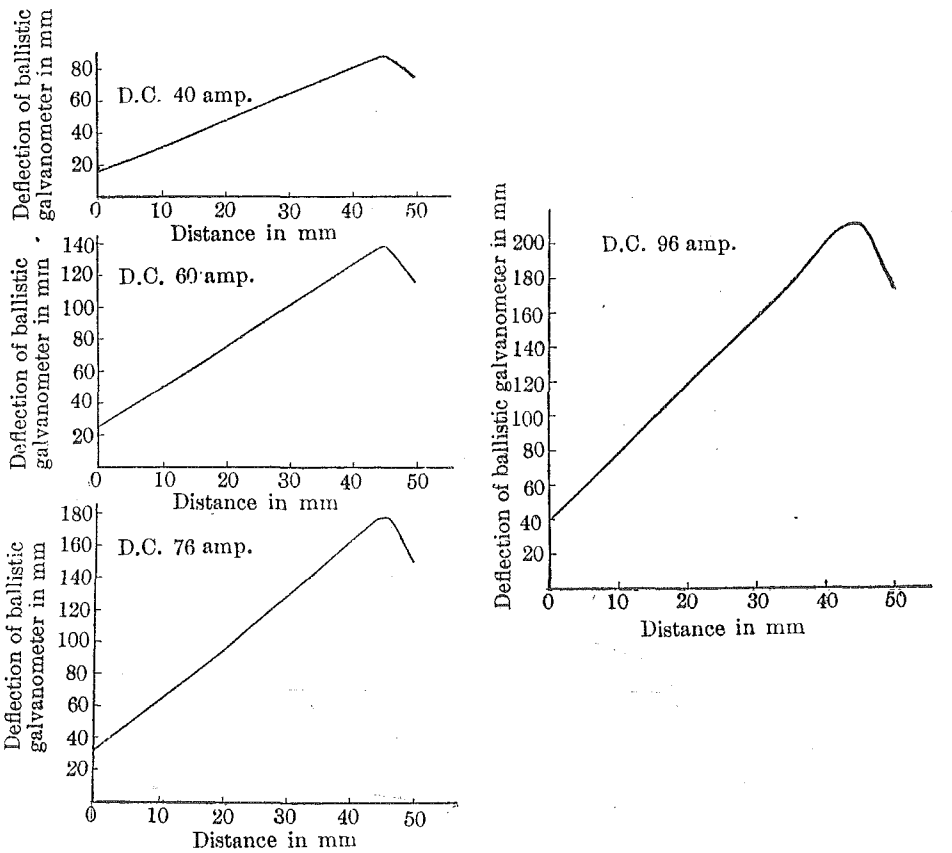

Fig. 35.

(B) CURRENT AND FIELD DISTRIBUTION IN THE CASE OF 60 CYCLES.

In this case the figures obtained are automatically recorded on the oscillogram by using the reduction gear above described.

The results in which the current of 200 amperes is used, are shown in Fig. 36 and indicate that the current density increases with

the height of slot conductor. Photographs in Fig. 36 are arranged in the order of 1–3–5–7–9–11 numbering from the one which is placed at the slot wall. Similarly the field distributions in the case of Fig. 36 are shown in Fig. 37.

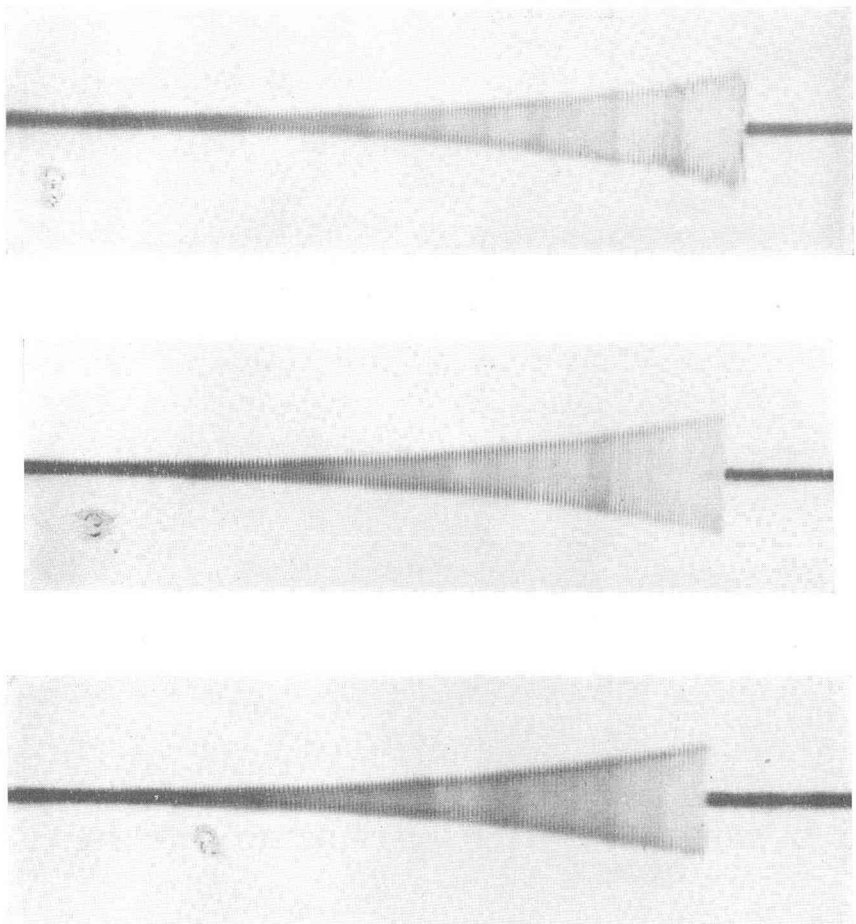

Fig. 36 (a).

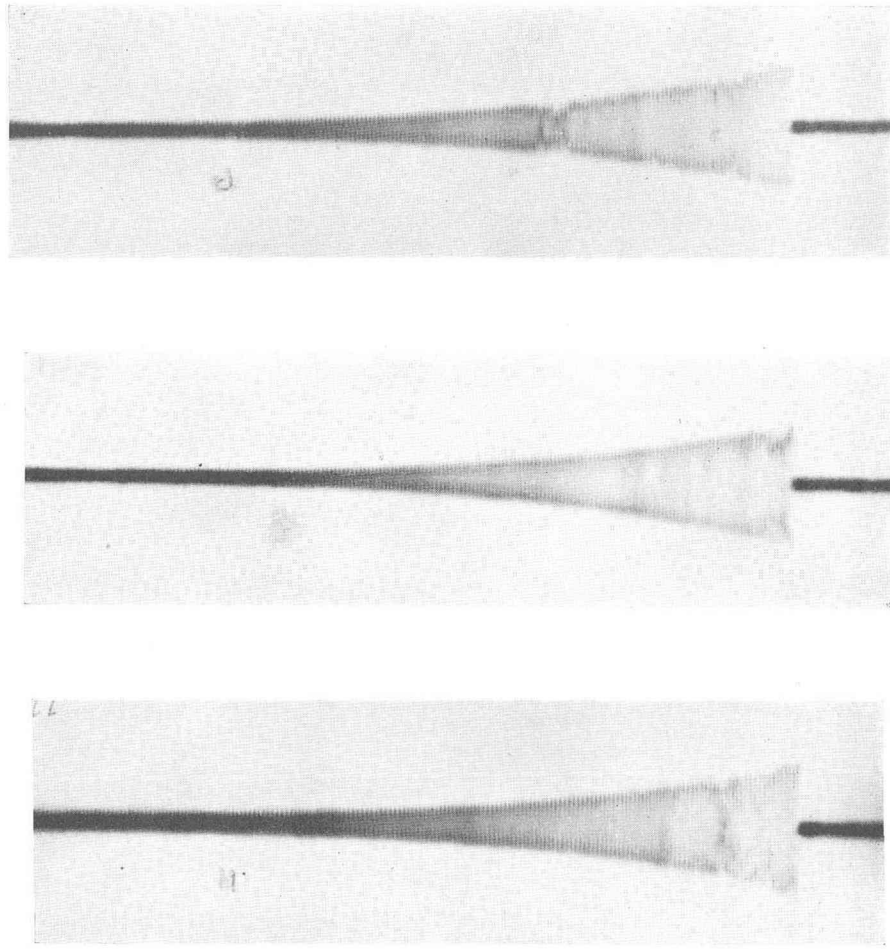

Fig. 36 (b).

(C) CURRENT AND FIELD DISTRIBUTION IN THE CASE OF 500 CYCLES.

The current and field distributions are shown in Fig. 38 and 39 respectively at 500 cycles, denoting extremely increasing character at the upper part of the conductor.

The field and current distributions in the slot conductor are explained already by the mathematical calculation and now by the

experimental investigation. The current distribution in the slot conductor is considered to be the one corresponding to the distribution of the heat sources developed in the slot conductor. Therefore by

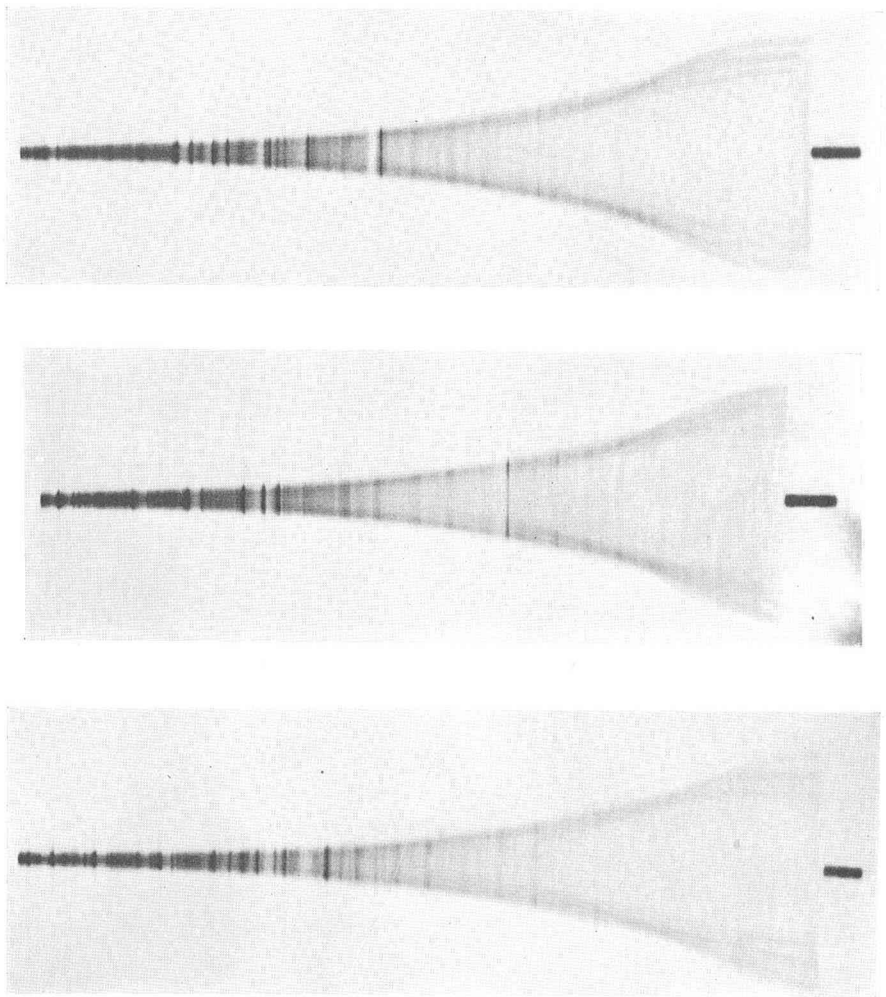

Fig. 37.

using this calculation, the temperature distribution in the slot may be easily calculated by finding these heat losses in the slot and the thermal condition surrounded the slot conductor.

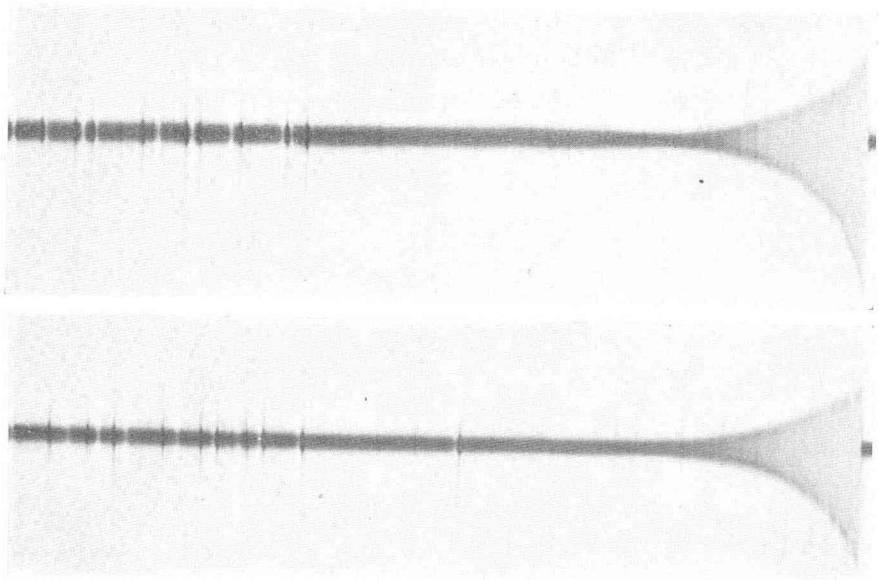

Fig. 38.

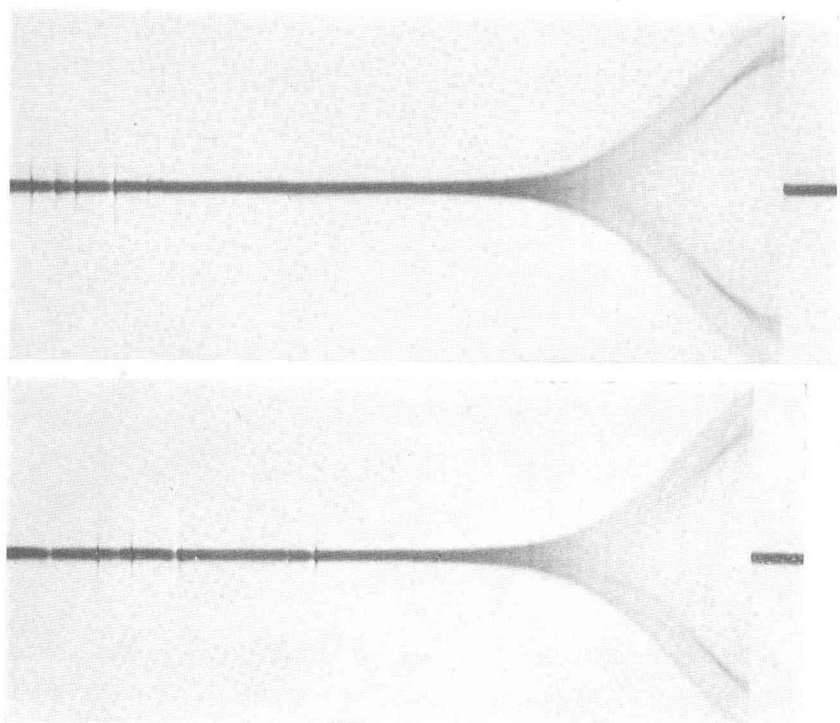

Fig. 39.

CHAPTER V.

TEMPERATURE DISTRIBUTION IN THE SLOT WINDING.

It is very difficult to measure directly the inner temperature of the slot by inserting a thermo-couple into the slot, because there exist great technical difficulties to insert a thermo-couple and such a technical operation can not be applied to an electric machine already constructed. Therefore the inner temperature of the slot is found only by mathematical calculation upon some special construction of the slot, when the power loss and the circumferential condition of the slot are given. The temperature in the slot may be decided by the power loss dissipated in the slot and the temperature at the outer circumference of the slot and also the thermal constants of material at the inner and the outer parts of the slot.

At the beginning, if the power loss is assumed to be distributed uniformly and also the heat to be diffused uniformly from the boundary of the slot, then it can be found that the temperature will be maximum at the centre of the slot. Besides the temperature is assumed to be gradually higher approaching to the centre of the armature, i.e., approaching to the bottom of the teeth, and then the highest temperature may be obtained at the bottom of the slot. Indeed, such a statement has been justified, that the temperature is the highest at the bottom of the teeth.

Next as for the power loss developed in the slot it may be distributed uniformly in the section of the slot conductor in the case of the direct current, but the power loss can not be considered to be uniform in the case of the alternating current, because the current density is not uniform in the section of the slot conductor and the maximum value of the current density must exist on the upper side of the slot conductor on account of the skin effect on the iron core and the teeth surrounding the slot.

In this chapter, the problem of the temperature in the slot is classified into the cases of no-loaded and loaded, and again the case of loading is classified into that of D.C. and A.C. In every case, the temperatures are found from the calculation varying the shape of the slot and the arrangement of the conductor in it. Specially attention is paid to the distribution of power loss due to the current distribution in the slot conductor.

(1) FUNDAMENTAL EQUATION OF HEAT CONDUCTION AND THE TEMPERATURE IN THE CASE OF NO-LOAD.

Fundamental equations of heat conduction known in general are as follows:—

$$(1) \qquad q = -\sigma \operatorname{grad} T ,$$

$$(2) \qquad \operatorname{div} q + Q = c\gamma \frac{\partial T}{\partial t} ,$$

where

q = density of heat current in watt/cm².
σ = thermal conductivity in watt/cm, °C.
Q = heat quantity in watt/cm²,
c = specific heat in watt, sec/gr, °C.
γ = density of material in gr/cm³.
T = inner temperature of conductor in °C.

In the case where the stationary state is alone considered, fundamental equation (3) from (1) and (2) is obtained as follows:—

$$(3) \qquad \Delta T = \frac{Q}{\sigma}$$

where the problem is considered to be two dimensional, and

$$\Delta = \operatorname{div} \cdot \operatorname{grad} = \frac{\partial^2}{\partial x^2} + \frac{\partial^2}{\partial y^2} ,$$

$$(4) \qquad Q = \frac{I_{max}^2}{2} \frac{\rho}{(b_0 h_0)^2} k , \qquad \rho = \rho_0(1+\alpha_0 T) .$$

K is the ratio of resistance in the case of A.C. and D.C.. This ratio is precisely discussed in chapter IV and it is expressed on the function (x, y) in general. The notations referred to in Fig. 40 are as follows:—

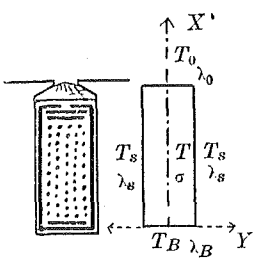

Fig. 40.

b_0 = width of slot in cm.
h_0 = depth of slot in cm.
ρ_0 = specific resistivity of slot winding in ohm, cm.
α_0 = temperature coefficient of resistance about slot winding.
T_s = mean temperature of teeth in °C.

Putting $$W = T - T_s ,$$

$$S_1 = \frac{I_{max}^2}{2\sigma} \frac{\rho_0}{(b_0 h_0)^2}(1+\alpha_0 T_s) ,$$

and

$$S_2 = \frac{I_{max}^2}{2\sigma} \frac{\rho_0 \alpha_0}{(b_0 h_0)^2} ,$$

and also combining (3) and (4), one obtains equation (5) as follows

$$(5) \qquad \frac{\partial^2 W}{\partial x^2} + \frac{\partial^2 W}{\partial y^2} = (S_1 + S_2 W)\, k(x, y)$$

where as k denotes the distribution of current in the slot from chapter IV, it depends on the distribution of heat source in the slot, and the constants S_1 and S_2 contain the temperature coefficient of resistance. If constant S_2 is put at zero, the solution of this equation may be simplified, but the temperature coefficient α_0 should not be neglected in the copper conductor compared with one of other material, because copper has a large temperature coefficient of resistance.

The equation may be established in the case of no-load as follows

$$(6) \qquad \frac{\partial^2 W}{\partial x^2} + \frac{\partial^2 W}{\partial y^2} = 0 .$$

This equation must be solved before the equation of loading is solved.

Both solutions of equations (5) and (6) must satisfy the boundary conditions (i), (ii), (iii) and (iv) for the slot having the notations as shown in Fig. 40.

If the mean temperature of teeth is denoted by T_s, the temperature of the core at the bottom of slot T_B and the temperature at the air gap by T_0, then four boundary conditions may be obtained as follows;

(i) at $x = 0 , \quad y = y ,$

$$\frac{\partial W}{\partial x} = \frac{\lambda_B}{\sigma}\left[W + (T_s - T_B)\right]$$

(ii) at $x = h_0 , \quad y = y ,$

$$-\frac{\partial W}{\partial x} = \frac{\lambda_0}{\sigma}\left[W + (T_s - T_0)\right]$$

(iii) at $x = x$, $y = +b_0/2$,

$$-\frac{\partial W}{\partial y} = \frac{\lambda_s}{\sigma} W$$

(iv) at $x = x$, $y = -b_0/2$,

$$+\frac{\partial W}{\partial y} = \frac{\lambda_s}{\sigma} W .$$

Boundary conditions (i), (ii), (iii) and (iv) are satisfied by the heat delivery through the insulating materials at the boundaries between the slot and the iron core, the slot and the air gap, and also the slot and both sides of teeth respectively. Constants λ_B, λ_0 and λ_s can not keep the constant value at any temperature, however they are taken as constants here, because only the case of stationary state is treated.

The solution of equation (6): no-load solution may be represented as follows:—

$$V = \left[A_\nu e^{2n_\nu \frac{h_0}{b_0}\left(1-\frac{x}{h_0}\right)} + B_\nu e^{2n_\nu \frac{h_0}{b_0}\frac{x}{h_0}}\right] \cos n_\nu \frac{2}{b_0} y$$

where the temperature is written with V instead of W, and also A_ν and B_ν are arbitrary constants to be determined from boundary conditions (i) and (ii). The value of n_ν is decided from boundary conditions (iii) and (iv). The no-load solution V must be satisfied by boundary conditions (iii) and (iv), hence

$$n_\nu \tan n_\nu = \frac{\lambda_s}{\sigma}\frac{b_0}{2} .$$

Let the roots of this equation be denoted by $n_1, n_2, n_3, \ldots, n_\nu, \ldots$ and if the following notations are used

$$m_\nu = 2n_\nu \frac{h_0}{b_0}, \qquad p_x = \frac{x}{h_0} \qquad \text{and} \qquad p_y = \frac{2}{b_0} y ,$$

the solution in the case of no-load will be

$$(7) \qquad V = \sum [A_\nu e^{m_\nu (1-p_x)} + B_\nu e^{m_\nu p_x}] \cos n_\nu p_y$$

Next, the arbitrary constants A_ν and B_ν must be determined by boundary conditions (i) and (ii) and also by the orthogonal condition. The orthogonal condition is,

$$\int_{-1}^{+1} \cos n_\nu p_y \cos n_\mu p_y \, dp_y = 0 \,, \quad [\mu \neq \nu]$$

and in the case $\mu = \nu$,

$$\int_{-1}^{+1} \cos n_\nu p_y \cos n_\nu p_y \, dp_y = 1 + \frac{1}{2n_\nu} \sin 2n_\nu \,.$$

Putting

$$\varphi(n_\nu) = \frac{\int_{-1}^{+1} \cos n_\nu p_y \, dp_y}{\int_{-1}^{+1} \cos^2 n_\nu p_y \, dp_y} = \frac{\frac{2}{n_\nu} \sin n_\nu}{1 + \frac{1}{2n_\nu} \sin 2n_\nu}$$

and inserting (7) into (i) and (ii), one obtains next formulae

$$-\left[\frac{m_\nu}{h_0} + \frac{\lambda_B}{\sigma}\right] e^{m_\nu} A_\nu + \left[\frac{m_\nu}{h_0} - \frac{\lambda_B}{\sigma}\right] B_\nu = \frac{\lambda_B}{\sigma} [T_s - T_B] \varphi(n_\nu) \,,$$

$$\left[\frac{m_\nu}{h_0} - \frac{\lambda_0}{\sigma}\right] A_\nu - \left[\frac{m_\nu}{h_0} + \frac{\lambda_0}{\sigma}\right] e^{m_\nu} B_\nu = \frac{\lambda_0}{\sigma} [T_s - T_0] \varphi(n_\nu) \,.$$

From these formulae the constants A_ν and B_ν can be determined.

(2) THE CASE WHERE MANY CONDUCTORS ARE INSERTED INTO THE SLOT.

Many conductors ($p = 1, 2, 3, \ldots, p, \ldots, p_0$.) are inserted into the slot as shown in Fig. 41. In such a case, it might be suitable to take the origin of coordinate at every conductor and accordingly to decide the constants $A_{1\nu}, B_{1\nu}, \ldots A_{p_0\nu}, B_{p_0\nu}$, whose subindex as 1, 2, 3, ..., p_0 are the number of conductors counting from those at the bottom of the slot.

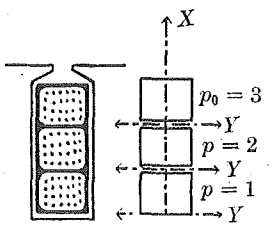

Fig. 41.

In such a case, the boundary conditions may be as follows:—

$$p = 1 \begin{cases} \text{at} \quad x = 0 \,, & \left[\frac{\partial V_1}{\partial x}\right]_{x=0} = \frac{\lambda_B}{\sigma}\left[(V_1)_{x=0} - (T_B - T_s)\right] \\ \text{at} \quad x = h_0 \,, & -\left[\frac{\partial V_1}{\partial x}\right]_{x=h_0} = \frac{\lambda_m}{\sigma}\left[(V_1)_{x=h_0} - (V_2)_{x=0}\right] \end{cases}$$

$$p=p\begin{cases}\text{at} & x=0, & \left[\frac{\partial V_p}{\partial x}\right]_{x=0}=\frac{\lambda_m}{\sigma}\left[(V_p)_{x=0}-(V_{p-1})_{x=h_0}\right]\\ \text{at} & x=h_0, & -\left[\frac{\partial V_p}{\partial x}\right]_{x=h_0}=\frac{\lambda_m}{\sigma}\left[(V_p)_{x=h_0}-(V_{p+1})_{x=0}\right]\end{cases}$$

$$p=p\begin{cases}\text{at} & x=0, & \left[\frac{\partial V_{p_0}}{\partial x}\right]_{x=0}=\frac{\lambda_m}{\sigma}\left[(V_{p_0})_{x=0}-(V_{p_0-1})_{x=h_0}\right]\\ \text{at} & x=h_0, & -\left[\frac{\partial V_{p_0}}{\partial x}\right]_{x=h_0}=\frac{\lambda_0}{\sigma}\left[(V_{p_0})_{x=h_0}-(T_0-T_s)\right].\end{cases}$$

Constants A_ν and B_ν are determined from the boundary conditions above described and λ_m is the coefficient of the heat diffusion in reference to the insulating material existing at the boundary of each slot conducter.

In general, the temperature at p-th conductor

$$(8)\qquad V_p=\sum_\nu\left[A_{p\nu}e^{m_\nu(1-p_x)}+B_{p\nu}e^{m_\nu p_x}\right]\cos n_\nu p_y$$

may be written.

Equation (7) is not only applied in the case where a single conductor is inserted into the slot, but also in the case where many small conductors are filled up uniformly in the slot. However, in such a case the heat quantity for some mean value must be chosen combined with those of the copper winding and the insulating materials surrounding them and in such a case, the heat sources developed in the slot may be taken as to uniform at every point in the slot even in the case of A.C.

It is found from the calculation that A_ν and B_ν are negative, i.e., there is in the slot a lower temperature than the outer peripheral temperature. Generally in the case of $|B_\nu|>|A_\nu|$, the temperature becomes higher toward the inner part of the slot and its temperature depends upon the values of T_0, T_B and T_s, moreover the temperature gradient in the slot may become the larger if λ_0/σ becomes larger or if $2/b_0 \fallingdotseq \lambda_B/\sigma$

(A) and (B) in Fig. 42 represent graphically the temperature distribution in the slot from the calculation by taking the constants as to be $h_0=7$, $b_0=2$ in the case of (A) and $h_0=4$, $b_0=1.5$ in the case of (B), and in both cases

$$\lambda_B \fallingdotseq \lambda_s \fallingdotseq 0.006 \text{ watt/cm}^2, \text{ °C.}$$

$$\lambda_0 = 0.004 \text{ watt/cm}^2, \text{ °C.}$$

The conductivity in the slot is taken at about $\sigma = 1.52$, assuming that its value is decreased by the existence of the insulating material in the slot, though the conductivity of copper conductor is 3.8 watt/cm, °C.. In this case, the circumferential temperature is assumed to be

$$T_s = 85\ ^\circ\text{C.} \qquad T_0 = 25\ ^\circ\text{C.} \qquad T_B = 70\ ^\circ\text{C.}$$

From both examples of numerical calculation, it can be concluded that the maximum temperature exists at a point a small distance upward from the bottom of the slot. As example (A) corresponds to the case where the depth of the slot is larger than its width, the mean temperature of case of (A) is higher than that of another case.

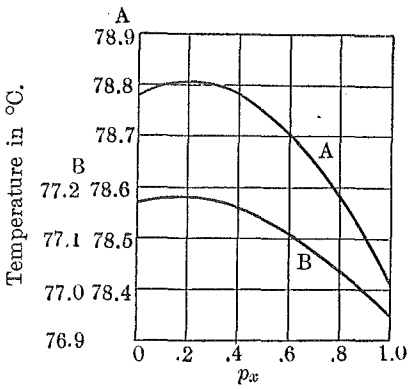

Fig. 42.

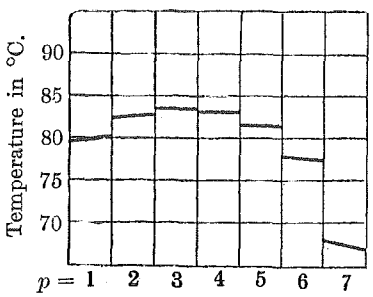

Fig. 43.

Fig. 43 represents the temperature distribution of every conductor or group of winding in the case where 7 conductors or groups having each dimension ($b_0 = 2$ cm, $h_0 = 1$ cm.) are arranged in the slot in the direction of x-axis only. In this case,

$$\lambda_m = 0.008 \text{ watt/cm}^2, \ ^\circ\text{C.}$$

and the other thermal constants are taken the same as those of Fig. 36.

To find the maximum temperature, put

$$\frac{\partial V}{\partial p_x} = 0 ,$$

then

$$\frac{A_\nu}{B_\nu} = e^{\varphi(T)}$$

and

$$p_x = \frac{1}{2} + \frac{1}{2m_\nu}\phi(T)\,,$$

where p_x is the position occupied by the maximum temperature. $p_x = 0$ means the position at the bottom and $p_x = 1$ means the position at the upper side of the slot.

Since the condition $A_\nu / B_\nu < 1$ is held here, there must exist the condition $\phi < 0$. Therefore it is found that the maximum temperature lies at some point on the way between the bottom and the middle point of the slot. If the temperature of the boundary is the same at the upper and the lower sides of slot, i.e., $T_B = T_0$ and constants of heat diffusion are kept $\lambda_0 = \lambda_B$ at the boundaries, then the maximum temperature must exist midway of the height of the slot, because $A_\nu = B_\nu$ is deduced. However the condition $\lambda_0 = \lambda_B$ is not kept in the ordinary slot, but the condition $\lambda_B > \lambda_0$ may be kept in general from the construction of the machine.

In order to investigate the transference of the spot having the highest temperature along the central line of the slot, the expression is used

$$\frac{A_\nu}{B_\nu} = \frac{\frac{m_\nu}{h_0}\lambda_B(e^{m_\nu} + \lambda_0) + \frac{\lambda_0\lambda_B}{\sigma}(e^{m_\nu} - 1)}{\frac{m_\nu}{h_0}(\lambda_0 e^{m_\nu} + \lambda_B) + \frac{\lambda_0\lambda_B}{\sigma}(e^{m_\nu} - 1)}$$

where $T_0 = T_B$.

From the fact that the condition $A_\nu / B_\nu > 1$ can be held, so long as λ_B becomes larger than λ_0, it can be ascertained that the spot of the highest temperature moves toward the upper side from the middle point of the slot as shown in Fig. 44.

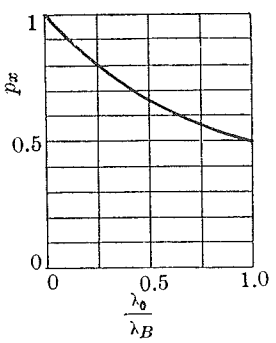

Fig. 44.

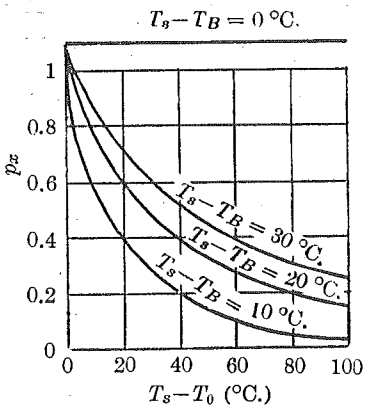

Fig. 45.

Fig. 45 represents the relation between the position of the highest temperature and the circumferential temperature of the slot, and from this figure, it is found that its position is displaced from the upper side toward the bottom side of the slot according as the temperature difference between T_s and T_0 becomes larger and also its displacement depends on the amount $(T_s - T_B)$.

If $T_s = T_B$ is kept, there appears no maximum temperature in the slot. The mean temperature is

$$V_{\text{mean}} = \frac{1}{m_\nu h_0}[e^{m_\nu} - 1][A_\nu + B_\nu] .$$

The mean temperature falls so long as the values $(T_s - T_0)$ and $(T_s - T_B)$ both become larger. If the circumferential temperature is taken as $T_B \fallingdotseq T_s$ and constants $\lambda_0 = \lambda_B = \lambda$ for the practical application, the mean value is

$$V_{\text{mean}} = -\frac{\lambda_0}{\sigma}[T_s - T_0] \frac{1}{m_\nu^2 + 2h_0 \frac{\lambda}{\sigma}(2 + m_\nu)} .$$

The larger m_ν and h_0 become, the higher the mean temperature becomes where m_ν is taken at some value which lies between zero and 1. This fact may be explained by the same reason at that given in the case where the height of slot h_0 and the ratio h_0/b_0 become larger.

The mean temperature depends also upon λ/σ; it is comparatively large so long as λ/σ is small. The value of σ may be large or small according to the size of the conductor, even though the slot has the same dimensions. Fig. 46 represents the mean temperature rise referring to m_ν.

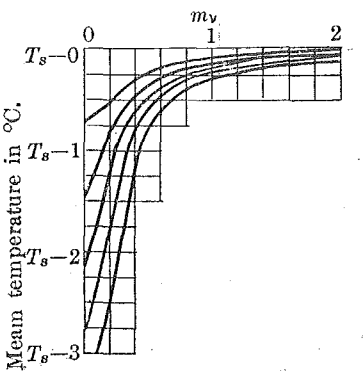

Fig. 46.

(3) THE SOLUTION IN THE CASE OF LOADING BY USING GREEN'S POTENTIAL FUNCTION.

If W and V are the potential functions of two dimensions, Green's formula of potential is

$$\int_s \left[V \frac{\partial W}{\partial n} - W \frac{\partial V}{\partial n} \right] ds = \iint_f [V \Delta W - W \Delta V] df ,$$

where the left side term of the equation denotes the line integral in the definite domain and the right side term denotes the surface integral. The normal of the integrating path is denoted by n.

Now, let us write the temperature with W and the logarithmic potential function with V, then

$$V = \log_e \frac{1}{r} , \qquad r = \sqrt{(x-\xi)^2 + (y-\eta)^2} .$$

It is certain that V is satisfied by the next equation

$$\frac{\partial^2 V}{\partial x^2} + \frac{\partial^2 V}{\partial y^2} = 0 .$$

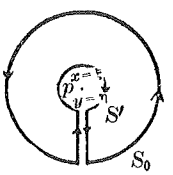

Fig. 47.

If the integrating surface contains the source at the point P whose coordinates are $x = \xi$, $y = \eta$, then the integrating path may be taken at the small circle S' around the point P and also at the large circle S_0 in which the small circle is contained as shown in Fig. 47.

Therefore,

$$(9) \qquad \int_{s'} \left[V \frac{\partial W}{\partial n} - W \frac{\partial V}{\partial n} \right] ds + \int_{s_0} \left[V \frac{\partial W}{\partial n} - W \frac{\partial V}{\partial n} \right] ds = \iint_{f_0} [V \Delta W - W \Delta V] df$$

where f_0 represents the surface enclosed by the line integrating path S_0. If n is taken as inward normal, then the first term of the left side of equation (9) may be written as follows,

$$-\int_{s'} \left[\log_e \frac{1}{r} \frac{\partial W}{\partial r} - W \frac{1}{r} \right] r d\theta .$$

If S' converges into zero, i.e., $x \to \xi$, $y \to \eta$, then $\frac{\partial W}{\partial r}$ may attain to the finite value and $r \log 1/r$ converges into zero, so the above expression may be written $2\pi W(\xi, \eta)$ as the result.

$$(10) \qquad W(\xi, \eta) = -\frac{1}{2\pi}\int_{s_0}\left[V\frac{\partial W}{\partial n} - W\frac{\partial V}{\partial n}\right]ds + \frac{1}{2\pi}\iint_{f_0} V \Delta W \, df$$

The first term at the right side of equation (10) is precisely determined in its form by boundary conditions (i), (ii), (iii) and (iv) or by other boundary conditions in the case where many conductors or groups of winding are inserted into the slot. The second term on the same side of the equation must be vanished in the case of no-loading that is,

$$\Delta W = 0 \, .$$

Therefore it is sure that the first term certainly corresponds to the solution at the no-loading. The first term is written by expression (7) or (8) according to the cases where one or many conductors are inserted into the slot.

$$(11) \qquad W = \sum [A_\nu e^{m_\nu (1-p_x)} + B_\nu e^{m_\nu p_x}] \cos n_\nu p_y$$

$$+ \frac{1}{2\pi}\int_0^{h_0}\int_{-\frac{1}{2}b_0}^{+\frac{1}{2}b_0} [S_1 + S_2 W] k(\xi, \eta) \log_e \frac{1}{r} \, d\xi \, d\eta \, .$$

This is Fredholm's integral equation.

(4) THE CASE OF UNIFORM CURRENT DISTRIBUTED IN THE SLOT.

When many conductors are packed up in the slot uniformly, then it is considered that the current density is uniformly distributed through out in the section of the slot. However, in the case where a single conductor is inserted into the slot, the fact that the current is uniformly distributed is confined to the case of direct current only. Therefore $k(x, y) = 1$ in this case, because the ratio of resistance in the cases of A.C. against that of D.C. is equal to 1.

The second term on the right side of (11) is written again with reference to r and θ as following,

$$\frac{S_1}{2\pi}\iint_{f_0} r\log_e\frac{1}{r}\,dr\,d\theta = S_1\int_{s_0} r\log_e\frac{1}{r}\,dr\,.$$

Integrating path S_0 is taken along the out-line of the slot. Put

$$dr = \frac{1}{r}(x-\xi)\,dx+\frac{1}{r}(y-\eta)dy$$

$$\log_e\frac{1}{r} \doteqdot \log_e\frac{1}{x-\xi}+\frac{1}{2}\left(\frac{y-\eta}{x-\xi}\right)^2+\cdots\cdots$$

$$\doteqdot \log_e\frac{1}{y-\eta}+\frac{1}{2}\left(\frac{x-\xi}{y-\eta}\right)^2+\cdots\cdots\,.$$

The term at the right side is

$$S_1\int_{s_0} r\log_e\frac{1}{r}\,dr$$

$$= S_1\int_0^{h_0}\log_e\frac{1}{x-\xi}(x-\xi)\,d\xi+S_1\int_{-\frac{1}{2}b_0}^{+\frac{1}{2}b_0}(y-\eta)\log_e\frac{1}{y-\eta}\,d\eta$$

where

at $\xi > x$, $(\xi-x)\log_e\dfrac{1}{\xi-x}$,

at $x > \xi$, $(x-\xi)\log_e\dfrac{1}{x-\xi}$,

at $\eta > y$, $(\eta-y)\log_e\dfrac{1}{\eta-y}$,

at $y > \eta$, $(y-\eta)\log_e\dfrac{1}{y-\eta}$.

The solution is obtained in the first approximation,

$$W_1 = \sum[A_\nu e^{m_\nu(1-p_\xi)}+B_\nu e^{m_\nu p_\xi}]$$

$$+\frac{h_0^2}{2}\left(\frac{1}{2}+\log_e\frac{1}{h_0}\right)S_1[p_\xi^2+(1-p_\xi)^2]$$

$$+\frac{h_0^2}{2}S_1\left[p_\xi^2\log_e\frac{1}{p_\xi}+(1-p_\xi)^2\log_e\frac{1}{1-p_\xi}\right]$$

$$+\frac{b_0}{8}\left(\frac{1}{2}+\log_e\frac{2}{b_0}\right)S_1[(1+p_\eta)^2+(1-p_\eta)^2]$$

$$+\frac{b_0^2}{8}S_1\left[(1+p_\eta)^2\log_e\frac{1}{1+p_\eta}+(1-p_\eta)^2\log_e\frac{1}{1-p_\eta}\right].$$

Putting

$$\begin{aligned} W_1 &= W_1 \\ W_2 &= W_1+\frac{S_2}{2\pi}\iint W_1\log\frac{1}{r}\,dx\,dy \\ &\vdots \\ W_{n+1} &= W_n+\frac{S_2}{2\pi}\iint W_n\log\frac{1}{r}\,dx\,dy \end{aligned}$$

the exact solution is obtained as follows,

$$W = W_1+\frac{S_2}{2\pi}W_2+\left(\frac{S_2}{2\pi}\right)^2W_3+\cdots\cdots+\left(\frac{S_2}{2\pi}\right)^{n-1}W_n+\cdots\cdots .$$

W is determined by means of successive approximations.

For the technical application, if only the first order of the solution is taken, solution W_1 is obtained, which can be again approximated by putting

$$p_\xi^2\log_e\frac{1}{p_\xi}+(1-p_\xi)^2\log_e\frac{1}{1-p_\xi}\fallingdotseq 0.347\sin\pi p_\xi ,$$

$$(1+p_\eta)^2\log_e\frac{1}{1+p_\eta}+(1-p_\eta)^2\log_e\frac{1}{1-p_\eta}\fallingdotseq -2.772\left(1-\cos\frac{\pi}{2}p_\eta\right).$$

Constants A_ν and B_ν are determined from boundary conditions (i) and (ii). Again, if the calculated result is inserted into the second term at the right side of equation (11), the term containing the temperature coefficient of resistance is obtained.

For an example, put

$h_0 = 4$ cm. $\qquad \lambda_0/\sigma = 0.00263$

$b_0 = 1.5$ cm. $\qquad \lambda_s/\sigma = \lambda_B/\sigma = 0.00295$

$T_0 = 20°\mathrm{C}.$ $\qquad T_s = 65°\mathrm{C}.$ $\qquad T_B = 60°\mathrm{C}.$

The constants are thus determined,

$$\begin{aligned} A_\nu &= -1.855+174.5\,S_1 , \\ B_\nu &= -2.47+174\,S_1 . \end{aligned}$$

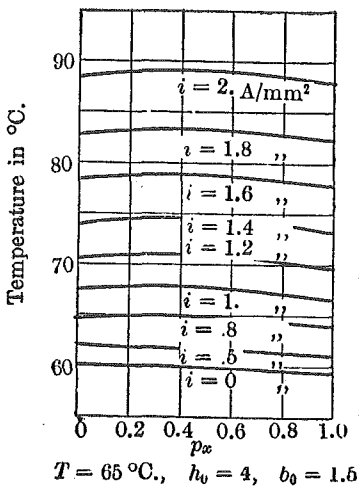

Fig. 48.

Fig. 48 represents graphically the temperature distributions along the direction of x-axis by taking the current density as parameter where

$$i = \frac{I_{max}}{\sqrt{2}} \frac{1}{b_0 h_0} .$$

From the calculation shown in Figs. 44 and 45 in the case of no-load, it is found that the point in which the highest temperature exists, moves to and fro along the central line of the slot as the thermal constants and the circumferential temperatures vary.

In the case of loading, two problems are investigated; 1) in what manner does the point of the highest temperature displace in the section of the slot? and 2) why does it displace in the section?

The transition of the spot of the highest temperature occurring in the case of loading is considered as follows: at the beginning, if the condition

$$0 < A_\nu / B_\nu < 1$$

is held in the slot, then the value $\log_e A_\nu / B_\nu$ may be negative. This fact means that the highest temperature exists in some place apart from the middle point toward the bottom of the slot and this case corresponds to the one of no-loading, i.e., $S_1 = 0$. Next, if the load current of slot conductor increases gradually, then the term A_ν / B_ν may become smaller till its value reaches zero. Therefore the highest temperature may displace its position toward the bottom of slot as S_1 increases.

Again with the increment of the load current, the term A_ν / B_ν changes its value as follows

$$(-\infty) \rightarrow (+\infty) \rightarrow (+1) .$$

Corresponding to these values, $(+\infty)$ and $(+1)$, $\log_e A_\nu / B_\nu$ may take the value $(+\infty)$ and (0) respectively.

Therefore for the reasons above mentioned, the point at which the highest temperature exists, may displace from the upper side to the bottom of the slot. Fig. 49 represents the relation between the

position of the highest temperature and the load current where $(T_s - T_B)$ is taken as parameter.

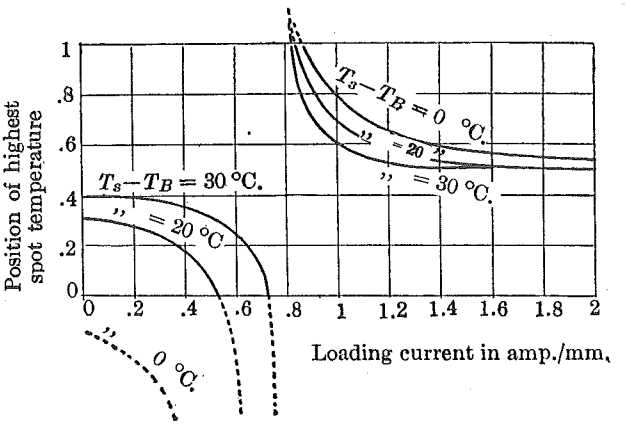

Fig. 49.

From this figure it is concluded that initially the highest temperature exists at the neighbourhood of the middle point of the slot. With increasing the load, the point of the highest temperature displaces toward the bottom of the slot and then it might be mathematically explained that the highest temperature displaces from $(-\infty)$ to $(+\infty)$ and returns back from $(+\infty)$ to the middle point of the slot.

Although the temperatures T_s and T_B are assumed to be constant in this calculation, they might change their values with increasing of the load, therefore the highest temperature would not always be confined to transiting its position on the locus as shown in Fig. 49 for a practical case.

Putting $A_\nu / B_\nu = 0$, one can obtain the next formula,

$$S_1 = \frac{\frac{\lambda_0}{\sigma}(T_s - T_0)\left[\frac{m_\nu}{h_0} - \frac{\lambda_B}{\sigma}\right] + \frac{\lambda_B}{\sigma}(T_s - T_B)\left[\frac{m_\nu}{h_0} + \frac{\lambda_0}{\sigma}\right] e^{m_\nu}}{\left[\left(\frac{m_\nu}{h_0} + \frac{\lambda_B}{\sigma}\right) e^{m_\nu} + \left(\frac{m_\nu}{h_0} - \frac{\lambda_0}{\sigma}\right)\right] h_0 \log_e \frac{1}{h_0}}.$$

If S_1 has a value to be satisfied by the above formula or a value smaller than it, then the position of the highest temperature may be at a point lower than the middle point of the slot. In such a case, the relation between $(T_s - T_0)$ and the current is represented as in Fig. 50. If the load current occupies its position at the point below

this curve as shown in Fig. 50, then the spot of the highest temperature should be at lower position far from the middle point of the slot.

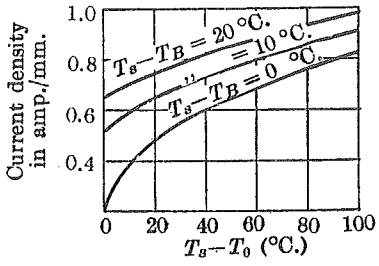

Fig. 50.

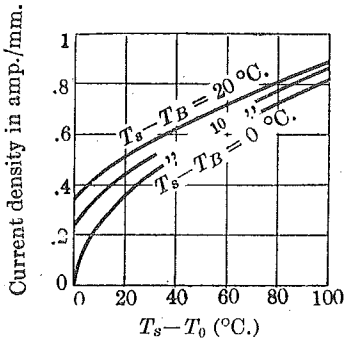

Fig. 51.

On the other hand, Fig. 51 shows the case where the spot of the highest temperature is at the upper side of the slot.

Putting $A_\nu / B_\nu = \infty$, one obtains

$$S_1 = \frac{\frac{\lambda_0}{\sigma}(T_s-T_0)\left[\frac{m_\nu}{h_0}+\frac{\lambda_B}{\sigma}\right]e^{m_\nu}+\frac{\lambda_B}{\sigma}(T_s-T_B)\left[\frac{m_\nu}{h_0}-\frac{\lambda_0}{\sigma}\right]}{\left[\left(\frac{m_\nu}{h_0}+\frac{\lambda_B}{\sigma}\right)e^{m_\nu}+\left(\frac{m_\nu}{h_0}-\frac{\lambda_0}{\sigma}\right)\right]h_0\log_e\frac{1}{h_0}}$$

Therefore in the case where S_1 has the value which is satisfied by this equation or has a larger one than that, the spot of the highest temperature may be above the middle point of the slot. The mean temperature of the slot is

$$V_{\text{mean}} = \frac{1}{h_0}\frac{-S_1 h_0\log_e\frac{1}{h_0}-\frac{\lambda_0}{\sigma}(T_s-T_0)}{\left(\frac{m_\nu}{h_0}+\frac{\lambda_B}{\sigma}\right)e^{m_\nu}-\left(\frac{m_\nu}{h_0}-\frac{\lambda_0}{\sigma}\right)}$$

$$+\frac{S_1}{6}h^2+\frac{S_1}{3}h_0^2\left[\frac{1}{3}+\log_e\frac{1}{h_0}\right]+S_1\frac{b_0^2}{4}\left[\frac{1}{2}+\log_e\frac{2}{b_0}\right]$$

and the results of numerical calculation are shown in Fig. 52.

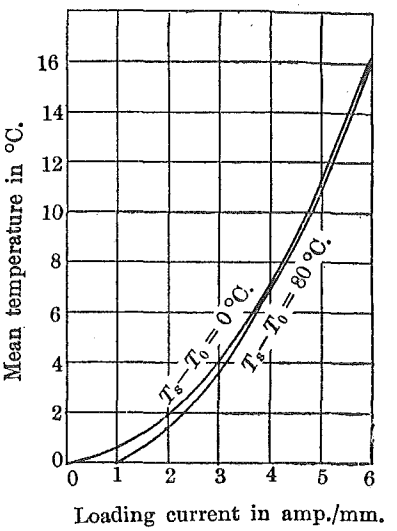

Fig. 52.

(5) THE CASE WHERE CURRENT DENSITY IS NOT UNIFORM.

In the case where a single conductor or several conductors are inserted into the slot, the current density in the conductor is not uniform depending upon the frequency of the source and the form of the slot. In such a case, rather the ratio of resistance $k(x, y)$, i.e., "Alternating current resistance" can be taken instead of the distribution of current in the slot.

For the case of a single conductor inserted into the slot, it follows

$$k(x, y) = (\alpha h_0 \beta b_0)^2 \frac{[\cosh 2\alpha x + \cos 2\alpha x][\cosh 2\beta y + \cos 2\beta y]}{[\cosh 2\alpha h_0 - \cos 2\alpha h_0][\cosh \beta b_0 - \cos \beta b_0]}$$

$$= C_0 [\cosh 2\alpha x + \cos 2\alpha x][\cosh 2\beta y + \cos 2\beta y] .$$

Form this equation,

$$\Delta W = C_0 (S_1 + S_2 W)[\cosh 2\alpha x + \cos 2\alpha x][\cosh 2\beta y + \cos 2\beta y] .$$

Inserting this relation into the second term at the right side of (11) and solving them, one obtains the solution in the case of non-uniform current,

$$W=\sum[A_\nu e^{m_\nu(1-p_\xi)}+B_\nu e^{m_\nu p_\xi}]+C_0h_0^2S\left(1+2\log_e\frac{1}{h_0}\right)[p_\xi^2+(1-p_\xi)^2]$$

$$+0.7\,C_0h_0^2S_1\sin\pi p_\xi+C_0\left(\frac{b_0}{2}\right)^2S_1\left(1+2\log_e\frac{2}{b_0}\right)[(1+p_\eta)^2+(1-p_\eta)^2]$$

$$-5.5\left(\frac{b_0}{2}\right)^2C_0S\left[1-\cos\frac{\pi}{2}p_\eta\right]+\frac{8}{3}\alpha^4C_0S_1\left[\frac{h_0^6}{6}\left(\frac{1}{6}+\log_e\frac{1}{h_0}\right)\right.$$

$$\left.-\frac{h_0^2}{5}\left(\frac{1}{5}+\log_e\frac{1}{h_0}\right)p_\xi+\frac{h_0^6}{15}\log_e\frac{1}{h_0}p_\xi^6+\frac{h_0^6}{15}p_\xi^6\log_e\frac{1}{p_\xi}\right]$$

$$+\frac{8}{3}\beta^4C_0S_1\left[\frac{1}{3}\left(\frac{b_0}{2}\right)^6\left(\frac{1}{6}+\log_e\frac{2}{b_1}\right)-\frac{2}{5}\left(\frac{b_0}{2}\right)^6\left(\frac{1}{5}+\log_e\frac{2}{b_0}\right)p_\eta\right.$$

$$\left.+\frac{2}{15}h_0^6\log_e\frac{2}{b_0}p_\eta^6+\frac{2}{15}h_0^6\log_e\frac{1}{p_\eta}\right].$$

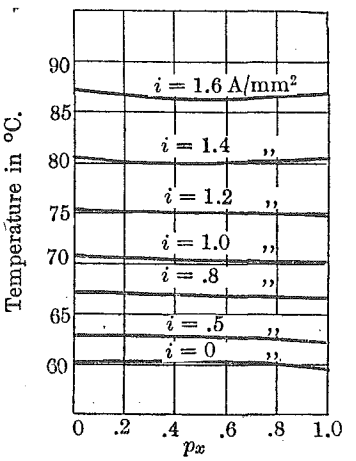

Fig. 53.

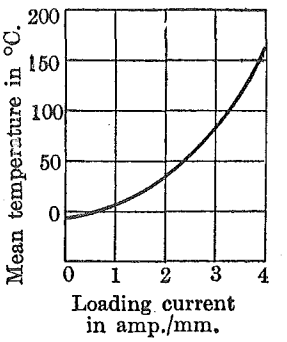

Fig. 54.

Fig. 53 shows the temperature distribution in the slot conductor having the same dimensions as shown in Fig. 48. Though the same current density is applied in both cases, the mean temperature and the temperature at the upper side of the slot indicated in Fig. 53, are higher than those in the case shown in Fig. 48, because current density distribution is not uniform in the case of Fig. 53.

The variation of the mean temperature is shown in Fig. 54 referring to the load current and in this case,

$$A_\nu = -1.855 + 242.5\, S_1 ,$$

$$B_\nu = -2.47 + 266\, S_1 .$$

The calculation may be performed for the case where many conductors are divided into several groups of winding in the slot like as the former case. However, "Alternating current-resistance" should be changed in each conductor or group, so they should be taken as k_1, k_2, k_3, k_4, ... about every conductor or group.

For an example, three conductors or groups are inserted into the slot and each conductor or group has the uniform current density at whole section, whose conductor or group of winding has the dimension

$$h_0 = 2 \text{ cm}, \qquad b_0 = 1 \text{ cm}.$$

and the boundary temperatures are

$$T_s = 65°\text{C}, \qquad T_B = 60°\text{C} \qquad \text{and} \qquad T_0 = 20°\text{C}.$$

and the thermal constants are

$$\sigma = 3.8 \times 10\% = 0.38, \qquad \lambda_B = 0.005, \qquad \lambda_m = 0.096$$

$$\text{and} \qquad \lambda_0 = 0.0035.$$

The calculated result from these data is shown in Fig. 55 (a).

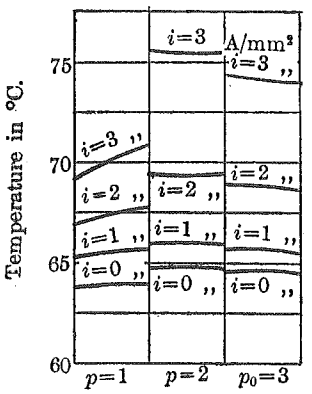

Fig. 55 (a).

In general, the highest temperature of the machine can be found by this mathematical calculation. However, the spot of the highest temperature might also occur at some other point owing to some defects in the construction of the machine. Yet in such a case, it can not be treated from the mathematical calculation, except for such a case as that when the spot having the highest temperature can be found from the mathematical calculation, provided the thermal constants, the dimension of slot and the circumferential temperature are known.

The circumferential temperature of the slot is treated as constant in this calculation, but its temperature may rise together with the load. Therefore, the actual temperature of the slot may become higher than those obtained from this calculation. The change of circum-

ferential temperature caused by the load must be investigated. However, it becomes a very complicated problem to take the circumferential temperature as the function of load at the beginning of the calculation.

(6) NUMERICAL EXAMPLE.

The dimensions of the slot and the slot conductor are shown in Fig. 55(b) taking the case of the synchronous alternator 31,000 kVA, 11,000 V at a certain hydro-electric power station for railway service.

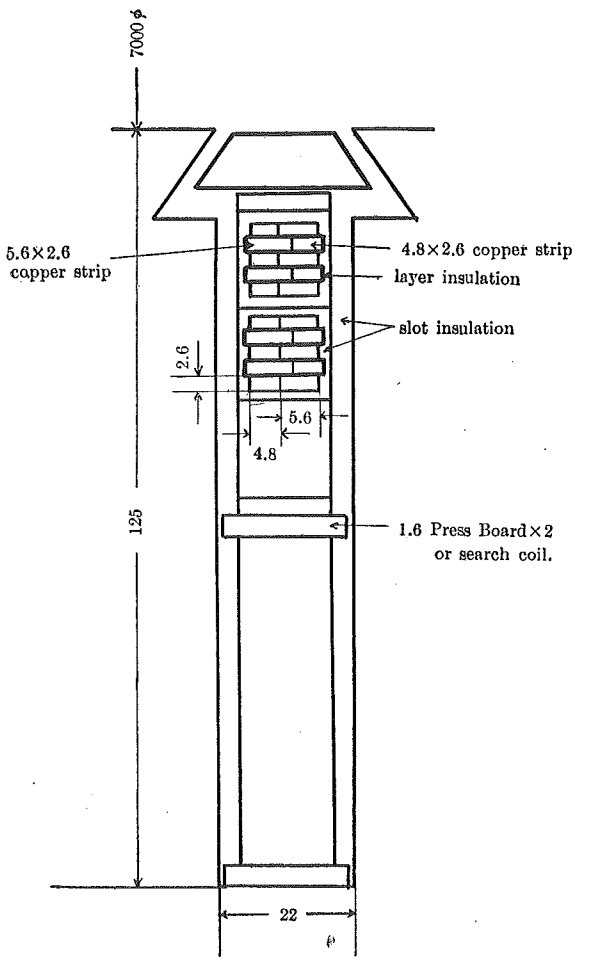

Fig. 55(b).

The slot and slot insulation are shown in Fig. 55(b); their main dimensions and cooling constants are:—

$$h_0 = 1.3 \text{ cm}, \qquad b_0 = 1.04 \text{ cm},$$

$$\lambda_s = 1.57 \times 10^{-3}, \qquad \sigma = 3.8,$$

$$n_\nu \tan n_\nu = \frac{\lambda_s}{\sigma}\frac{b_0}{2}, \qquad n_\nu = 0.01466,$$

$$m_\nu = 0.03665,$$

$$\lambda_B \fallingdotseq \lambda_0 = 1.4 \times 10^{-3} \text{ watt/cm}^2, \text{ °C},$$

$$\lambda_m = 0.0065.$$

The temperature at the boundary of the slot:—

$$T_s = 80°\text{C},$$

$$T_B = 65°\text{C},$$

$$T_0 = 40°\text{C}.$$

The calculation constants $A_1, A_2, \ldots, B_1, B_2, \ldots$ can be determined as follows:—

$$A_1 = 9, \qquad B_1 = 8,$$

$$A_2 = 3.85, \qquad B_2 = 3.4,$$

$$A_3 = 0.9, \qquad B_3 = 0.58,$$

$$A_4 = -1.2, \qquad B_4 = -1.5,$$

$$A_5 = -3.4, \qquad B_5 = -3.8,$$

$$A_6 = -5.51, \qquad B_6 = -5.97.$$

The temperature distribution of each conductor is shown in Fig. 55(c) in the case of no-load.

The temperatures at full load are shown in Fig. 55(d) where

the copper loss of the stator = 155 kW,

the stray load loss = 50 kW,

total winding loss = 205 kW.

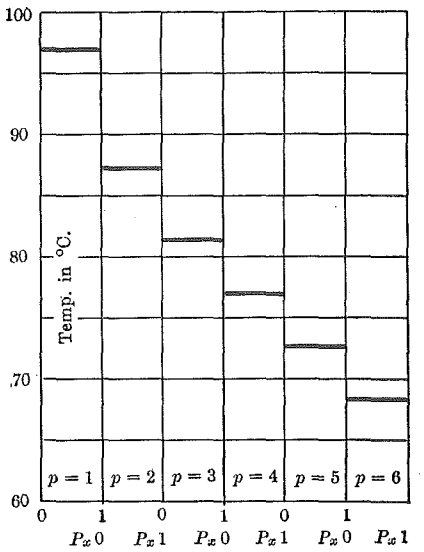

Fig. 55 (c).

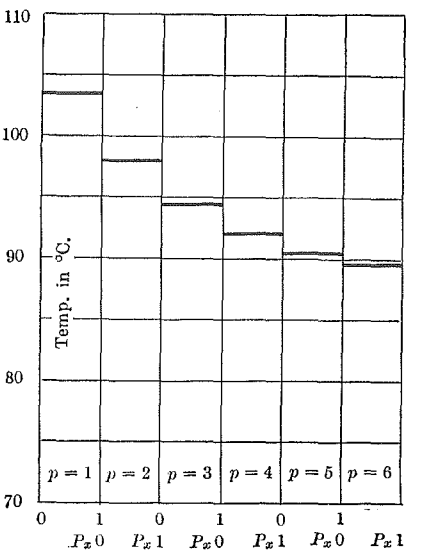

Fig. 55 (d).

From the above values, the copper loss per unit volume is found then

$$S_1 = \frac{\text{loss/unit volume}}{4.2} = 6.43 \times 10^{-2} .$$

The temperatures are found for each conductor by inserting the numerical values into the formula above described.

CHAPTER VI.

SURFACE COOLING AND TEMPERATURE RISE OF ELECTRIC MACHINE.

The law of cooling, i.e., the so-called "Newton's cooling law" is generally used for the heat dissipation at the surface in the range of lower temperatures. This law is based upon the fact that the heat quantity dissipated from the surface is proportional to the temperature difference between the surface and the cooling medium. The proportional constant in Newton's cooling law is determined suitably according to the circumferential conditions. For the surface such as that of an electric machine, the great amount of heat dissipated from the surface is not chiefly due to the heat radiation, but due to the heat conduction and convection in the outer cooling medium. In order to make clear the mechanism of the heat dissipation from the surface of electric machine, the heat conduction and the heat convection in the cooling medium must be investigated. Since the surfaces of the general electric machine are cooled by natural ventilation as well as by forced ventilation, the heat dissipation has been treated from this point of view in this chapter.

(1) NEWTON'S CONSTANT AT THE SURFACES.

Newton's constant means, as is generally known, the heat emissibility from the surfaces, denoted by the heat quantity from the unit area per sec. and per unit temperature difference between the surface and the cooling medium. For the general electric machine, it is favourable that the dimension of this unit is expressed as in watt/cm^2, °C.

To measure the Newton's constant of the vertical and horizontal planes, a polished metal plane used as the lid of a wooden box is taken as a test sample and heated from one side. The wooden box is filled up with asbestos wool as the heat insulator and a nichrom wire is inserted as a heat element in this box. The dimension of the lid of the wooden box is 25 cm × 30 cm. Newton's constant of the horizontal or vertical plane is obtained by keeping the metal plate horizontally or vertically respectively. The surface temperature is measured by a thermo-couple (copper and constantan). The surface temperature is measured after it is heated for long time in a small room.

If the measurement is begun before the surface temperature sufficiently attains the steady state, some other physical constants may be contained in the experimental results, such as:— the thermal conductivity and the specific heat of the material used in construction of the apparatus.

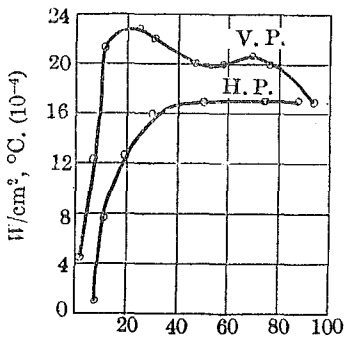

V. P.: vertical plane.
H. P.: horizontal plane.

Fig. 56.

Experimental results are shown in Fig. 56 referring to the horizontal and the vertical planes. The curves in Fig. 56 represent the relation between Newton's constant and the surface temperature, the room temperature being taken as zero. Newton's constant rises with the surface temperature in the lower range of the temperature and attains to the saturated value and in the case of the vertical plane it seems somewhat likely to fall after having reached the saturated value. The vertical plane is more favourable than the horizontal plane for the best dissipation from the surface. It is sure that the heat dissipation depends on the vertical length of the surface, unless the surface is large enough.

Thus it is concluded that Newton's constant varies with the direction of the place horizontally or vertically and the constant varies with the temperature difference between the surface and the cooling medium.

Newton's constants referring to the polished metal cylinders keeping their axes horizontal are shown in Fig. 57. Judging from the experimental results, the value of Newton's constant depends on the diameter of the cylinder:— the larger the diameter of the cylinder, the less Newton's constant becomes. The experiments were performed with a small polished brass cylinders up to 0.95 cm in diameter and from them it is concluded that very small wire has a large value of Newton's constant in comparison with larger ones.

When forced ventilation is applied to the heating surface, the heat diffusion from the surface may well become large and accordingly Newton's constant may also be large, for the air flow carries away the heat diffused from the surface.

Inserting the metal cylinder in the wind tunnel and keeping the velocity of air flow constant, the results are shown in Fig. 58 and

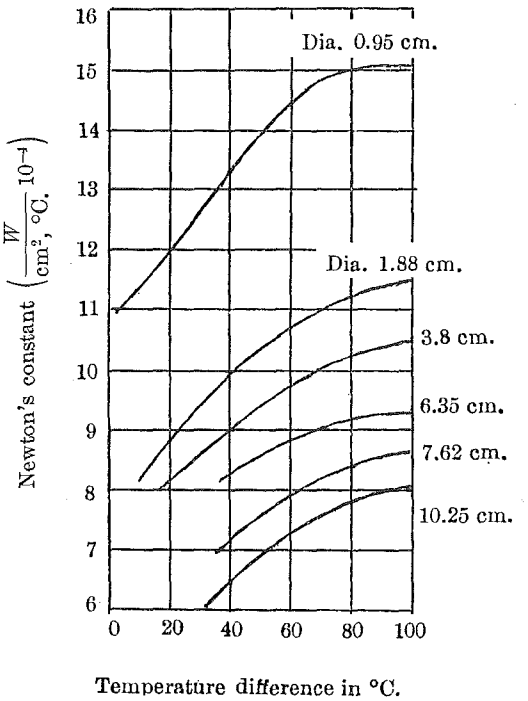

Fig. 57.

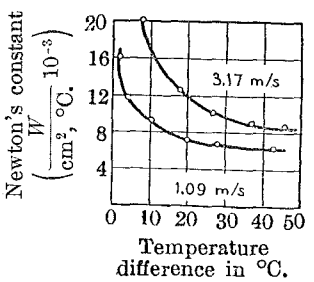

Fig. 58.

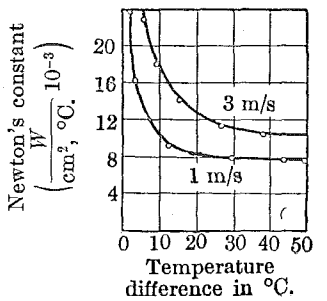

Fig. 59

Fig. 59. Fig. 58 indicates the case when the axes of the cylinders are parallel and Fig. 59 when perpendicular to the direction of air flow. Newton's constant is represented by the curve which decreases at the beginning and then attains to the constant value.

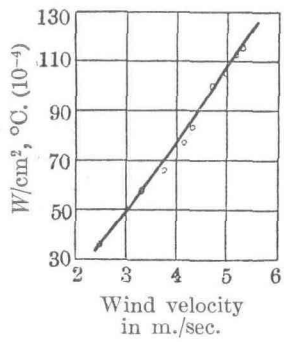

Fig. 60.

Next, by taking the wind velocity to be variable and the supplied heat energy to be constant, it is found that the relative character between Newton's constant and the wind velocity are expressed by a linear ascending line as shown in Fig. 60.

(2) OBSERVATION BY THE SCHLIEREN METHOD.

For investigating the air motion due to the heat conduction and convection, the Schlieren method is used. By means of the Schlieren method the heat diffusion from the surface can be made visible and photographs of the upward air current can be taken. The apparatus of this method is shown in Fig. 61.

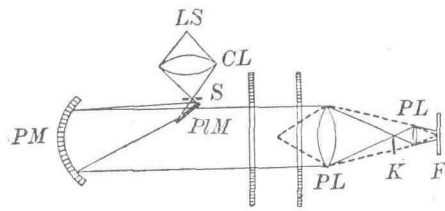

CL: condenser lens.
PL: photographic lens.
PlM: plane mirror.
PM: parabolic mirror.
LS: light source.
S: slit.
K: knife edge.
F: film or plate.

Fig. 61.

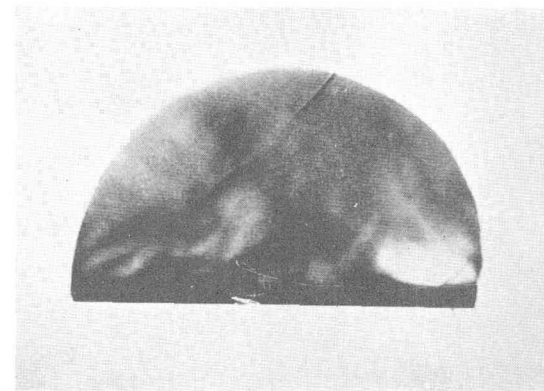

Fig. 62.

The photograph in Fig. 62 is taken in the case where the metal plate is placed horizontally and its temperature kept at 40~50°C. This photograph is reproduced as a negative figure for convenience; the black part in the photograph is the bright part which is produced by the flowing air. The horizontal line like the bow-string of a half circle in this figure corresponds to the surface of the metal plate and the black band above it, corresponds to the conduction layer while the air stream above this band shows the fairly turbulent air flow.

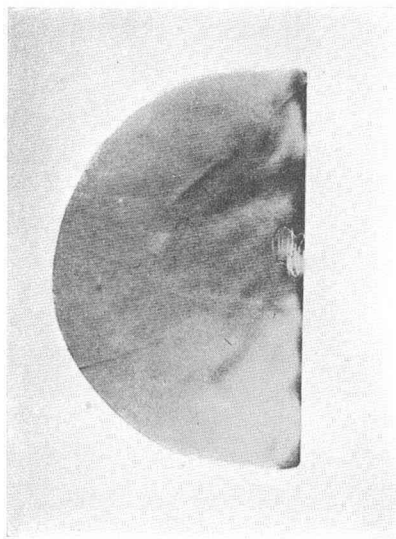

Fig. 63.

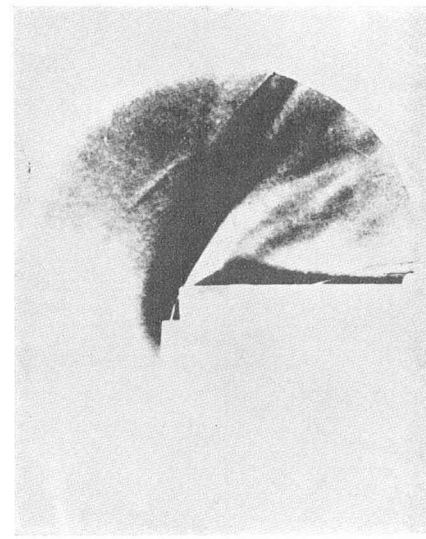

Fig. 64.

Figs. 63 and 64 are photographs taken in the case where the metal-plate is placed vertically and the air flow along the hot surface seems to be continuous, however, sometimes there appears a lump flowing upward along the heated wall. Fig. 64 shows the air flow at the upper end of the vertical surface due to convection.

The thickness of the conduction layer is observed by Schlieren method. When the temperature of the heated wall is low, the air flow due to the heat convection can not be observed. In the range in which the heat convection is not observed by Schlieren method, the variation of the thickness of the conduction layer can be found:— the thickness of the conduction layer increases with the temperature of the heated surface. By raising the temperature over this range, the air stream due to the heat convection appears gradually in the cooling medium and then the conduction layer becomes narrow with the increase of the flowing speed of the heat convection.

Figs. 65 and 66 show the air flows due to the heat convection with reference to the surface of the metal cylinder. The air flows rise upward along both sides of the cylinder and then meet at the vertex of the cylinder. If the cylinder rotates about its axis, the convecting flow is disturbed as shown in Fig. 67; one part of the flows goes in the direction of rotation while the other part is blown off.

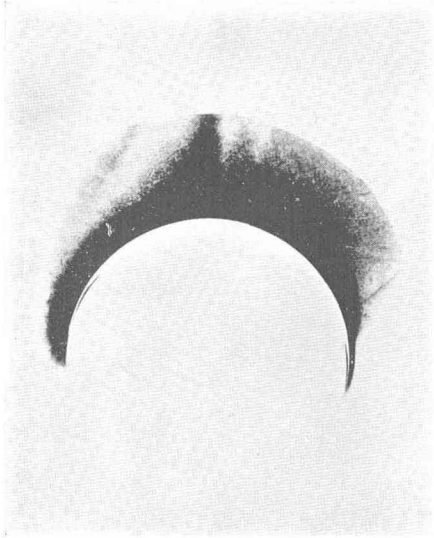

Fig. 65.

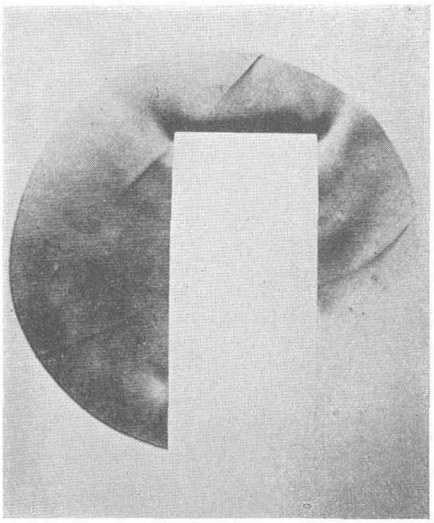

Fig. 66.

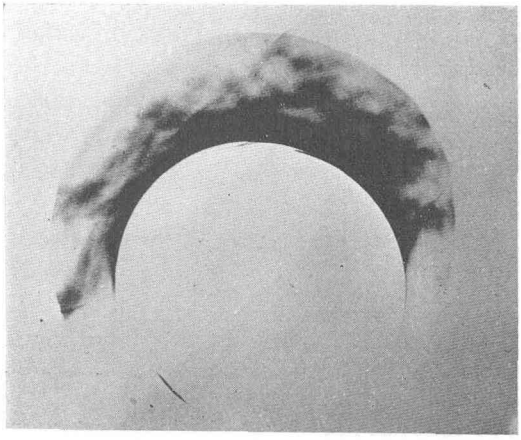

Fig. 67.

Air flows along the inner surface of the metal cylinder whose axis is kept horizontal, are shown in Fig. 68.

Rising air is suspended at the lower part of the inner surface of the ring for a moment and then rises upward forming a lump along the side surfaces. Two air lumps rising along the left and right of the circumferential surface, meet with each other at the vertex and then a stationary eddy current motion appears in the vertex.

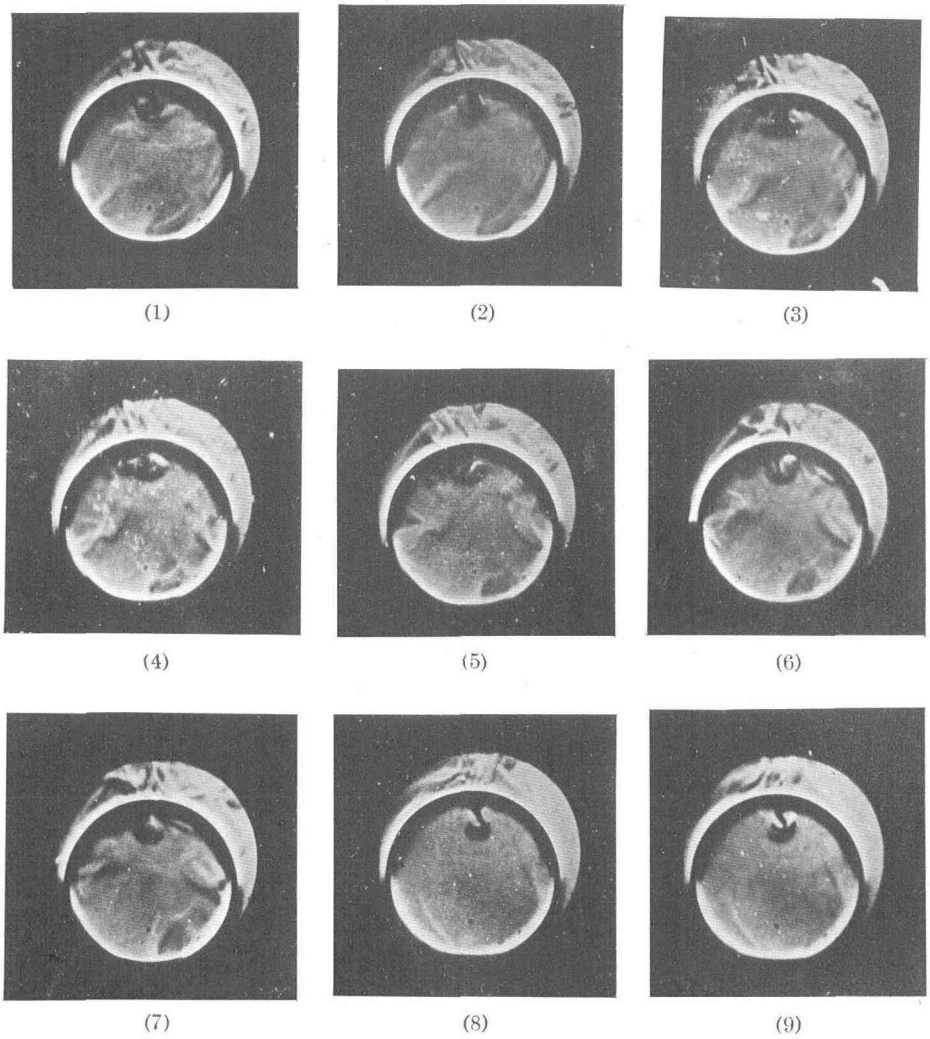

Fig. 68.

Next the convections about the electric rotating machine and the apparatus in practical use are observed. The photographs of the natural convection (Fig. 70) at the vertex of the outer periphery of the small direct current machine which is shown in Fig. 69 were taken. If the curvature of the outer shell is small or the surface is not smooth, the photograph resembles the one shown in Fig. 62 where the metal plate is placed horizontally, but if the curvature is large,

the heat convection is like that from the cylinderical surface shown in Fig. 65. Convection at the neighbourhood of the pole is shown in Fig. 71 where a stagnation of uprising air flow appears at the upper polar arc.

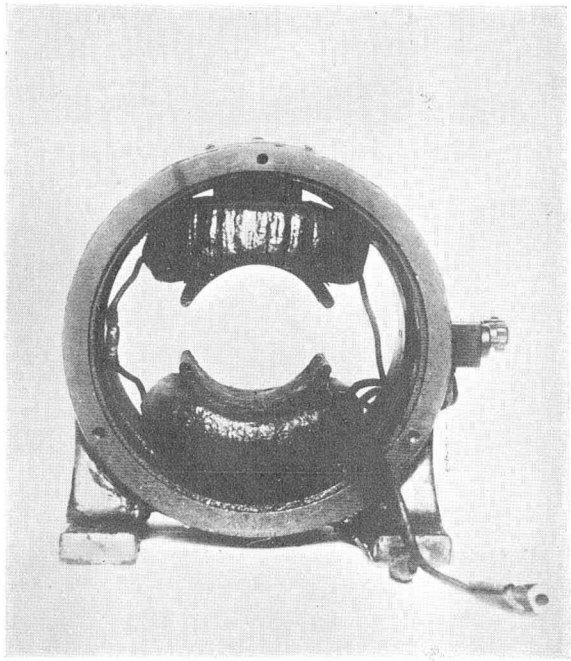

Fig. 69.

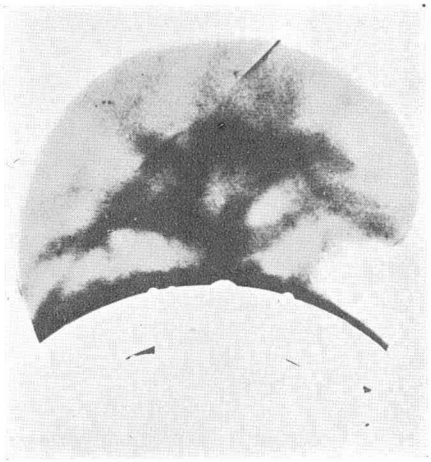

Fig. 70

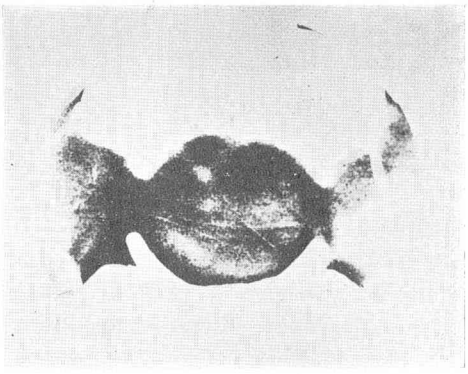

Fig. 71.

Next, the air flow motion is observed at the inner surface of the stator of an alternating current machine as shown in Fig. 72. This

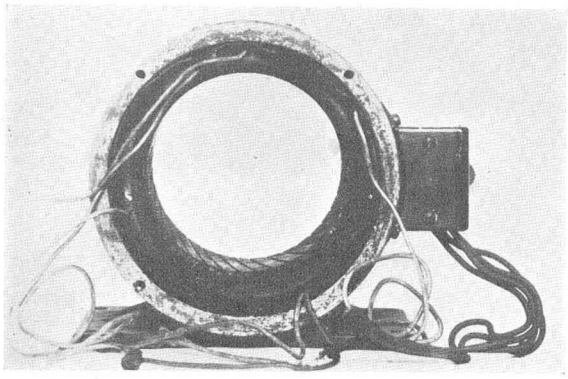

Fig. 72.

flow is similar to the one shown in Fig. 73 which illustrate the air flow at the inner surface of the metal cylinder, although the inner surface of machine is not perfectly similar to that of the metal cylinder at rest condition on account of the existance of the slot and slot conductors. From this figure the eddy motion at the upper part of the inner surface of a cylinder can be observed.

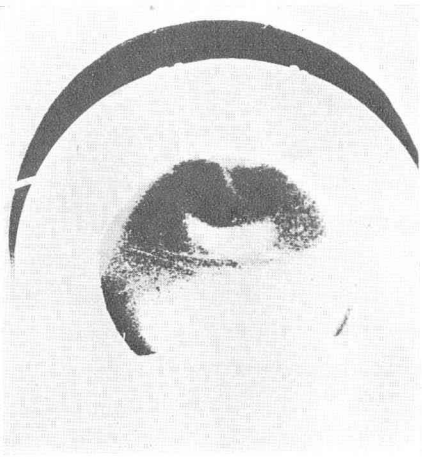

Fig. 73.

In order to test whether the heating of the periphery of the rotor is uniform or not, the armature is drawn out as shown in Fig. 74 from the stator and its winding is heated by the alternating current, passing through two carbon contactors placing at the armature periphery. The cases of uniform and the non-uniform heating are obtained by placing two carbon contactors symmetrically or non-symmetrically to the armature periphery.

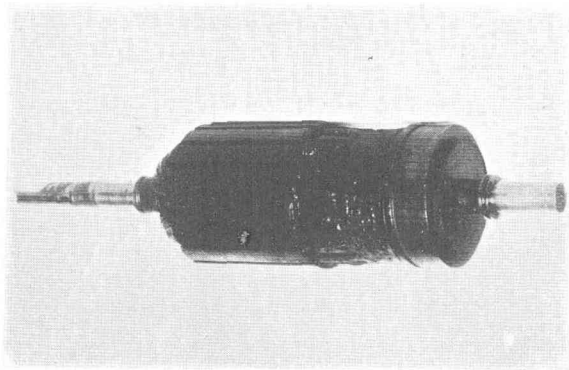

Fig. 74.

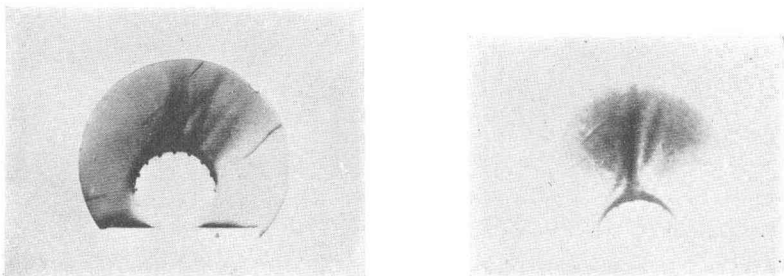

(a) (b)

Fig. 75.

The photographs (a) and (b) as shown in Fig. 75 are taken corresponding to uniformly and non-uniformly heated cases. In the case of (a) there appears one stream line at the vertex, but in the case of (b) there appears a turbulent stream.

From these experimental results, the spot where the temperature is the highest along the peripheral surface of the rotor can be detected.

For example;—if the slot winding marked with (×) in Fig. 76 is overheated, and the air flow at the periphery is inspected by means of the Schlieren method, then the stream line at the vertex may change with the rotating of the rotor. If the turbulent stream appears as shown in Fig. 76 (a) at any position and the rotor is rotated until the stream line appears as shown in Fig. 76 (b), then at the moment the vertex is the spot overheated. Thus the spot where the temperature is the highest can be detected easily.

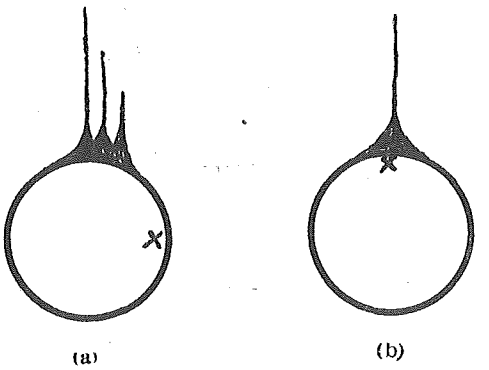

Fig. 76.

(3) TEMPERATURE DISTRIBUTION IN THE OUTER COOLING MEDIUM.

For seeking the temperatures in the cooling medium at every distance from the heating surface, they are measured with the thermocouple which is wound several times as a spiral and with the micro-displacing apparatus like that in the sliding microscope.

Horizontal metal plane.

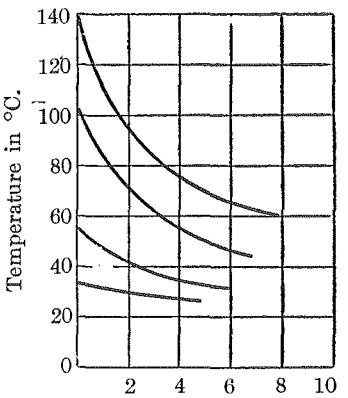

Fig. 77.

Vertical metal plane.

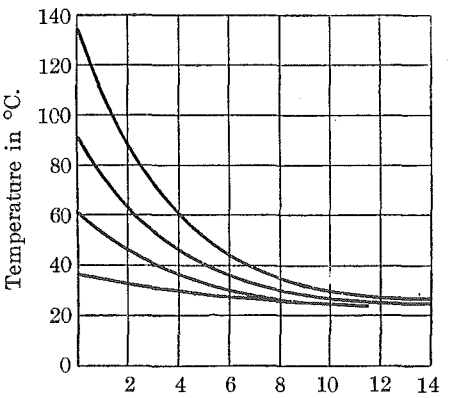

Fig. 78.

The results of the measurement are shown in Figs. 77 and 78 referring to the horizontal and vertical planes respectively. Temperature distribution far from the horizontal plane is measured and shown in Fig. 77 where the surface temperature is taken as a parameter in this curve. The measurements are made as far from the surface as the temperature is stable.

The conduction layer which exists in the range where the temperature is stable and also the uprising turbulent flow where the temperature is unstable in consequence of the replacement of hot air by the new cooling air are observed. In general, with the rise of the temperature, the disturbance due to the air flow from outer cooling medium is more vigorously. In Fig. 78 where the heated metal plate is placed vertically, the curves of temperature distribution indicate no irregularity or discontinuity, and the temperature decreases smoothly to the room temperature with the distance from the plate. In general, the air motion due to heat convection is parallel without any disturbances. In this point the flow is totally different from that of a horizontal plane. If the temperature is measured at the end part, the boundary condition may have considerable influences. Therefore the measurements are only performed at the central part of the heating surface.

From the result of this experiment, it can be concluded that the temperature distribution in the cooling medium is generally expressed by a curve resembling the exponential curve and the thickness of the conduction film is about 3~4 mm in maximum range from the observation by the Schlieren method.

If the temperature distribution due to the pure thermal conduction is expressed by the linear drooping curve, the difference between the linear drooping curve and the curve obtained from the experiments like the exponential one, should be due to the heat dissipated by the heat convection. From this consideration, it may be found that the difference of both curves is very little at the neighbourhood of the heated surface and the heat is carried only away by the thermal conduction at the neighbourhood of the heated wall. From these results, the heat from the surface is carried away by the conduction or convection in the range of distance 4~5 mm in both cases where the heated metal plates are placed horizontally and vertically.

(4) VELOCITY OF HEAT CONVECTION.

It is well known that air density is reduced by heating and the air rises up yielding the convecting flow at parts adjacent part to the heated wall. The velocity of the uprising air is very slow, so that the flow may be disturbed by introducing the apparatus or instrument with which the velocity of air is measured. Therefore, the Schlieren method is suitable to measure the air velocity because this method does not disturb the phenomena of the heat convection. The metallic surfaces to be tested are electrically heated by inserting the nichrom wire in the back part and the temperature is measured by the thermocouple (copper and constantan).

In the case where the heated surface is vertical, the uprising air flow may be laminated along the surfaces. If a shock is given at the lower part of the vertical surface for the purpose of making the impulse, and if the time is measured with which the impulse passes through two points whose distance is already measured, the mean velocity of the flow can be calculated from this measurement. The shock given at the lower part of the vertical plane, rises upward riding on the continuous heat flow due to heat convection. The propagation of the impulse is taken by kinematograph as shown in Fig. 79 and the results of this experiment are shown in Fig. 80. The velocity due to heat convection increases with the surface temperature and attains to the saturated condition at about 60°C.

The experimental result with reference to the horizontal surface is shown in Fig. 81 and the heat convection is started from the heated surface perpendicularly in front of the turbulent stream due to the disturbance from the outer cooling air.

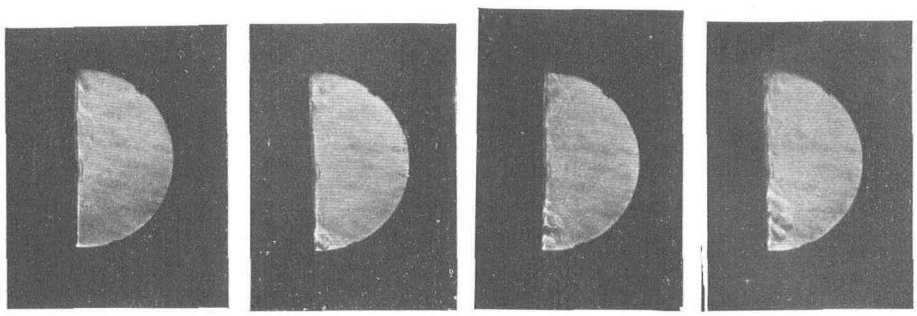

(1) (2) (3) (4)

Fig. 79.

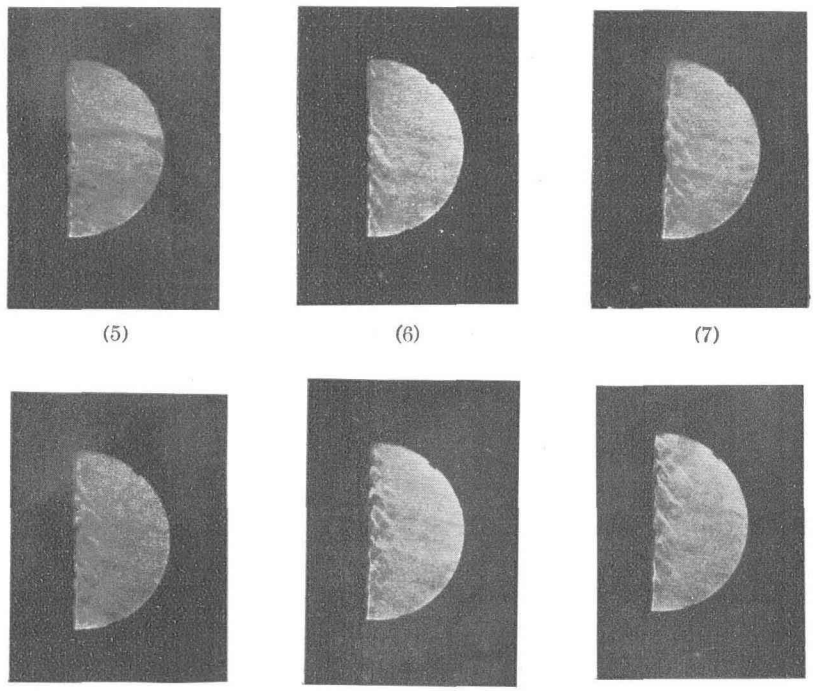

Fig. 79.

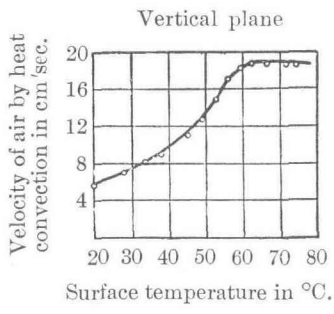

Fig. 80.

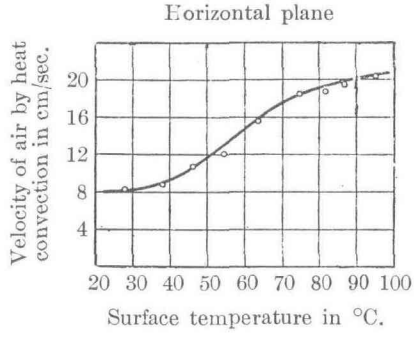

Fig. 81.

The turbulent flow is unstable, because the supplied air replaces the rising air flow from the outer circumference. The velocity increases very slightly with the temperature and the saturated velocity is about 20 cm/sec. the same as in the case of the vertical surface.

Fig. 82 represents the relation between the velocity of the uprising air along the peripheral surface and the surface temperature of the metal cylinder whose axis is horizontal. This curve is similar to the one obtained by using the horizontal or vertical plane. In this case, the vertical rising flow appears at the vertex of the cylinder and the air flows along the surfaces from the left and right sides of the cylinder come across with each other at the vertex. It is remarkable that the saturated velocity is the same respectively in the three cases where the heated surfaces are placed horizontally, vertically or where the surface form is cylinderical.

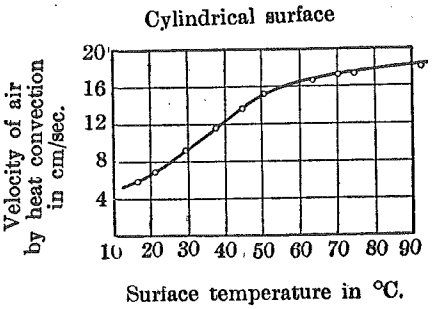

Fig. 82.

This can be explained from the existence of the two inverse flows:—the fresh air is supplied to fill up the space which is occupied by the uprising air of the heat convection, which is observed by the Schlieren method. If the surface temperature becomes higher, the speed of the uprising air becomes rapid and then the supplied air is more accelerated. As both streams are flowing in opposite directions in the vicinity of the heated surface as shown in Fig. 83 (a) and (b), the velocities of the two inverse flows may attain to equilibrium.

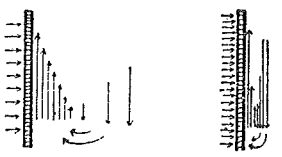

Fig. 83.

From these experimental observations, the heat diffusion depends not only upon the velocity of the heat convection along the heated wall, but also upon the thickness of the conduction layer in the cooling medium. Indeed it is observed that the conduction layer along the heated wall becomes thinner as the surface temperature becomes higher.

(5) CONDUCTION LAYER ABOUT HEATED SURFACE.

Next the variation of Newton's constant is investigated and it is found that Newton's constant depends upon the surface temperature of the heated wall:—the constant increases with the increase of the surface temperature. Especially referring to the cylinderical surface above described, the value of Newton's constant depends on the dia-

meter of the cylinder; the less the diameter of the cylinder becomes, the larger the value of Newton's constant becomes. Along with these experimental measurements, the existence and the variation of the pure conduction layer adhering to the heated wall is observed. With reference to the pure thermal conduction layer, it is found that the thickness of the layer is about 3~4 mm at the maximum condition and the temperature distribution in this layer is like to the exponential drooping curve.

From the experimental results, let us consider the heat diffusion as follows.

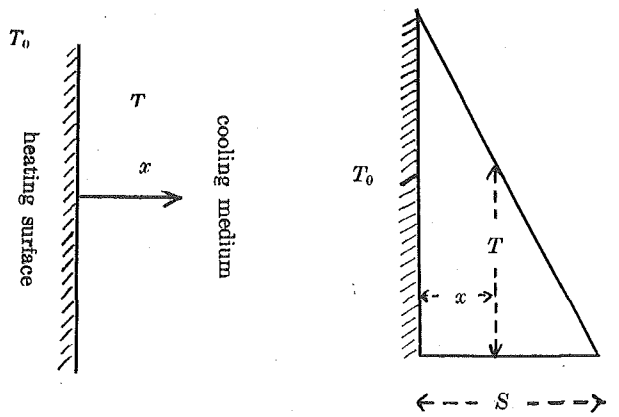

Fig. 84.

In the heated wall as shown in Fig. 84, denote the surface temperature by T_0, the temperature in the cooling medium by T and the thermal conductivity by σ, then the product $\sigma \frac{\partial T}{\partial x}$ of the temperature gradient $\frac{\partial T}{\partial x}$ in the cooling medium and the thermal conductivity σ, expresses the quantity of the heat emission from the heated surface per unit area.

Therefore Newton's constant λ is denoted by the formula

$$\lambda = -\sigma \frac{\partial T}{\partial x} \frac{1}{T_0} .$$

Now, if the temperature distribution in the cooling medium is assumed to be expressed by the linear drooping curve, then the mean temperature gradient at the distance x from the heated wall may be expressed as

$$\frac{dT}{dx} = \frac{T_0}{S} \tag{1}$$

where S shows the distance from the heated wall, at which the temperature of the cooling medium falls to the room temperature. Therefore, Newton's constant can be described;

$$\lambda = \sigma \frac{T_0}{S} \frac{1}{T_0} = \frac{\sigma}{S} . \tag{2}$$

From the above formula, it can be ascertained that Newton's constant depends on the thickness of the conduction layer S.

In order to manifest the cause, by which Newton's constant varies with the surface temperature, the heat conduction layer is observed by means of the Schlieren method.

As the results, it is concluded that the thickness of the conduction layer S decreases with the rise of the surface temperature T_0 and reaches to some final value. Therefore it can be expressed approximately.

$$S = \frac{\sigma}{K}[1+e^{-\alpha T_0}] . \tag{3}$$

Inserting (3) into formula (2), one obtains Newton's constant as follows:—

$$\lambda = \frac{\sigma}{S} \fallingdotseq K[1-e^{-\alpha T_0}]$$

where K is the saturated or the maximum value of Newton's constant and α is the index referring to the degree of rise of the exponential curve. Newton's constant given in the above formula has the saturated character and coincides with the experimental results.

The thermal conductivity of air is taken to be

$$\sigma = 0.681 \times 10^{-4} \text{ calorie/cm, °C, sec.}$$

and its unit is transformed as

$$\sigma = 4.2 \times 0.681 \times 10^{-4} \text{ watt/cm, °C.}$$

If the order of Newton's constant about the plane is assumed to have the following value

$$\lambda = 10^{-3} \text{ watt/cm}^2\text{, °C.}$$

then the thickness of the conduction layer may be gotten from the numerical calculation as following:—

$$S = \frac{\sigma}{\lambda} = \frac{4.2 \times 0.681 \times 10^{-4}}{10^{-3}} \fallingdotseq 0.3 \text{ cm.}$$

The thickness S attains to about 3 mm and coincides with the actual experimental result.

(6) HEAT DIFFUSION FROM CYLINDRICAL SURFACE.

Next the relation between Newton's constant and the surface temperature of the cylindrical surface is investigated. Denote the outer radius by r and assume the axis to be infinitely long and the surface temperature to be at T_0 as shown in Fig. 85.

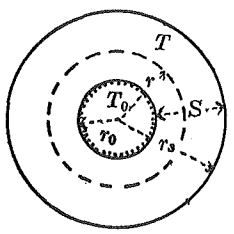

Fig. 85.

If the total heat emission from the surface per unit axial length at any distance from the heating surface is measured, then the total heat emission which occurs through out the cylindrical surface at radius r may be obtained as follows

$$2\pi r \frac{dT}{dr} \sigma$$

where σ = thermal conductivity of the cooling medium,
r = radial distance of the point to be considered,
T = temperature at the point to be considered.

Therefore, the heat emission per unit temperature and unit area i.e., Newton's constant can be written

$$\lambda = \frac{2\pi r}{2\pi r_0} \frac{dT}{dr} \frac{\sigma}{T_0}.$$

If the temperature distribution in the cooling medium is assumed to be represented by a straight line and r_s to be the radial distance of the point at which the temperature falls to the room temperature, then the mean temperature gradient

$$\frac{dT}{dr} = \frac{T_0}{r_s - r_0} = \frac{T_0}{S}$$

where $S = r_s - r_0$, Therefore Newton's constant may be represented as follows:—

$$\lambda = \sigma\left[\frac{1}{S}+\frac{1}{r_0}\right].$$

This formula denotes the heat diffusion, Newton's constant being referred to the cylindrical surface. From this formula, it can be ascertained that Newton's constant depends not only upon the thickness of the conduction layer, but also upon the diameter of the heated cylinder; Newton's constant is inversely proportional to the diameter of the heated cylinder. This calculated result coincides with the experimental one already shown in Fig. 57. If the thickness of the conduction layer is represented by the following formula referred to the variation of the surface temperature T_0,

$$S = \frac{\sigma}{K}[1+e^{-\alpha T_0}]$$

then the thickness of the conduction layer is decreased with the rise of the surface temperature. Newton's constant λ may be represented by the approximate formula

$$\lambda \fallingdotseq \frac{\sigma}{r_0}+K[1-e^{\alpha T_0}].$$

This formula expresses the character of saturation with the surface temperature.

Now to test whether the formula obtained from the consideration about the conduction layer coincides with experimental result of the heat diffusion from the cylindrical surface having various diameters, the data of Newton's constant at about 50°C in reference to the cylindrical surface is taken as shown in Table V and the thermal conductivity of the air in such values:—

$$\sigma = 2.86\times10^{-4} \text{ watt/cm, °C.}$$

and if, inserting the data in Table V into the for formula

Table V.

Diameter in cm.	Newton's const. at 50°C. (w/cm², °C)
0.95	13.9×10^{-4}
1.88	10.4×10^{-4}
3.8	9.4×10^{-4}
6.35	8.6×10^{-4}
7.62	7.85×10^{-4}
10.25	7.5×10^{-4}

$$\frac{1}{S}=\left[\frac{\lambda}{\sigma}-\frac{1}{r_0}\right]$$

the thickness of the conduction layer is calculated, then Table VI can be obtained. It may be remarked that the thickness of the conduction layer is about 3.6 mm independent of the diameter of the cylinder.

Table VI.

r_0 (cm)	λ/δ	$1/S$	S (mm)
0.478	4.86	2.76	3.63
0.94	3.64	2.575	3.86
1.9	3.29	2.763	3.64
3.175	3.00	2.685	3.62
3.81	2.88	2.6175	3.81
5.175	2.70	2.63	3.73

(7) RELATION BETWEEN SURFACE TEMPERATURE AND THICKNESS OF CONDUCTION LAYER.

Next it is investigated why the thickness of the conduction layer varies with the surface temperature. When the apparatus for testing the heat emission is inserted in the wind tunnel and Newton's constant with variation of the wind velocity is measured, the relation between Newton's constant and the wind velocity is obtained as shown in the experimental result already described.

These experimental data represent the variation of Newton's constant obtained by using a forced air flow at a velocity within the range of 1~5 meter/sec. and the relation between the current and the velocity, represents approximately a straight line. This experimental curve is exterpolated up to the range of 0~1 meter/sec. in the velocity and if this exterpolation is possible, Newton's constant corresponding to the wind velocity of 20 cm/sec. can be found. The wind velocity of 20 cm/sec. corresponds to the saturated speed due to natural convection and Newton's constant corresponds to its speed at about $6\sim7\times10^{-4}$ watt/cm^2, °C.

Therefore this value of Newton's constant should correspond to the case where the velocity of natural convection alone exists. However, the value of Newton's constant obtained directly from the experimental measurement was about twice or thrice larger than those

obtained by the above exterpolation. The differences of the two values may be considered to be those corresponding to the effect due to the heat conduction. From this it is concluded that the heat conduction exerts great influence on the heat diffusion from the surface.

If the part adjacent to the heated wall is investigated by Schlieren method in the case where the temperature at the surface is very low, then the conduction layer can be observed to be thicker with increasing of surface temperature when the heat convection does not appear in the cooling medium. If the temperature of the heated wall rises beyond this range, then vigorous natural convection can be observed. In the range of surface temperature at which the heat convection does not appear in the cooling medium, Newton's constant must decrease with the rising of the surface temperature of the heated wall, because the conduction layer becomes thicker with the rise of temperature.

If the heat convection is suppressed by means of evacuation or forced ventilation, the Newton's constant may show a decreasing character with the rising of the surface temperature of the heated wall. This decreasing character might escape our notice in the experiment of the cooling medium of normal condition, because natural convection appear with a slight rise of the surface temperature.

In the case where the natural convection appears in the cooling medium, the thickness of the conduction layer must decrease together with the temperature rise of the heated surface. Consequently the heat conduction may attain to the saturated state. Therefore it is explained that Newton's constant follows the uprising curve similar to the exponential curve.

(8) CHARACTERISTICS OF HEAT DIFFUSION BY EVACUATION AND FORCED VENTILATION.

The variation of Newton's constant due to the surface temperature depends on the characteristics of the heat diffusion influenced by heat convection and conduction from the surface to the cooling medium.

Next the characteristics of the pure heat conduction alone are investigated. At the beginning an attempt is made to find the character of the pure thermal conduction not influenced by heat convection. The air in the cooling medium is evacuated in order to suppress the air convection. The experimental results in the evacuated vessel are graphed in Fig. 86. The curve in this figure shows that Newton's constants take large value at the beginning and then decrease with

rising of surface temperature: this fact means that the thickness of the conduction layer increases with rising of the surface temperature.

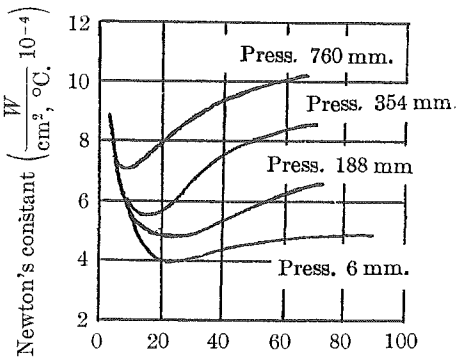

Brass cylinder dia. 3.17 cm.
length 30 cm.

Fig. 86.

If the heat convection appears more or less in the evacuated medium, the value of Newton's constant rises very slowly with increase of the temperature. The thermal conductivity of gas may be independent of the gas pressure and this law may hold in the range of pressure 760~1 mm. Accordingly the pressure of the cooling air is kept within that range and the heat diffusion from a metal cylinder inserted into a large glass vessel is measured. Therefore the thermal conductivity of gas may be considered to be constant. The minimum point exists in the curve denoting the relation between Newton's constant and surface temperature as shown in Fig. 86. The higher the pressure of the evacuating cooling air becomes, the higher becomes the temperature at which the minimum point appears and the higher becomes the rising of the characteristic curve, as shown in the characteristic curve of the heat diffusion. This uprising character may be considered as the effect of heat convection.

On the other hand, the apparatus is subjected to forced ventilation of a constant velocity by inserting it in the wind tunnel. In the case where forced ventilation is applied at a constant velocity the heat convection is considered to be constant. From the curves in Fig. 87, the characteristic curve takes a large value at the beginning and then decreases to a constant value. This pheno-

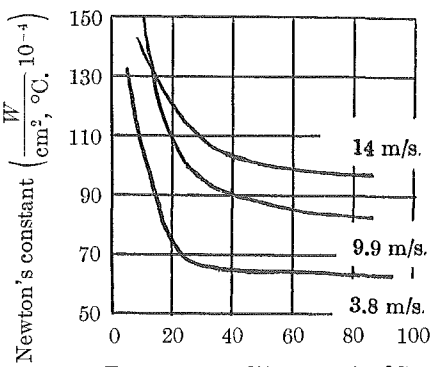

Diameter 1.88 cm.
Axial length 30 cm.

Fig. 87.

menon is explained by the fact that the thickness of the conduction layer increases with the rise of the surface temperature.

(9) SURFACE CONDITION.

For testing the variation of Newton's constant due to the surface condition. The heated surface is painted with "selvet" from the market as the simple cases and after making it dry, the experiment is performed. The result of the measurements is shown in Figs. 88 and 89. The difference between the painted and the non-painted surface is expressed in Fig. 88 with reference to brass cylinders with diameters 0.95 cm and 1.88 cm respectively.

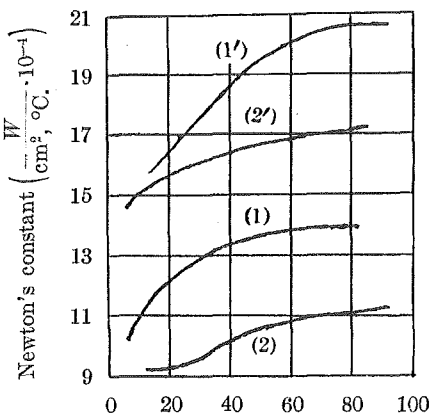

(1′), (2′). painted with black coloured "selvet."
(1), (2). non-painted.
(1′), (1). Brass cylinder having dia. 0.95 cm. and length 30 cm.
(2′), (2). Brass cylinder dia. 1.88 cm. and length 30 cm.

Fig. 88.

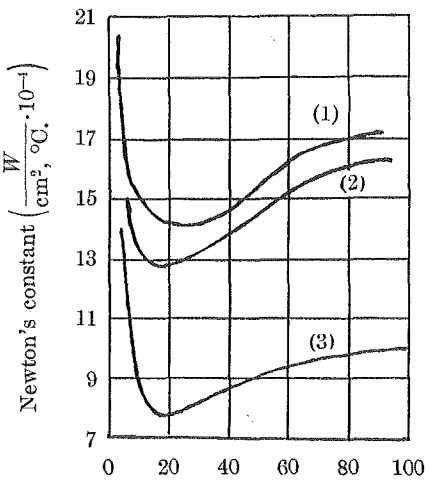

(1). painted with black coloured "selvet."
(2). painted with white coloured "selvet."
(3). polished metal surface.
Brass cylinder having dia. 3.8 cm. and length 40 cm.

Fig. 89.

From the experimental result, it is concluded that the painted surface is more favourable to diffuse the heat than the one non-painted. To test whether the painted colour exerts influence on the surface cooling or not experiments were made using various colours of "selvet"

paint. From the results, it is found that the other colours: red, blue, gray, yellow and etc., except white and black, take values between the curves of the white and black.

(10) CURVE OF TEMPERATURE RISE.

It is a very essential problem to determine the curve of the temperature rise of the electric machine, for the saturated temperature at full load running is taken as the highest allowable temperature for the materials constituting of the electric machine and a very long time is needed to find the saturated temperature of a large electric machine. Therefore the temperature rise curve at the range of under saturated state or the equivalent saturated temperature from over-loading for a short time is found from the experiment and the saturated temperature can be found only by extending the curve thus obtained up to the saturated part.

However, if the temperature of heated electric machine in the stationary state is given, as the power supply and the heat diffusion are constant, it is sufficient to determine the Newton's constant suitable for the external condition.

Newton's constant varies with the temperature of the heated surface and the surface condition. As Newton's constant varies with the surface temperature even if the surface condition is kept constant, every point on the curve of temperature rise may be influenced by the variation of Newton's constant. If Newton's constant is taken as constant during the process of temperature rise at the surface, then the curve of temperature rise may follow the exponential curve under the assumption of the constancy of heat supply. However, in practice, the curve obtained from the experiment is well known not to follow the exponential curve. Therefore, Newton's constant must be considered to be a function of the surface temperature.

Newton's constant is expressed by the following formula,

$$\lambda = \lambda_0[1-e^{-\alpha\theta}], \tag{1}$$

where λ_0 = maximum value of Newton's constant.
θ = surface temperature.

For the temperature rise of the heated body, the following equation

$$\frac{d\theta}{dt}+\frac{A}{SW}\lambda\theta = \frac{Q}{SW}, \tag{2}$$

is obtained where

W = weight of heated body.
A = surface area of heated body.
Q = consumed heat loss in watt assumed as constant.
S = specific heat of heating material.

Putting

$$\frac{SW}{A\lambda_0} = T_0 , \qquad \frac{Q}{A\lambda_0} = \vartheta .$$

one can write (2) as

$$\frac{d\theta}{dt} + \frac{1}{T_0}[1-e^{-\alpha\theta}]\theta = \frac{\vartheta}{T_0} . \tag{3}$$

To gain the saturated temperature, put

$$\frac{d\theta}{dt} = 0 ,$$

then

$$\vartheta = [1-e^{-\alpha\theta}]\theta , \tag{4}$$

If θ_f is satisfied by the above formula, the solution of (3) is

$$\int_{\theta_f} \frac{d\theta}{\vartheta-(1-e^{-\alpha\theta})\theta} = \frac{t}{T_0} . \tag{5}$$

By series integration, it follows

$$\frac{t}{T_0} = -\log_e\left[1-\frac{(1-e^{\alpha\theta})\theta}{\vartheta}\right] + \left(\frac{\theta}{\vartheta}\right)e^{-\alpha\theta} - \frac{1}{2}\left(\frac{\theta}{\vartheta}\right)^2 + \cdots\cdots . \tag{6}$$

The curve of temperature rise $\theta = f(t)$ may be obtained by the graphical method. At the beginning the curve represented by the term of the right hand of equation (6) is drawn as a function of the variable θ, and also the curve represented by $\frac{t}{T_0}$ as a function of t is drawn. If the two curves thus obtained are cut by any horizontal line and the values of θ and t are found at the points of the two curves at intersections by this horizontal line, then from such values

of θ and t, one can obtain the curve of temperature rise as shown in Fig. 90. In Fig. 90, two curves are represented; one corresponds to the case where Newton's constant is taken as $\lambda = \text{const.}$, the other corresponds to $\lambda \neq \text{const.}$

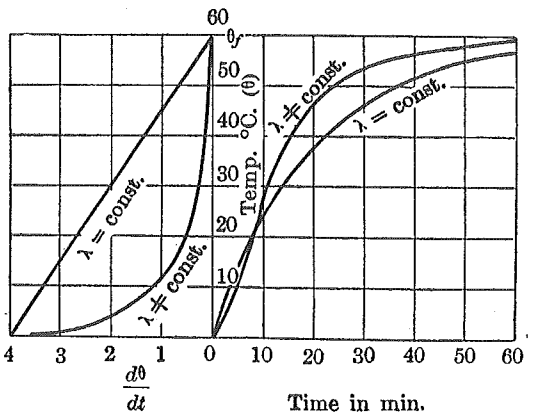

Fig. 90.

As the electric machines in practical use are very complicated and constructed of many kinds of materials, the temperature rise may not follow the exponential curve. The curve $\lambda \neq \text{const.}$ is like the one obtained by Jehle and Osborn. They treated the curve of temperature rise as the summation of the two kinds of the exponential curve and explained the complicated case of the practical machine to be composed of two kinds of heat capacities. However, the temperature rise of the machine or apparatus may not follow the pure exponential curve, even if the machine or apparatus is not composed of complicated materials.

CHAPTER VII.

SUMMARY.

The heat flow in the armature of electric machines has been classified into the radial and axial flows. The inner temperature of the armature is calculated about the above two flows independently.

In chapter II, the writer has calculated the inner temperature in each part of the armature under the consideration that the heat flow occurs in the radial direction alone and he has investigated the mean temperature in the iron core and the fluctuation of temperature corresponding to the temperatures of slot and teeth which exerts effects on the iron core and the cooling surface. The temperatures of the teeth and iron core have been found by this calculation and the influences of construction of teeth and iron core on their temperature have been discussed.

On the other hand, in chapter III only the axial temperature in reference to the slot, teeth and iron core is treated and the temperatures of each part of the armature is obtained. From the calculation in the axial direction, the temperatures of every point of the armature is found in the cases of no-load and short-circuit as special cases.

Next in chapters IV and V are described the precise investigation of the temperature in the slot winding. For his investigating the temperature in the slot, the writer's chapter IV may be consulted, in which the current and field distribution using the calculated formula and the experimental results is discussed precisely. From this calculation, the variation of current distribution due to the type of slot, the arrangement of conductors and the frequency of the source is found. As to the type of slot; open, semi-open and totally enclosed slots, and as to the arrangement, the variation of the current distribution due to the arrangement of the slot conductor have been investigated. If there is a side clearance (contained in the slot insulation) between the slot and conductor, great influence may be exerted upon the distribution of current. In the case where the side clearance was very small, it is enough to treat the distribution of the direction of y-axis as uniform, but in the case where the side clearance was not small enough to be neglected, the distribution of current could not be treated as uniform. Though the distribution of the heat loss in the slot could be found as the extension of this calculation, it was not convenient to treat the distribution of heat loss for the purpose of finding the

temperature distribution in the slot. At the end of this chapter, "Alternating current resistance" is calculated about the single conductor and many conductors inserted into the slot. It is important for the machine in practical use to find the over-heated point in the slot winding at which the damage to the machine frequently occurs. The temperature of the slot conductor has been treated in chapter V, being discussed by using the calculated formula deduced from the fundamental equation of heat conduction. The inner temperature from the thermal equilibrium in the outside and inside of the slot is found in the case of loading and the effects of the thermal constants on the temperature distribution are discussed. The temperature distribution for loading is expressed by the formula deduced from the fundamental equation by using Green's potential function. From these calculations, the maximum and the mean temperatures are obtained, and the position to be occupied by the highest temperature is discussed, since it is the most essential problem in engineering. The transference of the point of the highest temperature was discussed mainly for various load.

In chapter VI, Newton's constant was investigated and the mechanism of heat diffusion from the cooling surface was discussed. The problem of surface cooling was considered to be the final stage of the heat flow from the inner part of the armature into the outer cooling medium. The following conclusions are obtained from the experimental results:— 1) that Newton's constant becomes larger with the increase of the surface temperature and then attains to the saturated value, 2) that the vertical plane is more favourable to cool the surface than the horizontal plane and 3) also that Newton's constant of the cylindrical surface depends on its diameter.

The heat disipation from the surface is carried out by heat conduction, convection and radiation, however the latter could be neglected when the surface temperature is not too high. It is possible to make the phenomena of heat conduction and convection visible by means of the Schlieren method. From a rather large number of observations and photographs by means of the Schlieren method, the conduction layer and the convection flow are detected and thus the speed of the heat convection is measured. The results of these experimental observations and photographs are compared with those of an actual machine. The periphery of the rotor of an electric machine is heated uniformly or non-uniformly and it is found by means of the Schlieren method that there is an exceeding difference between the uniform and non-uniform heating. From these facts, the over-heating point is

detected on the periphery of the rotor and the method to detect the position of the over-heating point on the periphery of the rotor is found.

The temperature distribution in the cooling medium was measured and it was found that the temperature in the cooling medium is denoted approximately by the exponential curve and there was more or less difference about the temperature distribution between the horizontal and vertical planes. From several experiments, it is ascertained that the pure thermal conduction existed in the layer $3\sim4$ mm in thickness in the neighbourhood of the heating surface. From the change of Newton's constant in the wind tunnel and the evacuated vessel, it is concluded that the change of Newton's constant depends on the change of the layer in the pure thermal conduction referring to the surface temperature. The saturated character of Newton's constant was explained in this chapter.

Next, the curve of the temperature rise of an electric machine was discussed by using the calculated formula obtained by the variations of Newton's constant. Up to the present, the curve of temperature rise has been expressed by the pure exponential function, but it was found not suitable to the practical application. The new curve of temperature rise can be expressed by the formula obtained from the author's theory of the variation of Newton's constant and this curve may be most efficient for practical application.

At the end of this essay, the author wishes to express his thanks to Prof. Y. Ikeda for his kind guidance and encouragement and also to express his thanks to Prof. T. Sômiya for his valuable advice in regard to this essay. As the author's information about electric machines was received from the lectures of Prof. G. Shimizu and useful suggestions have been gained from his lecture, the author also expresses thanks to Prof. G. Shimizu.

Reference.

Arnold: Wechselstromtechnik, IV.

Y. Ikeka: Memoirs of the Faculty of Engineering, Hokkaido Imperial University Vol. 1, (1928), pp. 193-209.

Y. Ikeda: Integral equation.

Y. Ikeda: Mathematics and electrical engineering.

Ernst Stumpp: Arbeiten aus dem Electrotechnischen Institut, Bd. V, 1929.

Carl Trettin: Wissenschaftliche Veröffentlichungen aus dem Siemenskonzern, Bd. IX, 1930.

Rogowski: Archiv für Electrotechnik, Bd. 2, 1913.

A. Moskwitin: Archiv für Electrotechnik, Bd. 25, 1931.

I. Schenfer u. A. Moskwitin: Archiv für Electrotechnik, Bd. 24, 1930.

H. Bucholz: Archiv für Electrotechnik, Bd. 15, Feb. 1934.

Ludwig Binder: Über Wärme übergang auf ruhige oder bewegte Luft.

H. Osborne: Electrotechnische Zeitschrift, Ht. 25, 1930. Bd.

H. Jehle: Electrotechnische Zeitschrift, Ht. 33, 1930.

Piercy and Winny: Philosophical Magazine, Vol. 16, No. 105, 1933.

M. Mori: Journal of Institute of Electrical Engineering of Japan, Vol. 53, No. 537, 1933.

M. Mori: Journal of Institute of Electrical Engineering of Japan, Vol. 53, No. 539, 1933.

M. Mori: Journal of Institute of Electrical Engineering of Japan, Vol. 54, No. 553, 1934.

M. Mori: Journal of Institute of Electrical Engineering of Japan, Vol. 54, No. 554, 1934.

M. Mori: Journal of Institute of Electrical Engineering of Japan, Vol. 55, No. 559, 1935.

M. Mori: Journal of Institute of Electrical Engineering of Japan, Vol. 55, No. 568, 1935.